University of Ferrara

DOCTORAL RESEARCH IN

BIOMEDICAL SCIENCE and BIOTECHNOLOGY

CYCL XXIX

COORDINATOR Prof. Paolo Pinton

Effects of environmental ozone exposure on mice olfactory bulb. Immunochemical, electrophysiological and behavioural studies

Scientific Sector BIO/09

PhD student

Dr. ABdElrahim Batran Ali Samah

Tutors

Prof. Belluzzi Ottorino

Prof. Rispoli Giorgio

Co-tutors

Dr. Pignatelli Angela

Dr. Benedusi Mascia

Year 2013/2016

DEDICATION

I dedicate this humble work to my parents, family, teachers and friends.

ABBREVIATIONS

µg	Microgram
4HNE	4-Hydroxynonenal
GFP	Green fluorescent protein
Non-ON zone	Non-olfactory nerve zone
DOPAC	3,4-dihydroxyphenylacetic acid
HCHO and RCHO	aldehydic species
RO_2	Alkoperoxyl
RO	Alkoxyl
APS	Ammounium persulfate
A.U	Arbitrary Units
ACSF	Artificial cerebrospinal fluid
ACSF	Artificial cerebro-spinal fluid
Ba^{2+}	Barium
BSA	Bovine Serum Albumin
BAL	Bronchoalveolar lavage
C57BL/6	C57 black 6
CB	Calbindin
CR	Calretinin
Cm	Centimeter
cAMP	Cyclic adenosine monophosphate
CYP1A1	Cytochrome P450, family 1, subfamily A, polypeptide 1
C°	degree celsius
D.W	Deioinsed Water
DNA	Deoxyribonucleic acid
LDTT	Dithiothreitol
DA	Dopamine
eGFP	Enhanced green fluorescent protein
EPL	External plexiform layer
ET	External tufted
e.g	For example
GΩ	Gigaohm
GL	Glomerular layer
GAD	Glutamic acid decarboxylase
g	Gram
GCL	Granule cell layer
Hz	Hertz
HVA	Homovanillic acid
h	Hour
RH	hydrocarbons
HCl	Hydrochloric acid
Ih	Hyperpolarization-activated current
HCN	Hyperpolarization-activated cyclic nucleotide–gated channel
IPL	Internal plexiform layer

hν	Light energy
MDA	Malondialdehyde
MMPs	Matrix metalloproteinases
mRNA	Messenger Ribonucleic acid
µl	microliter
µm	micrometer
ml	milliliter
mM	Millimolar
mOsm	Milliosmole
mV	Millivolt
min	minute
MCL	Mitral cell layer
M	Molar
MW	Molecular weight
nM	Nano Molar
nm	Nanometer
NO	Nitric oxide
NO_2	Nitrogen dioxide
Nrf2	Nuclear factor (erythroid-derived 2)-like 2
NF-κB	Nuclear factor kappa-light-chain-enhancer of activated B cells
NF-κB inhibitor α	Nuclear factor of kappa light polypeptide gene enhancer in B-cells inhibitor, alpha
OB	Olfactory bulb
ONL	Olfactory nerve layer
ON zone	Olfactory nerve zone
OSN	Olfactory sensory neuron
OBP	olfactory-binding-protein
O_2	Oxygen
ROS	Oxygen species
O_3	Ozone
PM	Particulate matter
ppm	parts per million
PG	Periglomerular
PBS	Phosphate Buffered Saline
PBS-T	Phosphate Buffered Saline - Tween
RIPA	RadioImmunoPrecipitation Assay
RPM	Revolutions per minute
SB	Sample buffer
Na	sodium
NaCl	Sodium Chloride
SDS	Sodium dodecyl sulfate
NaOH	sodium hydroxide
SD	Standard Deviation
SSA	Superficial short-axon
TEMED	Tetramethylethylenediamine

TEMED	Tetramethylethylenediamine
TNFα	Tumor necrosis factor alpha
TH	Tyrosine hydroxylase
UV	Ultraviolet
vs	versus
v/v	Volume per volume
w/v	Weight per volume
WT	Wild type
GABA	γ-amino butyric acid

ABSTRACT

Objectives: This work aimed to study the effect(s) of environmental ozone (O_3) exposure on the olfactory bulbs (OB) of Swiss Webster and C57BL/6J mouse strains, by using immunochemical (Western blot), and electrophysiological (patch clamp) techniques. In addition, to behavioural experiments (olfactory habituation/dishabituation test).

Method: Swiss Webster and C57BL/6J mice were exposed to different O_3 doses for different durations. Then, the effect of O_3 exposure was evaluated by measuring the levels of oxidative stress biomarkers (4HNE and CYP1A1) in plasma and/or in the olfactory bulb (OB) samples, in control and O_3 exposed mice. In addition, the excitability profiles of bulbar dopaminergic cells were measured in C57BL/6J mice. Moreover, the effect of O_3 exposure on the olfactory response to social and non-social odours was also evaluated in the two strains. Finally, the body weight of the exposed mice was measured before and after O_3 exposure for the two strains.

Results: Concerning Swiss Webster mouse strain, O_3 exposure to doses of 0.2 ppm 2 h/2 times/1 day, 0.5 ppm 30 min/once, 0.5 ppm 60 min/once and 0.2 ppm 2 h/2 times/2 days, did not cause any sufferance to the tested mice. The biochemical results showed a significant increase in the level of the oxidative stress biomarkers and OB total proteins levels in O_3 exposed mice compared to the air exposed mice. In addition, the body weight of the O_3 exposed mice was significantly reduced after the exposure.

Furthermore, the biochemical results of C57BL/6J mice did show any significant differences in the plasma 4HNE and OB total proteins of mice exposed to 0.8 ppm 2h/2 times/5 days (GFP and WT), 0.5 ppm 30 min/once and 0.5 ppm 60 min/once O_3 doses compared to air exposed mice. However, the OB 4HNE was statistically increased in the 0.8 ppm 2h/2 times/5 days O_3 dose exposed WT mice. On the other hand, this marker was statistically insignificant in the other O_3 doses exposed mice compared to control mice. Moreover, the CYP 1A1 was not detected in the GFP mice. Furthermore, the body weight of the all O_3 exposed mice was statistically reduced after the exposure except for 0.5 ppm O_3 doses exposed mice for 60 min once. However, the electrophysiological experiments showed a significant alteration in the spontaneous firing activity of bulbar DA neurones following O_3 exposure, with overall reduction in the firing frequency, membrane resistance, rheobase and chronaxie with reorganization of spontaneous firing in bursts. Moreover, the variation in the number of the DA neurons between O_3 and control mice was statistically insignificant. Regarding the behavioural experiment results, the effect of O_3

exposure was different in the two strains. C57BL / 6J mice were less sensitive in comparison to Swiss Webster mice, while the latter showed high loss of olfactory sensitivity to environmental odours following O_3 exposure. In addition, concerning Swiss Webster mice, the females were more vulnerable to O_3 exposure than males.

Conclusion: In the current study, O_3 exposure caused an increase in the level of the proteins involved in the oxidative stress state in the OB of Swiss Webster mouse strain. While in C57BL/6J mouse strain this effect was not observed, but the electrophysiological studies showed a significant change in the firing properties of the OB DA cells. Also, the behavioural test showed deterioration in the olfactory function which was strain and sex dependant. Finally, O_3 exposure caused a significant decrease in the body weight of the tested mice in both strains.

RIASSUNTO

Scopo del lavoro: Lo scopo di questo lavoro è stato quello di studiare gli effetti dei danni provocati dalla applicazione di differenti dosi di ozono sul bulbo olfattorio (OB) di topi della linea Swiss Webster e C57BL/6J attraverso analisi immunochimica (Western Blot), elettrofisiologica (patch-clamp) e studi comportamentali (abituazione e disabituazione).

Materiali e Metodi: topi dei ceppi Swiss Webster e C57BL / 6J sono stati esposti ad ozono per tempi e dosi differenti. Gli effetti dell'esposizione ad ozono sono stati valutati misurando i livelli di espressione di marker specifici dello stress ossidativo, quali 4HNE e CYP1A1 sia nell'OB che a livello plasmatico. Successivamente, questi valori sono stati paragonati a quelli ottenuti facendo lo stesso tipo di indagine sui topi di controllo, esposti all'aria. Quindi, sono state valutate le caratteristiche elettrofisiologiche di base dei neuroni dopaminergici del bulbo olfattorio dei topi C57BL/6J esposti ad ozono. Inoltre è stato valutato l'effetto dell'ozono sulla risposta olfattiva a odori sociali e non. Per tutti gli animali è stato inoltre valutato il peso prima e dopo i diversi trattamenti.

Risultati: In topi del ceppo Swiss Webster, esposizioni all'ozono a dosi di, 0.2 ppm 2 h / 2 volte / 1 giorno, 0.5 ppm 30 min / una volta e 0.5 ppm 60 min / una volta, non hanno causato alcuna sofferenza ai topi. I risultati dell'analisi biochimica hanno mostrato un aumento significativo della proteina plasmatica 4HNE e della proteina bulbare 4HNE in topi esposti ad ozono rispetto ai topi di controllo. Il peso corporeo dei topi esposti era significativamente ridotto rispetto ai controlli.

In topi del ceppo C57BL/6J, l'analisi biochimica non ha mostrato variazioni significative nei livelli di 4HNE nei topi esposti a ozono 0.8 ppm 2h / 2 volte / 5 giorni (GFP e WT), 0.5 ppm 30 min / una volta e 0.5 ppm 60 min / una volta rispetto ai topi di controllo esposti all'aria, la proteina CYP1A1 non è stata rilevata in questo ceppo di topi. Gli esperimenti elettrofisiologici hanno mostrato una significativa alterazione della scarica spontanea nei neuroni DA bulbari in seguito ad esposizione a ozono, con una riduzione complessiva della frequenza di scarica, e una riorganizzazione dell'attività spontanea in burst. Nessuna variazione significativa del numero di neuroni DA è stata osservata in seguito ad esposizione all'ozono.

Gli studi comportamentali hanno mostrato effetti diversi nei due ceppi. Il C57BL/6J è risultato essere meno sensibile rispetto allo Swiss Webster. In quest'ultimo è stata messa in evidenza anche una diversità di genere nella risposta.

Conclusioni: In questo lavoro, è stato dimostrato che l'esposizione ad ozono causa un aumento dei livelli di espressione delle proteine coinvolte nello stress ossidativo a livello del bulbo olfattorio dei topi Swiss Webster, ma non nei topi C57BL/6J. Anche le proprietà elettrofisiologiche dei neuroni dopaminergici dei topi C57BL/6J sono modificate in seguito alla esposizione a differenti dosi di ozono. Infine i test comportamentali hanno mostrato un deterioramento della funzione olfattiva in risposta alla esposizione all'ozono sesso- e ceppo-dipendente.

I risultati indicano che i topi Swiss Webster sono più sensibili all'esposizione all'ozono rispetto C57BL/6J, mostrando attivazione dei marcatori di stress ossidativo a concentrazioni di ozono inferiori. Tuttavia, i C57BL/6J mostrano una significativa alterazione nella funzione dei neuroni DA bulbari che molto probabilmente compromette la funzione olfattiva.

LIST OF CONTENTS

LIST OF FIGURES

LIST OF TABLES

1. INTRODUCTION

1.1 Definitions of air pollution

Pollution is defined as "any harmful, or undesirable change in the physical, chemical or biological quality of air, water or soil," quoted from The Longman Dictionary of Environmental Science, (Lawrence et al., 1998). Also, it has been defined as any direct or indirect human introduction of substances into the environment which harm the living resources, influence human health, and deteriorate the environmental quality. However, the former definition has a lack, because pollution might occur naturally. Moreover, contamination is one of the terms that is correlated to pollution, and it is defined as the presence of elevated concentrations of one of the environment components (air, water, soil, etc.), and it is not necessary causing harmful effects. Beside the above terms, the atmospheric air pollution is another term which is correlated to pollution, and it refers to the abnormal presence and/or an increase in the concentration of gases or particulate matters. But, this definition is not complete, because the Eearth's atmosphere has been affected by many factors like the natural disasters, which led to the change in the atmosphere over time, (Yang and Omaye, 2009).

Furthermore, Lawrence et al., (1998) gave a thorough definition of air pollution. He defined it as the presence of substances or energy in the atmosphere in certain amount for a particular duration of time, which could be harmful to human life or leading to particular changes in the weather and climate. In addition, smog is another term which is commonly used for pollution, and it is a mixture of smoke and fog which are accumulated and suspended over large cities such as London, (Yang and Omaye, 2009).

1.2 Ozone gas (O_3)

Ozone (O_3) is an allotropic form of oxygen (O_2). It is formed due to strong flow of electricity in the air like the thunderstorm. In addition, it has different characteristics with a distinguished odour and tends to accumulate around high-voltage apparatus. However, O_3 is different from O_2 by being less stable, strongly irritating, more active, dissociate rapidly at room temperature, and it is heavier than O_2, (Yang and Omaye, 2009).

1.2.1 Ozone formation

Ozone is formed in the atmosphere through a complex series of photochemical reactions which involve three steps: photo activation, photo dissociation and free radical reactions, (Mudway and Kelly, 2000). In addition, these photochemical reactions require reactive

hydrocarbons, sunlight and nitrogen dioxide (NO_2). Therefore, the formation of O_3 starts when NO_2 absorbs shorter-wavelength UV light in the troposphere leading to the following reactions:

NO_2 + UV photons ($h\nu$) → O + NO

$O + O_2 \rightarrow O_3$

$O_3 + NO \rightarrow NO_2 + O_2$

The formed oxides of nitrogen: NO and NO_2 (NO_x) are primary pollutants, and are usually produced by the motor vehicles. Furthermore, there are some organic components which participate in O_3 formation and they include: methane, the natural biogenic decay product, olefinic hydrocarbons and other compounds which are produced due to some human anthropogenic activities, such as agriculture, mining, and transportation. In addition, O_3 formation has other two resources: the first one is the outdoor source which includes methane (formed from agriculture and animal industry), and NO_x (comes from fossil fuel), while the second one is the outdoor resource which have a role in increasing the concentration of O_3 in the modern world to 40 ppm, and it contains: laser printers, copy machines, and electrostatic air cleaners, (Altshuller, 1987; Yang and Omaye, 2009).

Moreover, there are some other compounds in the photochemical smog which might undergo photo decomposition to produce free radicals that participate directly or indirectly in the conversion of NO to NO_2, such as Hydroxyl and hydroperoxyl radicals which are formed by the photo dissociation reactions from a wide range of compounds including nitrous acid and formaldehyde. Furthermore, Alkoxyl (RO) and alkoperoxyl (RO_2) radicals which are formed from the interaction of radicals with aldehydic species (HCHO and RCHO) and hydrocarbons (RH), were also shown to oxidise NO**.** to NO_2, (Mudway and Kelly, 2000).

1.3 Mechanism of O_3 toxicity

Ozone initiates an intracellular oxidative stress through ozonide and hydroperoxide formation. This mechanism of oxidative damage involves the activation of Nrf2, heat shock protein 70, NF-κB, protein-1 fos and c-jun oncogenes also, it increases the expression levels of a wide range of proinflammatory cytokines (TNFα and interleukin 1β), chemokines (e.g., interleukin 8), and adhesion genes, (Bassett et al., 2001; Nichols et al., 2001).

When O_3 is inhaled it produces reactive oxygen species (ROS) depending on the exposure dose, then it induces its toxic effects firstly in the pulmonary system leading to some

alterations in structure and function of alveolar cell membrane, (Dorado-Martínez et al., 2001). Moreover, as the lungs are the most important vital barriers against O_3 exposure, they act as a defence mechanism by producing an antioxidant components such as: superoxide dismutase, catalase and glutathione peroxidase, (Rahman et al., 1991). Then, If the free radicals overwhelm the antioxidant defence systems in the lungs, they diffuse to the other organs and reach the central nervous system through the bloodstream producing further oxidative stress state which might affect the whole organism systems, (Dorado-Martínez et al., 2001).

Furthermore, the oxidative stress state caused by O_3 exposure produces an increase in lipid peroxidation in different brain structures, (Rivas-Arancibia et al., 2000). Moreover, exposure to 1ppm O_3 dose caused an oxidative stress state which led to neural changes, (Colín-Barenque et al., 1999).

1.4 The biological harm full effects of O_3 exposure and ozone toxicity

The biological harmful effects due to O_3 exposure are attributed to its ability to cause ozonation, which is the oxidation and peroxidation of biomolecules (Glutathione, thiol or amino groups and unsaturated C=C bonds), either directly or indirectly through secondary reactive toxic reactions. In addition, O_3 reacts with amino acids such as: cysteine, Methionine, Tryptophan, Tyrosine and Histidine, and some other molecules like uric acid and ascorbic acid. Also, it reacts with proteins such as Albumin. Moreover, when it oxidizes lipids it produces highly reactive aldehyde group, (Bocci, 1996; Menzel, 1984). Furthermore, the produced peroxides and the free radicals induce further toxic effects and biochemical chain reactions (such as endoperoxide production, enzymatic inactivation) which lead to the production of more free radicles causing further cellular membrane oxidation, organelles lipoperoxidation and production of aldehyde groups, (Cross et al., 1992; Halliwell and Gutteridge, 1984; Mustafa, 1990). In addition, these free radicals can modulate the lipid peroxidation of some organs, e.g. lung, heart and brain, (Rahman et al., 1991). O_3 oxidizes lipids directly to ozonides by changing them to aldehydes. Moreover, the lining fluid on the lung reacts with O_3 produces components which strength the oxidative damage, e.g. organic hydrogen peroxides, aldehydes, and organic radicals, (Fakhrzadeh et al., 2004a; Salvi, 2001; Timblin et al., 1998).

1.5 Acute O_3 exposure

Acute O_3 exposure causes damage in the lung ciliated epithelial cell, the respiratory airways and type 1 epithelial cells in the alveolar region. However, these effects are exclusively localized at the junction of the terminal bronchioles and the alveolar ducts, as evidenced from the death of cells and accumulation of inflammatory cells. Furthermore, in acute O_3 exposures the response of the lung includes two phases: the first one is the initial injury-phase, which is characterized by loss of some enzymatic activities and cell damage, followed by the repairing-phase (second phase), which is associated with an increase in the proliferation and in the metabolic activities of metabolically active cells, e.g., the alveolar type 2 cells and the bronchiolar clara cells, finally it leads to an impairment of lung function and tissue damage. In addition, the repair-phase is associated with an accumulation of inflammatory cells mainly the macrophages in the lung and an increase in the nitric oxide production, (Laskin et al., 1994; Mustafa, 1990).

1.6 Chronic O_3 exposure

Chronic O_3 exposure can cause or increase lung diseases. Also, it might affect other body systems such as the circulatory system, spleen and the central nervous system, (extra pulmonary effects), (Mustafa, 1990). In addition, some experimental data concerning chronic O_3 exposure for 18 months showed restrictive lung disease caused by obliterative bronchiolitis and reduction in the spirometric indices in adults and children, (Mudway and Kelly, 2000).

Furthermore, the harmful effects due to chronic O_3 exposure have been studied also in rats and monkeys. In both animal models signs of bronchitis, (Chang et al., 1992), fibrosis, (Stockstill et al., 1995), and bronchiolar metaplasia of the alveolar ducts have been observed, (Mudway and Kelly, 2000).

1.7 The defence mechanisms against reactive oxygen species (ROS)

In the normal metabolic process free radicals and some ROS are produced within the human body, but if their production overwhelms the antioxidant defence enzymes, an oxidative stress state will be generated, (Bocci, 1996).

Various antioxidants, like ascorbic acid, uric acid and thiols act as powerful scavengers for O_3 and NO_2 free radicals in the body fluids, they protect the lung lining fluid against inhaled air pollutants, (Yang and Omaye, 2009) .

Ozone is strong oxidizing agent, it can stimulate the cellular antioxidant enzymes which inhibit the oxidative stress state, (Bocci, 1996). Furthermore, the dose and the time of exposure affect the body response to the oxidative stress state that might be generated. After the occurrence of the oxidative stress state, part of ROS will be neutralized by the antioxidant defence system such as superoxide dismutase, catalase, glutathione and ascorbic acid. Whereas, in the plasma uric acid, ascorbic acid, and albumin will be oxidised, leading to loss of their protection ability against O_3 harmful effects. However, when these ROS are produced chronically or in an increased amount, they produce tissue damage, (Kodavanti et al., 1995). Moreover, when the ROS are not neutralized by the antioxidant defence system, they cross the alveolar-capillary barrier and reach distant organs (e.g. nervous system) through the blood stream. The central nervous system is one of the most vulnerable systems to the oxidative damage, due to the increase rate of oxygen consumption, high concentrations of iron, high content of polyunsaturated fatty acids, the endogenous production of free radicals, and to the low antioxidant enzyme, (Colín-Barenque et al., 1999).

1.8 The most affected organs by O_3 exposure

The respiratory tract, cutaneous tissue, and exposed ocular tissue are the most biological tissues which are affected by atmospheric O_3 exposure, either directly or indirectly, (Lee et al., 2013). The alveolar capillaries are the most sensitive parts of the lung to acute O_3 exposure, (Aviado and Salem, 1968; Lippmann, 2009), when they exposed to O_3 their wall becomes thick due to formation of edema fluid, (Yang and Omaye, 2009).

1.8.1 The Lungs

Some experimental studies showed that O_3 exposure has harmful effects on the respiratory tract, (Fabbri et al., 1984; Holtzman et al., 1983; Johnston et al., 2005; O'Byrne et al., 1984). Also, it has been reported that O_3 exposure can cause biological harmful effects in human and experimental animals such as: decrease in pulmonary function, respiratory airway inflammation and increase in the airway responsiveness, (Koren et al., 1989). In addition , O_3 has a role in the activation of nuclear factor-κB (NF-κB) in human nasal epithelial cells and animal lungs, (Haddad et al., 1996; Nichols et al., 2001).

There are several mechanisms which have been suggested to explain the adverse effects of air pollutants. The most consistent and the most widely accepted one is the explanation of Arbex et al., (2012). He mentioned that when air pollutants such as particulate matter (PM) of various sizes and gases (O_3 and nitrogen oxides), come in direct contact with the respiratory epithelium in high concentrations, they form oxygen and nitrogen free radicals,

which in turn induce oxidative stress in the airways. In other words, air pollutants cause an increase in the free radicals which are not neutralized by antioxidant defence system leading to an inflammatory response with the release of inflammatory cells and mediators (cytokines, chemokines, and adhesion molecules), then these inflammatory cells and mediators reach the blood circulation, causing subclinical inflammation which has a negative effect on the respiratory system, then it causes further systemic effects, (Arbex et al., 2012).

In addition, several epidemiological studies have shown that exposure to PM and gaseous air pollutants is associated with higher incidence of upper airway symptoms, such as: cough, laryngospasm, rhinorrhea, vocal fold dysfunction, and nasal obstruction, (Shusterman, 2011). Furthermore, it leads to lower airway symptoms, e.g., cough, dyspnea, and wheezing, especially in children, cough and wheezing in adults with and without chronic lung disease, (Kelly and Fussell, 2011).

1.8.2 The Eyes

The ocular irritation is one of the adverse effects of O_3 exposure. It is caused due to the direct exposure of the ocular surface to O_3, (Schmut et al., 1994). An in vivo experimental study in mouse model has shown that O_3 exposure affects the ocular integrity of the ocular surface by altering the mucin-secreting cells and by the production of inflammatory cytokines in tears. On the other hand, an in vitro studies have found that O_3 exposure can lead to an increase in: NF-κB nuclear translocation, κB-dependent transcriptional activity, NF-κB inhibitor α (IκBα) proteolysis, and expression of phosphorylated IκBα (p-IκBα), (Lee et al., 2013).

1.8.3 The Skin

The upper layer of the human skin epidermis acts as a barrier, but is also one of the first targets of air pollutants either from environmental origin or from anthropic origin. The skin problems arise when an abnormal exposure to environmental air pollutant exceeds the skin's normal defensive ability, (Valacchi et al., 2012) .

Air pollutants induce severe change in the normal functions of: lipids, DNA and/or proteins of the human skin, causing oxidative damage, (Adelman et al., 1988; Ames et al., 1995; Gaboriau et al., 1993; Kampa and Castanas, 2008; Karten et al., 1997; Menzel, 1994; Stadtman, 1992), leading to skin aging, inflammatory or allergic conditions such as atopic dermatitis, psoriasis, acne, and skin cancer, (Baudouin et al., 2002; Kohen, 1999). In addition, results from experimental studies in murine skin have shown that O_3 can induce

damage in the epidermis, increases malondialdehyde (MDA) level, and reduces the level of antioxidants such as tocopherol and ascorbic acid, (Schroeder et al., 2006; Thiele et al., 1997; Weber et al., 1999). In addition, these effects can lead to barrier perturbations, production of lipid ozonation products and inflammation, (Schroeder et al., 2006; Valacchi et al., 2012). The first target of the skin layers to O_3 exposure is the stratum corneum, which contains high level of unsaturated fatty acids and lipids, (He et al., 2006; Packer and Valacchi, 2002). Moreover, O_3 exposure can lead to generation of ROS and disturbance of matrix metallo proteinases (MMPs) activity, (Rittié and Fisher, 2002; Schroeder et al., 2006). Furthermore, tropospheric O_3 exposure has been associated with many diseases such as: urticaria, eczema, and dermatitis, (Xu et al., 2011). Also, O_3 exposure has been shown to inhibit wound healing in cutaneous tissues, (Lim et al., 2006; Valacchi et al., 2002).

1.8.4 Nervous system

The nervous system is one of the most susceptible systems to the oxidative damage which is produced due to exposure to air pollutants, (Olanow, 1993). This susceptibility is due to the increase rate of oxygen consumption, high concentrations of iron, high content of polyunsaturated fatty acids, the endogenous production of free radicals, and to moderate antioxidant enzyme activity, (Colín-Barenque et al., 1999; Rivas-Arancibia et al., 2003).

The role of oxidative stress on the nervous system has been addressed by several studies. In some regions of the nervous system, the ROS can induce osmotic stress which cases release of dopamine and simultaneous decrease in its DOPAC and HVA metabolites, result in alteration in the transport or metabolism of this catecholamine, (Rivas-Arancibia et al., 2003). In addition, LaVoie and Hastings, (1999) reported that under certain oxidizing conditions dopamine is predisposed to form chinones which react with cysteine forming residues. Moreover, these residues are able to block the function of some proteins. Furthermore, the oxidative stress which is produced due to air pollutants exposure has a functional role in the pathological process of some neurodegenerative diseases such as amyotrophic lateral sclerosis, Parkinson's, Alzheimer's and Huntington's diseases, (Beckman and Ames, 1998; Olanow, 1993; Simonian and Coyle, 1996; Smith et al., 2000), and in aging process, (Barja and Herrero, 2000; Carney et al., 1994; Fukagawa et al., 2000).

1.8.4.1 Olfactory bulbs (OB)

The olfactory system receptors are exposed directly to air pollutants making them more susceptive to the harmful effect of toxic substances and airborne pollutants causing damage to their neural tissue, (Benignus and Prah, 1982). Furthermore, reviewed articles by Ajmani et al., (2016) from 1950 to 2015 focused on human epidemiologic and pathophysiologic studies with some experimental studies on animals, showed a relationship between environmental air pollutant exposure and olfactory function. Moreover, these studies have explained how air pollutants enter the OB issues. When air pollutants come in direct contact with the olfactory epithelium they translocate to the olfactory bulb, and migrate to the olfactory cortex, **figure (1.1)**. Then, deposited at each site of the OB, causing direct damage and disruption of tissue morphology or inducing local inflammation and harmful cellular stress responses. Moreover, Benignus and Prah (1982) mentioned that air pollutants can cause indirect damage through the circulatory system when the lung antioxidant system component failed to clear the toxic free radicals.

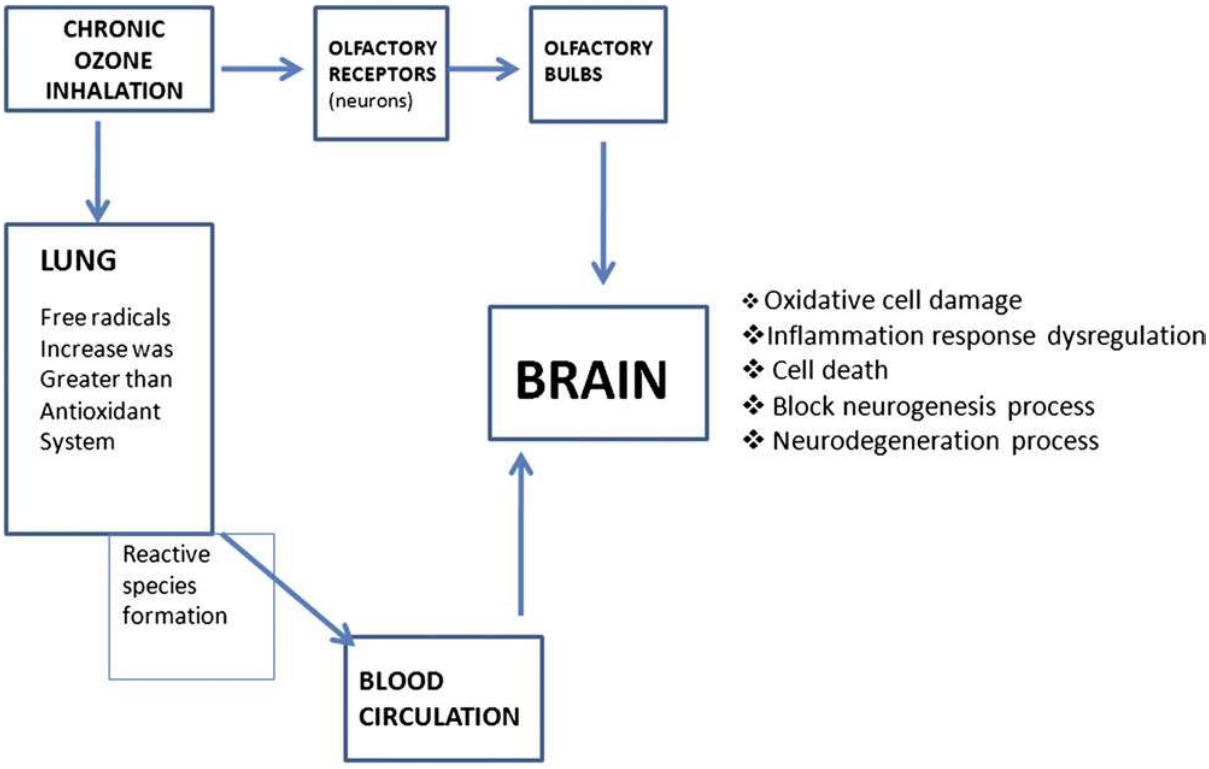

Figure 1. 1: Chronic ozone exposure pathways. The figure shows how chronic ozone inhalation can cause damage in the brain, (Rivas-Arancibia et al., 2010).

1.9 Ozone and the sense of smell

The olfactory sensory neurons can detect different odourous molecules, and transmit the information about these odourous molecules to the OB through their axon for information processing, (Mori et al., 1999). In addition, an electrophysiological study found that the olfactory receptors are sensitive to one or two different odorous categories. Moreover, the different types of odorous molecules evoke different activities in different areas of the olfactory bulb, (Getchell and Shepherd, 1978).

Calderón-Garcidueñas, (2003) reviewed the mechanism by which air pollutant and volatile molecules reach the OB region. As shown in **figure 1.2,** when an air borne pollutants or volatile molecules enter the nasal cavity through the inspired air, they bind to the ciliated epithelium in the mucosa by the action of specialized protein called olfactory-binding-protein (OBP). Then, from the mucus membranes they can be transported through the olfactory nerve to the bulb. However, in some conditions they can reach the olfactory cortex and other regions of the brain.

The effects of oxidative stress on the olfactory bulbs have taken many researchers attention because it is the primary site for coding the odourous information. Therefore, any alteration in its components will lead to alteration in the stimulation process, result in changing of the olfactory and behavioural responses. Moreover, olfactory bulb is the main organ which is involved in memory-mindedness and perception of odours, (Kendrick et al., 1997; Sánchez-Andrade et al., 2005). In addition, in animal models odour perception has an adaptive value for animal's survival. Furthermore, some authors found that the plasticity of the nervous system allows individuals to adapt themselves to any changes in the surrounding environment through memory and learning processes, (Carney et al., 1994; Olanow, 1993).

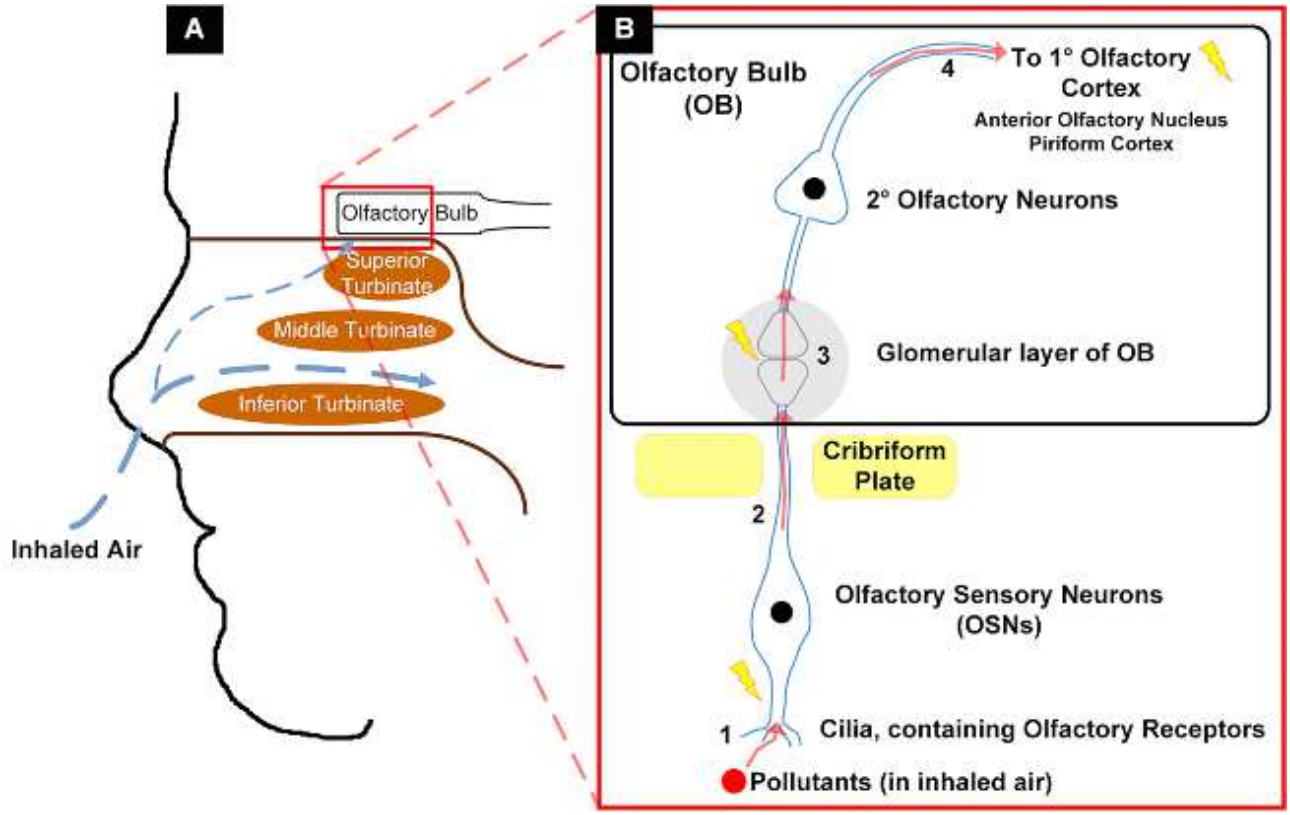

Figure 1. 2: The mechanism of air pollution entry into olfactory tissues. (A): The inspired air reaches the olfactory mucosa after its passages through the nasal cavity. **(B):** the passages of air pollutants in the olfactory tissues, **1:** the olfactory sensory neurons uptake the air pollutant, **2:** the transportation of air pollutant from the olfactory sensory neurons axons through cribriform plate to the olfactory bulb, **3:** the uptake of air pollutant by olfactory secondary neurons, **4:** the transportation of air pollutants from the olfactory secondary neurons to the primary olfactory cortex, (Ajmani et al., 2016).

1.10 Olfactory System

The olfactory system is one of the sense organs which is responsible for information processing, to discriminate between different odours, detection of volatile airborne molecules (aromatic compounds), and chemical compounds which come from the outdoor environment and can profoundly influence animal behavior. Therefore, the olfactory system provides essential information for animal survival. Moreover, in mammalian it regulates a wide range of multiple and integrative functions (Lledo et al., 2005). Furthermore, it composes of olfactory epithelium which has sensory functions and of the main olfactory bulb (OB), the site for information processing (Shipley and Ennis, 1996).

1.10.1 Olfactory bulb structure

The structure of the olfactory bulbs is made up of six layers, olfactory nerve layer, glomerular layer, external plexiform layer, mitral cell layer, internal plexiform layer, and granule cell layer, (Kosaka and Kosaka, 2009), **(figure 1.3** and **figure 1.4).**

The first layer is the olfactory nerve layer (ONL) which contains axonal fibers of the olfactory sensory neurons. This layer is formed by bipolar neurons, towards the inside the neurons crosses the ethmoid bone then join with other neurons and forms the nerve tract. From the outside in the dendritic portion of the neuron, it generates a globular structure called the olfactory vesicle, which is rich in cilia and contains the olfactory receptors. It has been estimated that about 50,000,000 sensory neurones are present in the nasal cavity of mice, (Allison and Warwick, 1949), and approximately 6,000,000 cells found in man, (Moran et al., 1982).

The next layer is the glomerular layer (GL), which tends to form glomerular like structures, which are formed between olfactory nerve layer axonal terminals, apical dendrites of mitral and middle tufted cells, and with the neuronal processes of the three types of interneurons that contributes to the glomerular formation, periglomerular (PG) cells, external tufted (ET) cells and superficial short-axon (SSA), (Kosaka and Kosaka, 2005; Kosaka et al., 1998; Pinching and Powell, 1971). In the external plexiform layer (EPL) located the middle and the deep tufted cells, both form dendro-dendritic synapses with the granule cell layer, (Jackowski et al., 1978; Schneider and Macrides, 1978; Schoenfeld et al., 1985).

The mitral cell layer (MCL) is located below the EPL layer, it is thin contains mitral cells, and fewest number of short-axon cells, (Price and Powell, 1970a; Schneider and Macrides, 1978). According to the shape and number of cells; Mitral cells are classified into two groups: type 1 mitral cells, represent the majority of mitral cells and extend their dendrites to the EPL and are great in number. Whereas, type 2 mitral cells have narrow dendrites and are few in number, (Mori et al., 1983; Orona et al., 1984) . In addition to this type of cell, short axis cells of Hensen (hSAC) and Cajal (cSAC) have been also identified, (Price and Powell, 1970c; Schneider and Macrides, 1978).

The next layer is the internal plexiform layer (IPL), which contains few cell bodies and the axonal fibres of projection neurons, (Price and Powell, 1970a; Schneider and Macrides, 1978).

The last innermost layer is the granule cell layer (GCL), which contains small roundish interneurons without axonal processes (granule cells), (Price and Powell, 1970b, 1970c). The granule cells project their peripheral dendrites in the EPL and contact the secondary dendrites of the output neurons. In addition, the granular cells represent the highest number of neurons among the bulbar neural cell population their number ranges approximately from 1,000,000 to 3,000,000, (Meisami and Safari, 1981).

Granule cells dendrites have appendices called spines or gemmules that in the PLL participate in reciprocal synapses between the granule cells and the mitral or tufted cells, result in formation of both pre and post connections, (Rall et al., 1966).

Also, they can be classified into three sub types, according to the arrangement of their dendrites and location of their cell bodies in the granule cell layer, (Price and Powell, 1970b; Schneider and Macrides, 1978).

Depending on the position of the soma and the extension of the dendritic shaft in the EPL, the granule cells can be divided into three types: median granulocytes (mGCs) or type 1 bodies: these cells are located in the central zone of GCL receiving signal from both mitral and tufted cells. The second type is the deep granular cells (dGCs): which is located deeply in the bulb and their dendrites connect to the mitral cells of the ELP. In addition, the last type is the granular cell (OGC): which are located in the peripheral zones of the GCL and can only create synapses with plump / tufted cells as their dendritic tree is poorly developed, (Price and Powell, 1970a)

Recently, Merkle et al., (2014) have revealed the discovery of four unknown interneurons which were generated in the rat brain ventricular area migrating into the granular layer. Two of them have been classified into 4 and 5 granular cell according to the shape of the soma, presence of the dendritic tree with the spines and the absence of the axon. Moreover, type 4 present predominate in GCL whereas type 5 reaches the deep region of the EPL.

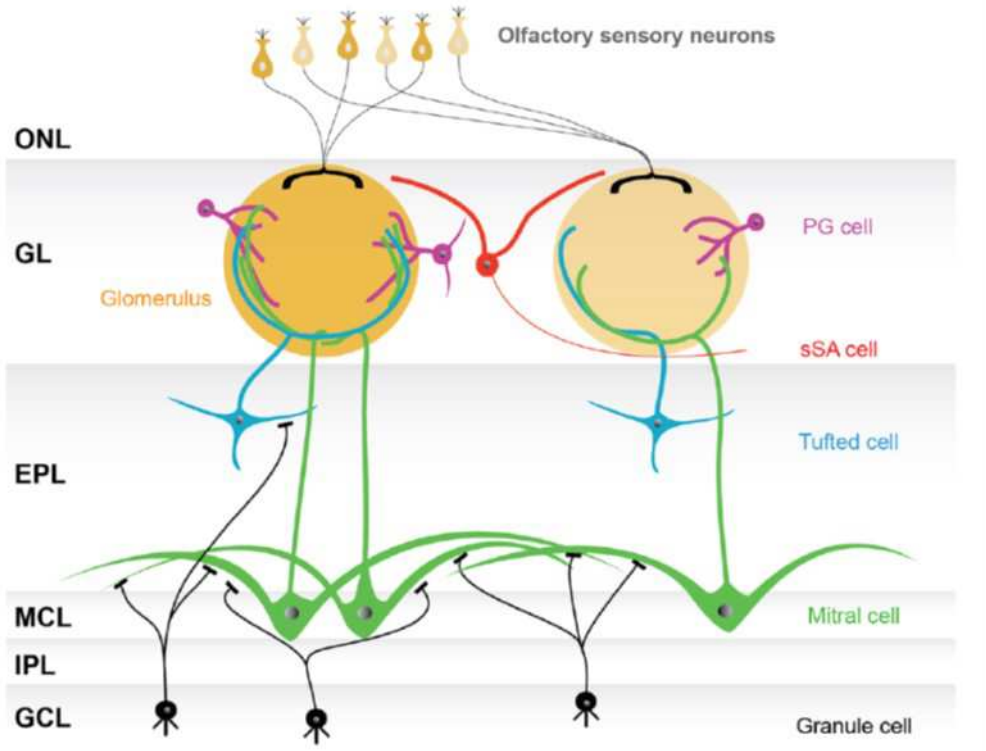

Figure 1. 3: The basic model of the olfactory bulb network.

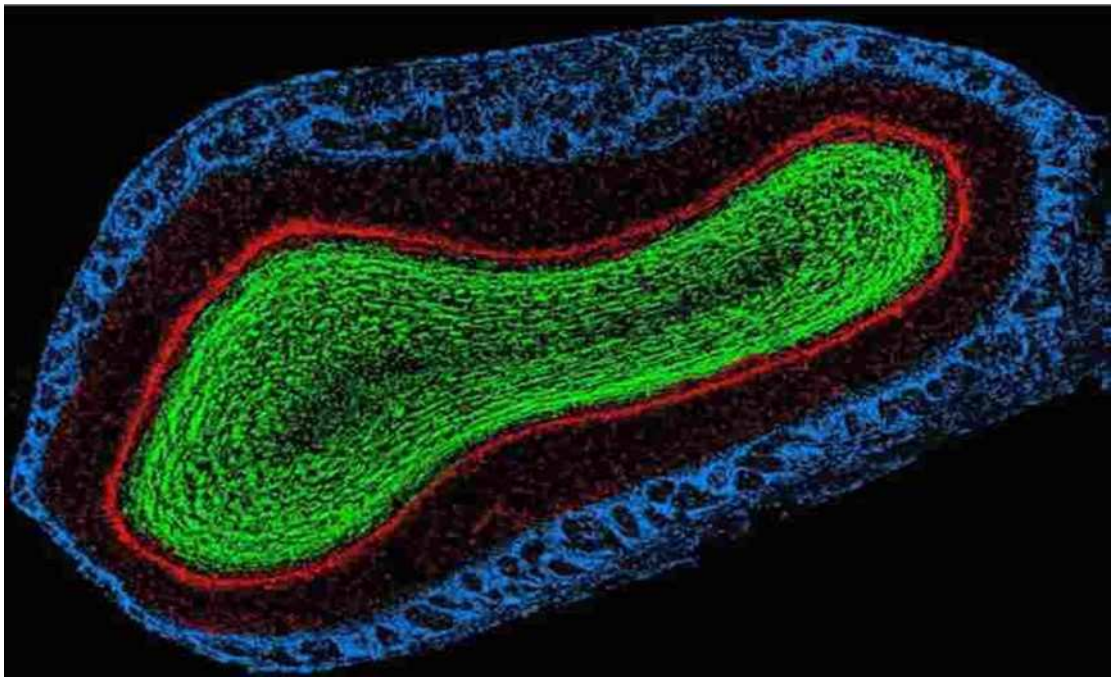

Figure 1. 4: Coronal section of the main olfactory bulb of an adult mouse male. The blue layer is the glomerular layer which contains periglomerular cells (juxtaglomerular cell bodies). The red layer is the Mitral cell layer, and contains cell bodies of mitral cells. The green layer is the granule cell layer and contains cell bodies of immature migrating neuroblasts (at the centre) and mature granule cells (superficially).

1.10.2 Cellular heterogeneity in the glomerulus

The glomerulus is rough globular structure surrounded by neuronal and glial cell bodies. Also, it is the first processing centre of the olfactory information. In addition, it contains dendrites of OSN axons, projection neurons and juxtaglomerular cells, (Kosaka et al., 1998; Pinching and Powell, 1971; Schoenfeld et al., 1985).

Each glomerulus is surrounded by numerous periglomerular cells with small somata (6-8 μm). The PG cell dendrites branch and terminate with one or two glomeruli, then contact with olfactory axons and dendrites of principal cells, (Hálasz and Greer, 1993; Pinching and Powell, 1971). The PG cells are the numerous cell population and are different in their morphological, physiological and neurochemical features, (Kosaka et al., 1997; Puopolo and Belluzzi, 1998; Toida et al., 2000).

The periglomerular cells (PG) with external tufted cells and superficial short-axon cells collectively named as the juxtaglomerular (JG) cells. The dendritic processes of external tufted cells and PG cells extend into the glomerular space, (Kosaka and Kosaka, 2005). Furthermore, each cell type of JG cells can be further classified basing on the morphological, chemical, and functional features, (Kosaka and Kosaka, 2011; Macrides et al., 1985; Nagayama et al., 2004).

The intraglomerular space is classified into two zones according to the synaptic organization. The first zone is the olfactory nerve zone (ON zone) and the second zone is the non-olfactory nerve zone (non-ON zone), (Chao et al., 1997; Kasowski et al., 1999; Kosaka et al., 1997), the PG neurons send their dendritic projections either to the olfactory nerve zone or to the non-olfactory nerve zone. Therefore, type 1 PG cells contact both intraglomerular compartments. Whereas, type 2 PG cells form dendro-dendritic synapses with the bulbar neurons, (Kosaka et al., 1998), (**figure 1.5**).

Moreover, experimental studies on mouse model have shown that PG cells express different chemical markers such as: tyrosine hydroxylase (TH), calbindin (CB) and calretinin (CR) (Kosaka and Kosaka, 2007; Parrish-Aungst et al., 2007). Furthermore, it has been reported that all PG cells synthesize γ-amino butyric acid (GABA) and express at least one of the two glutamic acid decarboxylase (GAD) isoforms, with the exception of a small percentage of CR-positive neurons, (Kosaka and Kosaka, 2007). In addition, several studies have calculated the number of PG cells, their findings have shown that CR-positive cells are the most abundant cell type, while the CB-positive cells are the fewest one, (Kosaka and Kosaka, 2007; Panzanelli et al., 2007; Parrish-Aungst et al., 2007; Whitman

and Greer, 2007). The CR- and the CB- positive cells belong to type 2PG cells. Whereas, TH-positive cells belong to type 1PG cells, (Kosaka and Kosaka, 2007).

The CB-positive neurons are present in neonates only, (Altman, 1962, 1969, Hinds, 1968a, 1968b). Whereas, the production of CR-positive cells increases in the adulthood. However, contrasting results were observed from experimental studies focusing on the age-dependent neurogenesis of TH-positive cells, (Batista-Brito et al., 2008; De Marchis et al., 2007).

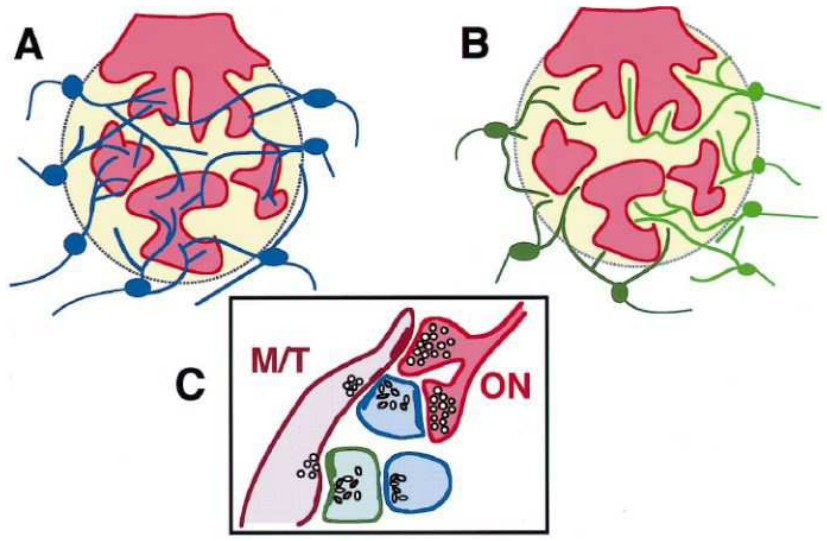

Figure 1. 5: Type 1 and type 2 periglomerular cells. A: Type 1 periglomerular cells sending their dendrites to the ON zone (red) and non-ON zone (yellow). **B:** Type 2 periglomerular cells sending their dendrites to the non-ON zone (yellow). **C:** synaptic connection between type 1 and type 2 PG cells in the glomerular space. Olfactory nerves (ONs, red) terminate into mitral/tufted cells (M/Ts, brown) and type 1 periglomerular cells (blue), but not type 2 periglomerular cells (green). Both type 1 (blue) and type 2 (green) periglomerular cells synapse apical dendrites of M/Ts (brown), (Kosaka et al., 1998).

1.10.3 Dopaminergic PG cells

The olfactory bulb (OB) is the first centre for processing the olfactory information, and is characterised by vigorous life-long activity-dependent plasticity which is responsible for the variety of odour-evoked behavioural responses. Also, it hosts the more numerous group of dopaminergic (DA) neurones in the central nervous system, identified as A16 in the standard classification, (Björklund and Dunnett, 2007). These DA cells are located in the entry of the bulbar circuitry and form direct contact with the olfactory nerve terminals. In addition, they play a key role in odour processing and in the adaptation of the bulbar network to external conditions, (Cave and Baker, 2009).

In the OB, DAergic neurons have been reported to be present only in the most external (glomerular) layer, (Halász et al., 1981), and it is generally accepted that they co-release dopamine (DA) and GABA from separate pools of vesicles, (Borisovska et al., 2013; Maher and Westbrook, 2008). The glomerular layer is populated by a variety of cell types which are described into three major classes of interneurons, i.e. periglomerular (PG), short-axon (SA) and external tufted (ET) cells. Since DA neurones are the only catecholaminergic neurones found in the OB, (Kratskin and Belluzzi, 2003), they are usually recognized by the expression of tyrosine hydroxylase (TH), the rate-limiting enzyme of catecholaminergic pathway. Moreover, it has been estimated that 10 to 16% of the neurons in the most external glomerular layer (GL) of adult animals are DAergic cells, (McLean and Shipley, 1988; Panzanelli et al., 2007) which include the two types of cells PG, (Gall et al., 1987; Kosaka et al., 1985), in addition to subpopulation of ET cells, (Halász, 1990).

From functional point of view, the first demonstration of the involvement of DA neurones in olfaction was proved by the impairment of olfactory discrimination in mice lacking functional dopamine receptors or transporters, (Sullivan and Wilson, 1995; Tillerson et al., 2006) and by the explanation of the well-known observation of Doty (2012). He mentioned that the olfactory impairment is one of the earliest non-motor traits of Parkinson's disease.

In the forebrain, the bulbar dopaminergic cells represent the majority of dopaminergic cells population, (Baker and Farbman, 1993; Cave and Baker, 2009) . These neurons are located in the GL, **(figure 1.3 and 1. 4).** Also, they represent 10-20% of all JG cells, (De Marchis et al., 2007; Kosaka and Kosaka, 2007; Panzanelli et al., 2007; Parrish-Aungst et al., 2007; Whitman and Greer, 2007).

Bulbar DA cells have attracted the attention of may scientific researchers in the last few years, because they are extremely plastic, (Baker et al., 1983; Bastien-Dionne et al., 2010), have a significant role in odour processing due to their position in the entry of the bulbar circuitry, (Borisovska et al., 2013) and are constantly generated throughout life, (Altman, 1969; Baker et al., 2001; Betarbet et al., 1996; Lazarini et al., 2014; Mizrahi et al., 2006; Ventura and Goldman, 2007; Winner et al., 2002).

The difficulty in distinguishing DA PG cells in living preparations was overcome by using transgenic mouse model, which carries the green fluorescent protein (GFP) under the control of the TH promoter (TH-GFP cells), (Matsushita et al., 2002; Sawamoto et al., 2001).

Therefore, the identification of the dopaminergic cells has been carried out by the detection of TH marker, a rate-limiting enzyme in the biosynthetic pathway of dopamine (DA), (Joh et al., 1973; Nagatsu et al., 1964). All of the TH-positive neurons are considered as dopaminergic cells in the absence of the other cells that produce other catecolamines in the OB, (**figure 1.5)**, (Baker et al., 1983; Joh et al., 1973; Nagatsu et al., 1964).

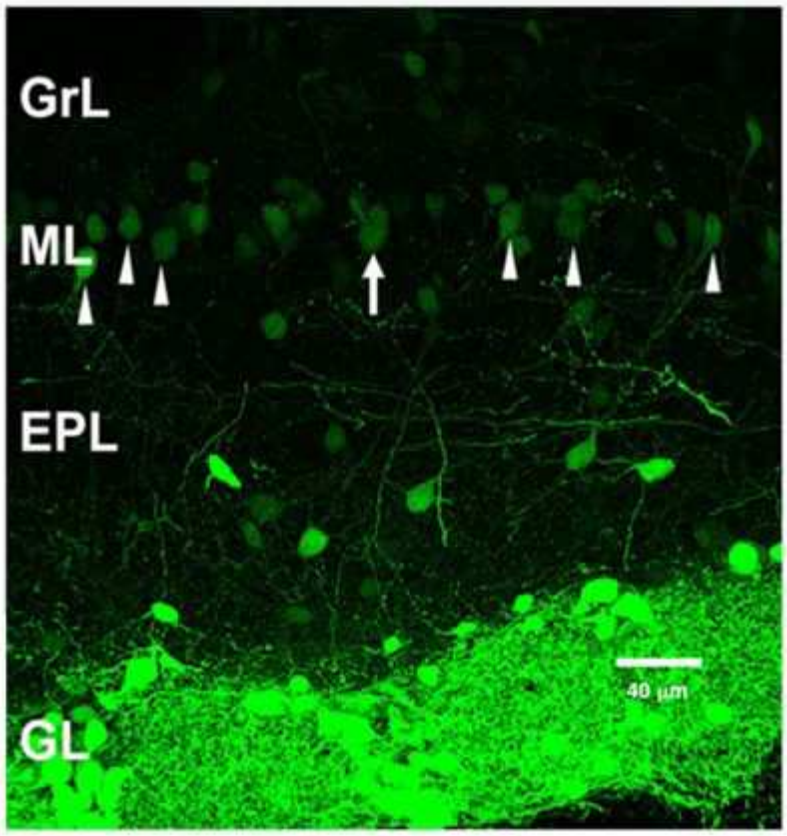

Figure 1. 6: The dopaminergic periglomerular cells. The figure shows coronal section of mouse OB shows dopaminergic cells expressing the GFP. Arrows show faint dopaminergic cells in the mitral cell layer in the mouse olfactory bulb.

According to their location and size, dopaminergic cells in the GL can be further subclassified into two different populations, (Baker et al., 1983; Kosaka and Kosaka, 2008; Pignatelli et al., 2005), the first one contains small PG cells (5 to 10 µm in diameter) and the other one includes larger neurons (10-15 µm in diameter), (Cave and Baker, 2009; Nagayama et al., 2004) . In addition, dopaminergic PG interneurons can be stimulated by the electrical activity which comes from the olfactory epithelium, (Aroniadou-Anderjaska et al., 1997; Ennis et al., 1996, 2001). Also, they influence the activity of glomerular components because they release dopamine and γ-amino butyric acid, (Berkowicz and Trombley, 2000; Ennis et al., 1996; Hsia et al., 1999).

1.10.4 What is known about the dopaminergic cells in olfactory bulb

The DA PG cells like other CNS neurons are able to generate rhythmic action potentials (pacemaker activity) in the absence of synaptic inputs , (Feigenspan et al., 1998; Grace and Onn, 1989; Hainsworth et al., 1991; Neuhoff et al., 2002, 2002; Yung et al., 1991). In addition, after blocking the glutamatergic and GABAergic synaptic transmission, the spontaneous activity of these neurons persists, suggesting that this ability is an intrinsic property of the cell membrane independent from the external synaptic inputs. Furthermore, this evidence is supported by an experiment conducted on dissociated TH-GFP cells. The result of this experiment showed that the frequency of spikes measured from dissociated cells was double compared with that measured from slices and this finding could be due to the inhibition of the intercellular contact between these neurons, (Pignatelli et al., 2005), (**figure 1.7).**

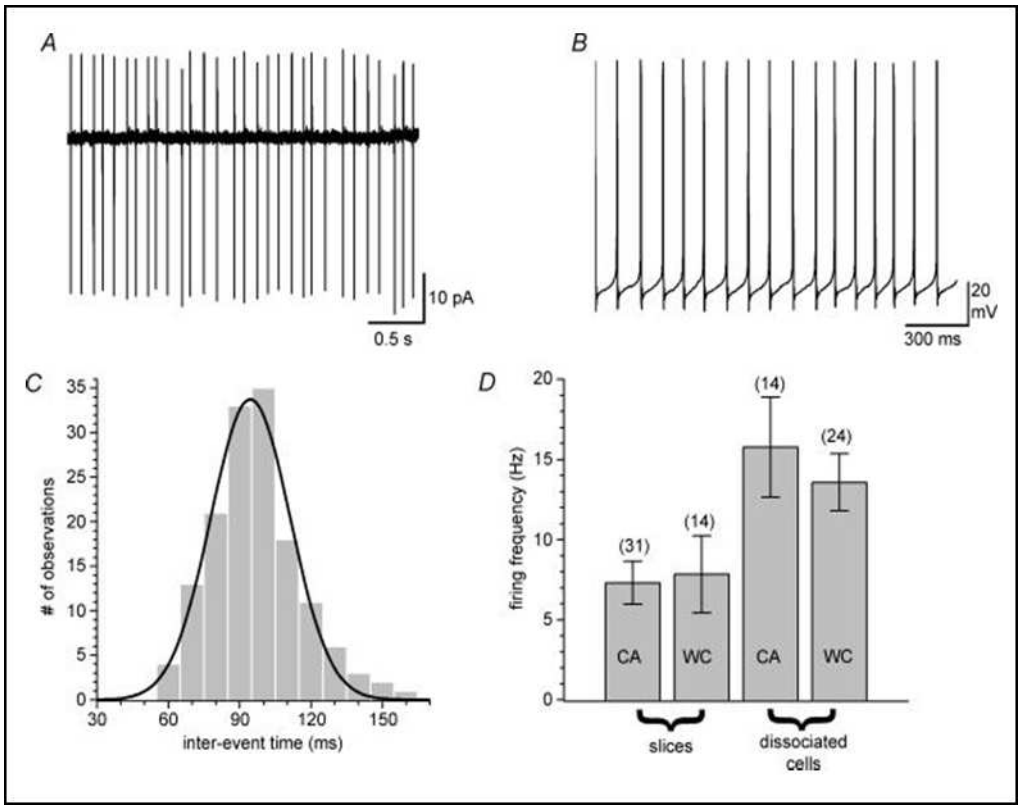

Figure 1. 7: The spontaneous firing activity of the TH-GFP+ cells. (A): Example of the current recorded in voltage-clamp cell-configuration. **(B):** Action potentials in the whole-cell and current-clamp configurations. **(C):** Frequency distribution of the cell shown in B. **(D):** The frequency of spontaneous firing activity in TH-GFP+ cells under different experimental conditions (CA, cell attached, WC, whole cell), (Pignatelli et al., 2005).

The first description of the dopaminergic PG cells has been provided by Pignatelli et al., (2005), by using an electrophysiological technique on transgenic mouse model which carries the green fluorescent protein (GFP) gene under the control of the TH promoter (TH-GFP cells), (Matsushita et al., 2002; Sawamoto et al., 2001). These cells are characterise by spontaneous activity, which was observed in the absence of synaptic inputs, (Feigenspan et al., 1998; Grace and Onn, 1989; Hainsworth et al., 1991; Neuhoff et al., 2002; Yung et al., 1991). This spontaneous activity is on the range of the theta frequency (4–12 Hz). The DA cell pacemaking machinery is composed of two small inward currents, a persistent sodium current (INa(P), 0.41 nS) and the T-type Ca^{2+} current (ICa(T), 0.35 nS), (Pignatelli et al., 2005).

The spontaneous activity of these cells can be blocked by TTX, which blocks fast voltage-activated Na-channels, by riluzole, a drug used in the therapy of amyotrophic lateral sclerosis, (Urbani and Belluzzi, 2000) which blocks the persistent sodium channel, and by blockers of the T-type Ca-channels.

Moreover, there are five different depolarization-activated conductances that were identified in mouse OB DA cells. The two currents which have the largest amplitude are the fast transient sodium current and the delayed rectifier potassium current. On the other hand, the smaller currents are the persistent sodium current and the two types of calcium conductances (L-type and T-type). Also, these currents have been kinetically characterized in order to understand the mechanism of the spontaneous firing and it has been found that only the persistent sodium currents and T-type calcium currents are necessary to sustain the auto- rhythmicity, (Pignatelli et al., 2005).

Recently, some studies have revealed other currents which are generated from these DA cells. Pignatelli et al., (2013) identified two hyperpolarization-activated currents in the DA cells of the mouse OB as well: a Ih hyperpolarization-activated current and Borin et al., (2014) detected the fast activating inward rectifier potassium current (Kir).

2. MATERIALS AND METHOD

2.1 Ethical statement

Care and use of animals was conducted according to guidelines established by European Council Directives (609/1986 and 63/2010) and Italian laws (DL 116/92 and D. Lgsl. 26/2014) for the protection of animals used for scientific purposes. The experimental protocols were approved by the Committee for Animal Welfare of the University of Ferrara (OBA), by the Directorate-General for Animal Health of the Ministry of Health, and supervised by the Campus Veterinarian of Ferrara University.

2.2 Mice stains

2.2.1 C57BL/6j strain

The C57BL/6 mouse is the most well-known inbred mouse strain, it has been widely used as a genetic background for congenic and mutant mice, its genome was fully sequenced in 2005 and has been used as a perfect research model for physiological and pathological in vivo experiments. (Johnson, 2016). There are different-substrains of C57BL/6 which differ in their phenotype. These include: C57BL/6J, C57BL/6JJmsSlc, C57BL/6JJcl, C57BL/6NJcl, C57BL/6CrSlc, C57BL/6NCrlCrlj, and C57BL/6NTac, (Mekada et al., 2009).

Experiments on dopaminergic neurons were performed using the transgenic strain "TH-GFP/21-31", which carries the eGFP transgene under the control of the TH promoter. The transgene of the transgenic mice C57 is build up from a construct containing the 9.0 kb 5′-flanking region of the rat tyrosine hydroxylase (TH) gene, the second intron of the rabbit β-globin gene, cDNA encoding GFP, and polyadenylation signals of the rabbit β-globin and simian virus 40 early genes, (Matsushita et al., 2002; Pignatelli et al., 2009; Sawamoto et al., 2001).

2.2.1.1 Identification of C57BL/6j GFP-positive mice

The identification of heterozygous mice expressing the GFP gene is carried out by directing a light source (FBL / Basic-B & N-01 lamp, FHS / LS1B lamp, with blue light filter (460 - 493nm), towards the frontal bone of a new born mouse, in complete darkness. Then, if the mouse carries the GFP protein, a green radiation will be emitted in the spectrum of 500-515 nm from the olfactory bulb region due to the excitation of the GFP protein by the beam. Furthermore, it is advisable to check the newly born mice (P1-P3) for

the expression of the GFP protein up to four days after birth, because after this time the identification becomes very difficult due to the thickening of the frontal bone, **(Figure 2.1).**

(A) **(B)** **(C)**

Figure 2. 1: The identification of transgenic mice. (A): the blue light source, **(B):** the emission filter, used to detect the GFP emission. **(C):** A P3 mouse showing GFP-positive OB (white arrow).

2.2.1.2 Green fluorescent protein (GFP)

The green fluorescent protein (GFP) was discovered firstly by Morin and Hastings (1971), then it was isolated from the jellyfish *Aequorea victoria* in 1962 by Group of scientists including: Roger Y. Tsien, Osamu Shimomura, and Martin Chalfie (Yang et al., 1996). It contains 238 amino acids (Prasher et al., 1992). Also, it has unique crystal structure, consisting of eleven barrelled strands of β- sheet, threaded by an α-helix. In addition, its chromophore is located in the α-helix, particularly close to the centre of the cylinder. (Yang et al., 1996). Furthermore, this protein has an excitation spectrum ranged from 400 to 470 nm, and an emission spectrum between 505 to 540 nm, (Tsien, 1998). Moreover, it exhibits bright green fluorescence when excited by a blue light, (Yang et al., 1996), (**Figure 2.2).**

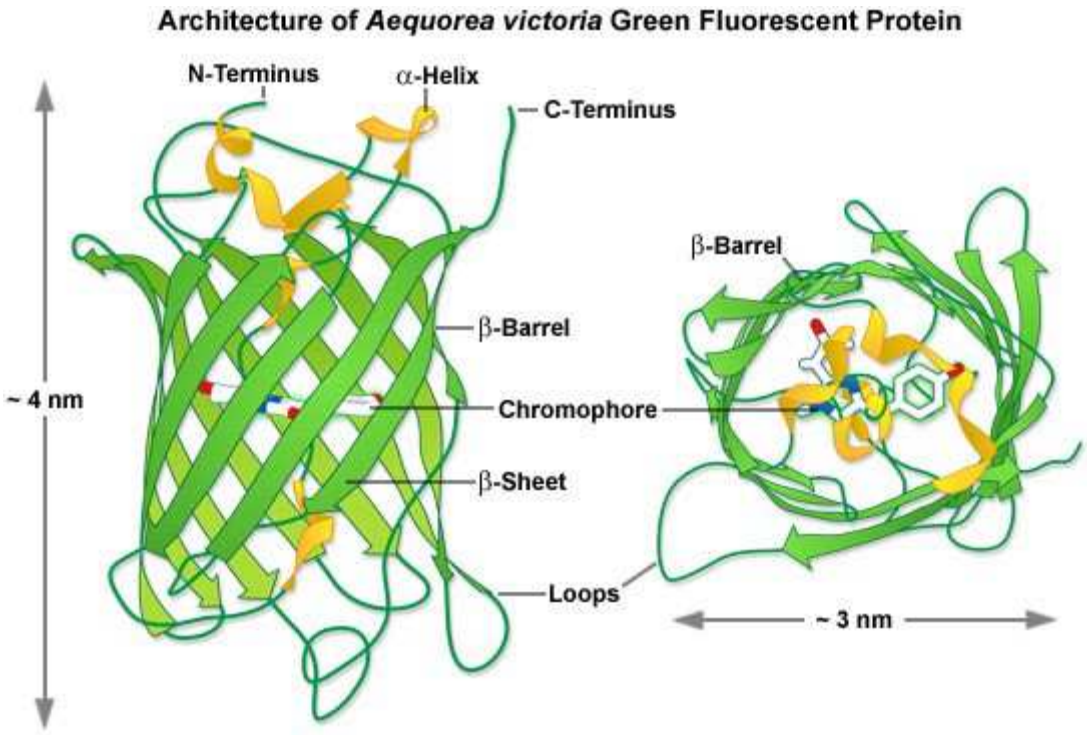

Figure 2. 2: The structure of Green fluorescent protein.

2.2.2 Swiss Webster

This strain appeared firstly in the United State and was originated from two males and seven females, which were obtained for the Rockefeller Institute in 1926 by Clara Lynch from Andre de Coulon in Lausanne, Switzerland. This stock resulted from the selective inbreeding by Dr. Leslie Webster using foundation animals from a large colony. Highly inbred at the time they were acquired by Carworth, then reduced to a single pair, and progeny outbred from that point forward formed a new stock. The descendants were widely distributed to many investigators and dealers. The outbred and the inbred stocks have been used for biomedical researches due to their high rate of productivity, sensitivity to certain infectious agents and their good health, (Lynch, 1969).

2.3 Electrophysiological parameters

Five electrophysiological parameters were analysed to understand the effect of ozone exposure on mice OB, these parameters included: the capacity (pF), the membrane resistance (Ω), the frequency of discharge (Hz), the rheobase (pA) and the chronaxie (ms).

-The first parameter was the membrane capacity that comes from the fact that the membrane acts as a capacitor, with two electrical conductors, i.e. inside and outside solutions, separated by a dielectric, the lipid bilayer.

Since the membrane capacity is proportional to the cell surface area, it is used as an indicator of the cell size, (Golowasch et al., 2009). In addition, the capacity and the resistance together determine how quickly the membrane potential changes in the response to an ionic current.

The second parameter was the membrane resistance, which indicates how easily the charges can cross the lipid bilayer through the ion channels, and therefore depends on the number, permeability and state of different ion channels.

The third parameter was the discharge frequency, which is defined as the number of action potentials per second, and is measured in Hertz. The excitability of nervous tissue is indicated as the ratio between the amplitude of a stimulus and its duration, and can be represented by the force-duration curve, (**Figure 2.3)**.

The fourth parameter was the rheobase, and it is the minimal intensity of a current pulse of infinite duration (pA) capable to excite the cell evoking an action potential. Although, this current is defined as of unlimited duration, conventionally, for practical purposes, it has a duration of 200 ms. (Ashley et al., 2005).

The protocol was applied by administering series of 200 ms current pulses of increasing amplitude until an action potential could be evoked.

The last parameter was the chronaxie, which represents the minimum time required for a constant electric current of twice the threshold voltage to excite a tissue, (Golowasch et al., 2009).

In our experiments, currents amplitude equal twice the rheobase with incremental duration have been given until an action potential was evoked.

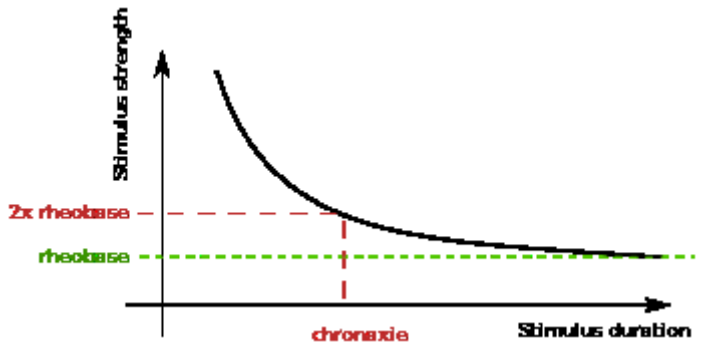

Figure 2. 3: The force-duration curve.

2.4 Ozone and air exposure conditions

Animals were kept in a small cage 32 cm length, 13 cm width and 14 height, then were placed in a closed chamber with a diffuser connected to a variable-flux ozone generator. Ozone was produced from high-voltage current circulated in a tube, this tube contains aluminum chips and two electrodes that allows the conversion of oxygen into ozone. The O_3 concentration in chamber was adjusted according to the selected protocol and was continuously monitored by the O_3 sensor.

2.4.1 Ozone exposure protocols

Different exposure protocols were used for the biochemical, electrophysiological and behavioural experiments.

The time interval between each two ozone exposures in each single day was 3 hours of air exposure, and 24 hours of air exposure between the last exposure in each day and the first exposure on the following day, in case of repeated exposure protocols for more than one day.

The exposure protocols are shown on the tables below for each experimental condition:

Table 2. 1: Biochemical experiment exposure protocols - Swiss Webster

Protocol number	Dose(ppm)	Time(min)/single exposure	Number of exposures/day	Exposure days
1	0.8	180	2	1
2	0.8	180	1	2
3*	0.4	120	2 in the 1st day+ 1in the2ed day	2
4	0.4	120	2	1
5	0.3	120	2	1
6	0.2	120	2	1
7	0.1	120	2	1
8	0.2	120	2	2
9	0.5	30	1	1
10	0.5	60	1	1

For protocol 3* mice were exposed for 2 times in the first day followed by single exposure on the second day.

Table 2. 2 :Biochemical experiment exposure protocol - C57BL/6J mice

Protocol number	Dose(ppm)	Time(min)/single exposure	Number of exposures/day	Number of exposure days
1	0.8	120	2	5
2	0.5	30	1	1
3	0.5	60	1	1

Table 2. 3: Electrophysiological exposure protocol

Protocol number	Dose(ppm)	Time(min)/single exposure	Number of exposure(s)/day	Number of exposure days
1	0.5	30	1	1
2*	0.5	30	2	2
			1	1
3*	0.8	120	2	4
			1	1
4*	0.8	120	2	4
			1	1

For protocol 3, mice were exposed two times for the first two days followed by single exposure on the third day, while for protocol 3* and 4* mice were exposed two times for the first four days followed by single exposure on the fifth day.

Table 2. 4: Behavioural experiment exposure protocols

Protocol number	Dose(ppm)	Time(min)/single exposure	Number of exposure(s)/day	Number of exposure days
1	0.8	120	1	1

2.5 Biochemical experiments

2.5.1 Samples preparation

Approximately 1ml of blood was collected during mice sacrificing in 1.5ml Eppendorf tube containing 100 µl Na^+ citrate, centrifuged at 2500g at 4 C° for 15 min. Then the plasma was collected in new Eppendorf tube and stored at -20 C° In addition, olfactory bulbs were collected and stored at -80 C° or freezed directly in liquid nitrogen at -190 C° for homogenization. Then 150 µl of lysis buffer was added to the homogenized olfactory bulb samples, centrifuged at 3500g at 4 C° for 15 min. Moreover, the supernatant liquid was collected in new Eppendorf tube and stored at -20 C°.

The following chemicals were used during sample preparation:

-1M Na^+ citrate (5ml): Na^+ citrate 1.47g, D.W 5ml

-The Lysis Buffer composes of: RIPA buffer PH 7.5 885µl, Orto vanadato 5µl, beta glycerol phosphate 10µl, proteinase inhibitor 100 µl.

-1M NaOH (5ml): 5M NaOH 1ml**,** D.W 4ml**.**

2.5.2 Bradford protein assay

This technique is used to determine protein concentration in biological samples. It was developed by Bradford. Moreover, it is very simple technique, fast and more sensitive than Lowry method, (Bradford, 1976).

In this work, the Bradford protein assay was used to measure the protein concentrations in plasma and homogenised olfactory bulb samples. The appropriate sample dilution was determined for each sample after testing several dilutions, starting from 1:5, by taking 2 µl from each diluted sample. Then 5µl from each diluted sample was placed in a single well on microtiter plate and close to it in another well 5µl of 4 µg protein standard (BSA). After that, 200µl of 1X Coomassie Brilliant Blue was added to the diluted sample and protein standard wells. Then the intensity of the reaction colour was correspondent to the amount of proteins in each sample. Moreover, if the intensity of the reaction colour in the diluted samples (olfactory bulb or plasma) was more intense than the standard reaction colour, the samples (OB and plasma samples) were further diluted until reaching reaction colour less intense than the standard protein reaction colour. As a result of that the 47 OB samples were diluted either 1:6 in a final volume of 60ul (2 µl of the homogenized

olfactory bulb sample were added to 58µl of D.W) or 1:12 in a final volume of 600 µl (2 µl of the smashed olfactory bulb sample were added to 598µl of D.W). On the other hand, the 39 plasma samples were diluted either1:70 in final volume of 700µl (2 µl of plasma sample were added to 698 µl of D.W) or 1:50 in a final volume of 500µl (2 µl of plasma sample were added to 498 µl of D.W). In addition, 15µl from each diluted sample (OB and plasma) were divided into 3 wells of microtiter plate, 5 µl in each single well. Furthermore, 5µl from each protein standard in a concentration of (0, 0.4, 0.6, 0.8, 1, 1.2,2, and 4 µg) was placed in a single well, followed by the addition of 200 µl 1X Coomassie Brilliant Blue to each well containing either BSA sample or the diluted samples (OB and plasma). Following that step, the microtiter plate was incubated for 15min at room temperature in the laboratory shaker, at 90 RPM speed. Moreover, by using the spectrophotometer the absorbance of the known standard protein samples concentration and of the olfactory bulb and plasma samples (unknown protein concentration) was read at 595 nm. Then, the standard curve was created by plotting the absorbance of BSA values (y-axis) versus their concentration in µg/ml (x-axis).

For knowing the concentration of unknown total proteins in each sample (OB and plasma) using the created standard curve of BSA, the following steps were followed: first the mean of each three absorbance values of each single sample was calculated, after that from the curve formula the diluted concentration values were obtained then were multiplied by the appropriated dilution factor for each single sample (OB and plasma).

-in the Bradford protein assay the 1X Coomassie brilliant blue (0.2ml) was prepared by mixing 0.04ml of 5% Coomassie brilliant blue 0.04 ml with 0.16ml of D.W

Table 2. 5: Preparation of BSA standards from 2mg/ml BSA stock

Standard number	BSA concentration (µg)	D.W volume (µl)	Volume of BSA(2mg/ml)
1	0	100	0
2	0.4	96	4
3	0.6	94	6
4	0.8	92	8
5	1	90	10
6	1.2	88	12

7	2	80	20
8	4	60	40

2.5.3 Western blot (WB) technique

Western blot is a commonly used technique in molecular and cell biology fields. Its aim is to identify particular protein from a mixture of proteins. In addition, this technique involves three steps: the first one is the separation of proteins by their size, the second one is the transformation of the separated proteins to a solid supporter and the last step is the marking of the target protein by specific primary and secondary antibodies for visualization, (Mahmood and Yang, 2012).

Before performing this technique, a specific amount of proteins (30µg) was calculated from the concentrations that were obtained from the Bradford assay in order to know the amount of proteins that must be taken from each sample.

The first step for carrying out this technique is the preparation of sample lysate. Which contained 4 µl of 1x SDS sample buffer, 2µl of LDTT, the calculated amount of proteins for each sample and D.W (to complete the final volume to 20µl), all of the components were mixed in 0.2 ml Eppendorf tube. Then mixture was centrifuged at 2.5 RPM for 5 min and placed in the thermocycler, heated at 70 C° for10 min, then stored at -80 C° for the electrophoresis step.

The second step was the preparation of polyacrylamide gel electrophoresis. It consists of two parts: the first part is the (10%) resolving gel, which contains: H_2O 2ml**,** 30% Acrylamide mix 1.7ml**,** 1.5M Tris (PH 8.8) 1.3ml**,** 10% SDS 0.05ml**,** 10%APS 0.05ml and TEMED 0.02ml. In addition, the second part is the stacking gel which consist of: H_2O 1.4ml, 30% Acrylamide 0.33 ml, 1.5M Tris (PH 6.8) 0.25ml, 10% SDS 0.02ml, 10%APS 0.02ml and TEMED 0.002ml.

The components of polyacrylamide gel electrophoresis were prepared as follow:

-1.5 M Tris-HCL, pH8.8: Tris base 27.23 g, Deionized water 80 ml**.** Then the pH was adjusted to 8.8 with 6N HCL, then deionized water was added up to 150 ml.

-1M Tris-HCL: Tris base (Giotto biotech) 24.448 g, deionized water 60 ml. Then the pH was adjusted to 6.8 with HCL, then deionized water was added up to 150ml.

-10%APS (Ammonium persulfate): APS 10g and D.W 100ml.

-10% SDS (Bio Rad Laboratories): SDS 10g and D.W 100ml.

-30%Acrylamide (10ml): 40%Acrylamide 7.5ml and DW 2.5ml.

Following polyacrylamide gel electrophoresis preparation, the protein electrophoresis was performed using the Mini-PROTEAN® Tetra Cell apparatus (Bio Rad). Gels were rinsed in1x running buffer using Pasteur pipette. Then the combs were removed, after that they were fixed in the casting stand, placed in the mini tank containing 1x running buffer. Furthermore, 20µl from each sample and 5µl from the protein marker mix were loaded into the gel and the electrophoresis machine was turned on, the voltage was adjusted to 140 mV for 1h and 40 min approximately.

After the electrophoresis has finished, the gels were transferred into nitrocellulose paper. In addition, the filter papers and the sponges were soaked in 1x transfer buffer, also the nitrocellulose membrane were soaked in D.W first then in the 1x transfer buffer. Sequentially the sandwich for the transfer was prepared as follow: for each single gel, first the spongy was placed on the transfer cassette over it the wetted filter paper, the gel, wetted nitrocellulose membrane, wetted filter paper and finally wetted spongy. After that air bubbles that lied between any of these layers were removed. Then the wet transfer system was applied according to the Bio Rad instructions.

Moreover, after the transfer has finished the nitrocellulose membranes were stained with commercial Ponceau red solution (0.1 % (w/v) in 5% (v/v) acetic acid) for 30 seconds to visualize the protein bands. Then the stained nitrocellulose membranes were washed by D.W to remove excess Ponceau red stain, scanned by a scanner. Furthermore, the nitrocellulose membranes were placed in plastic boxes for blocking by 5% non-fatty dry milk in 1x PBS-T for 1h. Following the blocking step, membranes were incubated with the specific primary antibody (4HNE 1:1000, for bulbs and plasma samples and CYPA1A11: 1000 for bulbs samples only), overnight at 4 C°. On the following day, membranes were placed in the laboratory agitator at room temperature at a speed of 90 RPM, washed three times with 1x PBS-T for 10 minutes each. Then were incubated with the suitable HRP-conjugated secondary antibodies which were anti-goat (1:5000) for 4HNE antibody (for

OB and plasma samples), and anti- rabbit (1:10000) for Cyp1A1 antibody, (for OB samples only). Moreover, the membranes were washed three times with 1x PBS-T for 10 min each, and with PBS 1x for 15 min. After the washing steps, membranes were incubated in the dark room with Western Lightning® Chemiluminescence Reagent Plus system substrate, by mixing equal volumes of enhanced luminol reagent (1ml) and the oxidizing reagent (1ml) for approximately 5 min. Then the membranes were placed in black box covered with plastic paper and exposed to autoradiography film X-ray in the dark room. In addition, the developed films were lined up in the correct orientation and the molecular weight (MW) ladder bands were marked into the film. Then the developed films were scanned for the quantitative analysis.

All olfactory bulbs membranes were then washed with PBS-T three times 10 min each, then with PBS for 15 min, in the laboratory agitator at room temperature at a speed of 90 RPM. After that membranes were incubated with B-Actin antibody (dilution 1:50000) for 1 h, washed with PBS-T three times 10 min each, then with PBS for 15 min, after that membranes were incubated in the dark room with Western Lightning® Chemiluminescence Reagent Plus system substrate as described above.

- Preparation of Western blot reagents and Antibodies:

- Ponceau S staining solution: 0.1% (w/v) in Ponceau S stain in 5%(v/v) acetic acid: Ponceau S1g, acetic acid 50 ml and D.W up to 1 L.

-1X Running Buffer: Tris Base 3g, Glycine (BDH laboratory) 14.3g, SDS 1g and D.w up to 1000ml.

-1%Transfer Buffer: Tris Base 3g**,** Glycine 14.3g**,** Methanol 200ml and D.w up to 1000ml

5% Milk solution: Milk 5g and 1x PBS-T 100ml.

-10% PBS: H Cl .200g**,** KH_2PO_4 2g**,** NaCl 80g**,** Na_2HPO_4 anidro 11.5g

-1%PBS: 10% PBS 100ml and D.W 900ml.

-1%PBS-T: 10% PBS 100ml**,** D.W 900ml and Tween 1ml.

-1%SB (sample buffer): 5%SB 1ml and 2-mercaptoetanolo 0.05ml.

-4HNE antibody (Biorad-1:1000 / 6ml): PBS-T 5.4ml**,** 5%milk 0.6 ml and 4HNE 0.006 ml

-CYP1A1 antibody (Thermo fisher -1:1000- 6 ml): PBS-T 5.4ml**,** 5%milk 0.6 ml and CYP1A1 0.006 ml.

-B-actin antibody (Biorad laboratory-1:50000-10ml): PBS-T 9ml**,** 0.5%milk 1ml and B-actin antibody 0.002ml**.**

-Anti-Goat antibody (Biorad- 1:5000- 10ml): PBS-T 9ml**,** 0.5%milk 1ml and Anti-Goat antibody 0.002ml.

-Anti-Rabbit antibody (Biorad-1:10000-10ml): PBS-T 9ml**,** 0.5%milk 1ml and Anti-Rabbit antibody 0.001ml.

2.6 Electrophysiological experiments

2.6.1 Slice preparation

Mice were beheaded by laboratory guillotine, then the brain was extracted by microsurgical procedure and immediately submerged in refrigerated high sucrose extracellular solution bubbled with carboxy mixture (95% O_2, 5% CO_2).

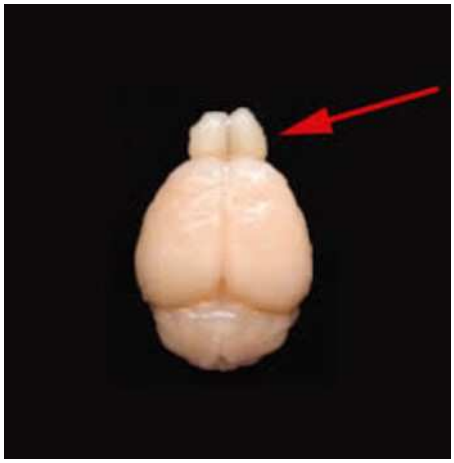

Figure 2. 4: Mouse brain. The red arrow indicates the olfactory bulbs.

Olfactory bulbs **figure 2.4**, were isolated and placed into a small petri dish filled with low temperature gelling agar (Sigma-Aldrich), then were kept in the freezer for a few seconds for solidification. After that, the olfactory bulbs were cut in cube shape supported by the

gel and were attached to the slicing chamber of vibroslicer using 3MTM VetbondTM Tissue Adhesive.

The slicing chamber was filled with refrigerated high sucrose extracellular solution. Then by using a vibrating microslicer (Campden Instruments Ltd), the olfactory bulbs were cut into several slices (150 µm thickness) in the coronal plane. Moreover, these slices were maintained in appropriate holding chamber inserted in a beaker filled with high sucrose extracellular solution continually bubbled with a mixture of carboxygen gas (95% O_2, 5% CO_2). Furthermore, for the electrophysiological recordings, the slice was placed in a recording chamber, fixed by a home-made grid of parallel nylon threads, (**Figure 2.5).**

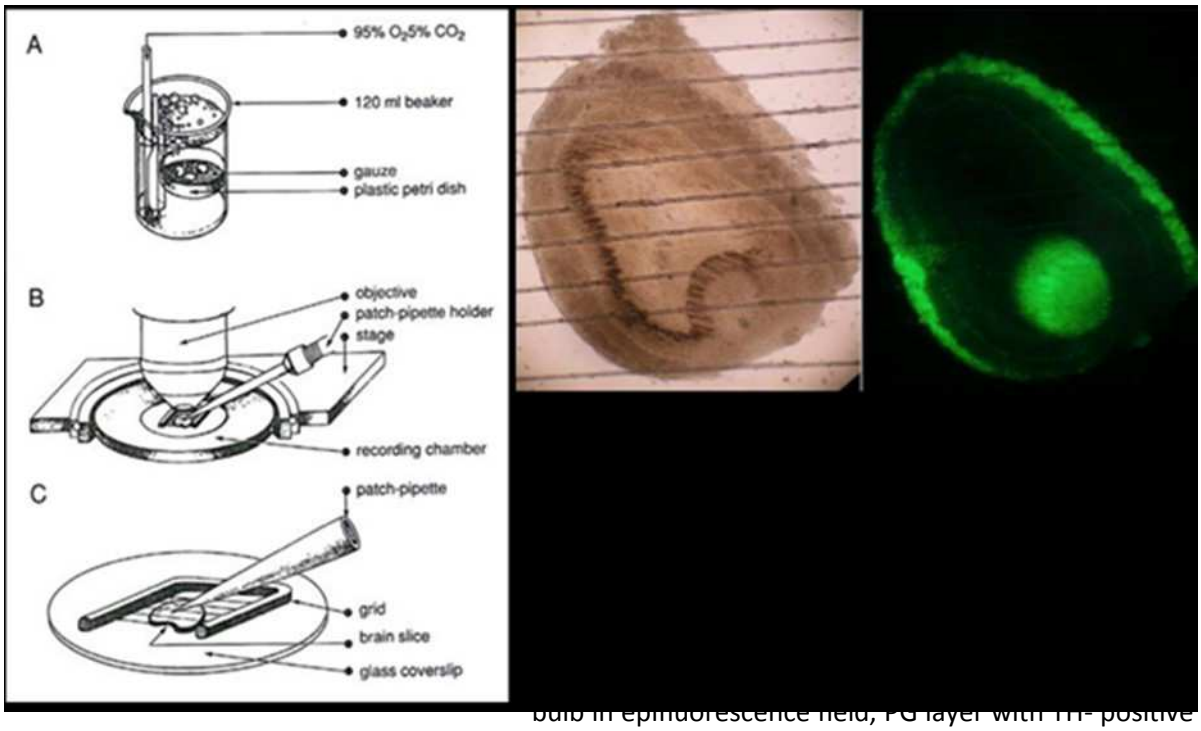

bulb in epifluorescence field, PG layer with TH- positive cells are seen at the border of the slice (green).

2.6.2 Patch clamp technique

This technique was introduced by Neher and Sakmann, (1976), it allows the measurement of ionic flows that pass through the cellular membrane channel, (either from a single-channel, small piece of cells or whole-cell) .

Depending on the researcher`s interest, different configurations can be used. Therefore, in this project two configurations were selected to study the effect of ozone exposure on the OB DA cells. The first one was the voltage-clamp configuration. In this configuration, a current was injected into a cell to record the variations in the cell membrane potential.

Whereas, the second one was the voltage clamp configuration, which allows the control of the membrane potential by recording currents that flow through the cell membrane.

The first step in this technique is touching the target cell with a large pipette followed by the application of gentle negative pressure to form a tight seal with high resistance (GΩ range). As a result, the small membrane patch will attach to the inside of the pipette tip and becomes electrically isolated, (Hamill et al., 1981). Then by application of negative voltage pulse or pressure the patch will rupture, result in the recording of ionic currents from the whole cell membrane. In addition, the cytosol was replaced by the intracellular pipette solution for washing out of the intracellular molecules such as cAMP, these conditions are for the whole-cell configuration.

In both configurations (current clamp and voltage clamp) the electrode was always connected to an amplifier that records the currents and the potential difference between the cell and the extracellular environment.

2.6.3 Preparation of electrodes

All of the micropipettes were produced in our laboratory by using capillaries made from borosilicate hard glass. The preparation of each micropipette started firstly by cutting the glass capillary tube (1.5 mm outer diameter) into pieces of 10 cm in length. Then it was flamed at the two ends. The second step was the insertion of the glass piece inside the Sutter puller (P-97), which heats the capillary glass at the centre and at the same time pulls the two ends in opposite directions. After a few seconds, the capillary divided into two electrodes. Each of the two electrodes had an inside diameter at the tip of less than one micron (μm).

2.6.4 Electrophysiological experiment solutions

The following solutions were used during the electrophysiological experiment:

The first was the High sucrose ACSF solution: which was used during the dissection and slice preparation. It has the following composition (mM) 215 sucrose, 3 KCl, 21 $NaHCO_3$, 1.25 NaH_2PO_4, 1.6 $CaCl_2$, 2 $MgCl_2$, and 10 glucose.

The second solution was the extracellular solution Bicarbonate buffer saline (BBS): it was used during the recording phase, It composed of (mM): 125 NaCl, 2.5 KCl, 26 $NaHCO_3$, 1.25 NaH_2PO_4, 2 $CaCl_2$, 1 $MgCl_2$, and 15 glucose, and was prepared from a 10-fold more concentrated stock solution, then glucose, $Ca^{2+}$and Mg^{2+} were added and the solution was continuously bubbled with a mixture of carboxygen gas (95% O_2, 5% CO_2) to maintain the pH as close as possible to physiological pH (7.4).

The third solution was the Intracellular (IC) solution: it was used to fill about half of the micropipette. In addition, its composition is similar to that present within the cell. This solution composed of (mM): 120 K-gluconate, 10 NaCl, 2 MgCl2, 0.5 CaCl2, 5 EGTA (ethylene glycol tetraacetic acid), 10 HEPES, 2 Na-ATP, 10 glucose.

2.7 The Olfactory Habituation/Dishabituation Test

This test is used to assess animals ability to smell and if they can distinguish same and different odourous stimuli, (Yang and Crawley, 2009).

Habituation is a progressive decrease in olfactory investigation or sniffing towards a repeated presentation of same odour. Whereas, dishabituation is the reinstatement of sniffing when a new odour is introduced, (Wersinger et al., 2007; Woodley and Baum, 2003; Wrenn et al., 2004). Moreover, the test depends on successive presentations of different odours. The most commonly used odours are water, two non-social odours, and two social odours. Furthermore, each odour is presented in three repeated trials for 2 minutes, (Wesson et al., 2008).

In the current experiment, a total number of 20 Swiss Webster mice (10 females and 10 males) and 10 C57BL/6 male mice were tested before and after O_3 exposure.

All of the mice were assessed for their ability to smell and distinguish non-social and social odours before O_3 exposure, then after three weeks the O_3 exposure was carried out and the test was repeated again after the exposure immediately.

Based on Yang and Crawley protocol, (2009) we decided to use two categories of odourous stimuli, the first one was the non-social odours which included: water, banana (amyl acetate, 1: 1000), mint (L-carvone 1: 100), peppermint (D-carvone 1: 100), (sigma-aldrich). The dilution of these odours was done at the starting time of the test. Whereas, the second category was the social odours which included: urine from the same sex and urine from opposite sex. Furthermore, the social odours were prepared by swapping the cotton of the applicator in a zigzag fashion several times in the cage of animals of the same sex (urine from the same sex) or in another mouse cage of opposite sex (urine from opposite sex), then the bedding was removed off from the cotton piece. The experiment was performed in a clean room which was free from any source of odours. The first step in the test was the pre-acclimation step: in which a clean dry cotton stick (Cotton-tipped wooden applicator) was fixed in a clean cage (the testing cag) at a distance of 15 cm far from the bottom of the cage. Then, the cage was positioned at the eye level at a distance of 2 meters, on a flat surface to ensure better scoring of the sniffing time. After that, each tested mouse

was entered in the testing cage and allowed to acclimate for 30 min without food and water This acclimation period is very important to avoid disturbing the tested mouse and to adapt it to the presence of the odour applicator, because animals are attracted by the presence of new object rather than the presence of new smell, (Yang and Crawley, 2009) .

Furthermore, the second step was the discrimination test: before starting the discrimination, the odourous stimuli were predetermined previously and were ordered as follow: water (neutral stimulus) which was presented three times (3x), banana (3x), D carvone (3x), L carvone (3x), social odour 1 (urine from the same sex 5x), social odour 2 (urine from opposite sex 5x), for C57BL / 6J mice experiment. While for Swiss Webster mice they were ordered as: water (3x), banana (3x), D carvone (3x), Almond (3x), social odour 1 (urine from the same sex 5x), social odour 2 (urine from opposite sex 5x). Moreover, banana was considered as neutral odour that the mice have never smelled before, while the two forms of carvone (L and D) were used to test mice`s ability to distinguish very similar odours.

The first step in the discrimination test was the immersion of the cotton part of the applicator in the selected odourus solution then fixing the applicator in the grill of the experimental cage. Furthermore, the test started when the tested mouse was covered by the grill containing the odourous applicator. Each odourous stimulus was presented for 2 minutes in each trial. Following this step, the cumulative time spent by each mouse in each trial was recorded during the 2 minutes by using a stop wash. The inter-trial interval time (time between two presented odours) was one min.

Furthermore, when the animal reached more than 2 cm from the odourous source, the sniffing time was not measured. Finally, at the end of each two minutes the applicator was removed carefully without touching any part of the experimental cage, then the test steps were repeated in the same way for the other odours stimuli.

2.8 Data analysis

For analysing the result of this work different programs and statistical tests were used. For the biochemical results: Image studio lite software was used for Western blots quantification, whereas, paired, unpaired t-tests and one- way ANOVA were used for the statistical analysis, using Graph pad prism (version 6) software. In addition, pCLAMP software for the electrophysiological data. Furthermore, regarding the behavioural experiments results, the comparison of the averages was performed by Student`s t-test for

unspecified data. Moreover, in the figures the significance levels at 0.05, 0.01, 0.001 or lower and were indicated by one, two or three asterisk(s), respectively.

3. OBJECTIVES

The objectives of this work were:

1. To test the sensitivity of Swiss Webster mouse strain to different O_3 doses.
2. To compare the expression levels of 4HNE and CYP1A1 oxidative stress biomarkers in the OB and plasma samples of O_3 and air exposed Swiss Webster and C75BL/6J mice, using western immunoblot technique.
3. To measure the OB protein level in O_3 and air exposed Swiss Webster and C75BL/6J mice, using the Bradford technique.
4. To observe the effect of O_3 exposure on the body weight of Swiss Webster and C75BL/6J mice before and after O_3 exposure.
5. To study the effect of different O_3 doses on the number and excitability profile of OB DA cells in C57BL/6J mice compared to the air exposed mice, using electrophysiological method (patch clamp technique).
6. To test the effect of O_3 exposure on the olfactory response to environmental odours in C57BL/6J and Swiss Webster mouse strain.
7. To test the effect of gender in the olfactory response to environmental odours following O_3 exposure in Swiss Webster mice strain.

4. RESULTS

In this work, we aimed to assess the effect(s) of different O_3 doses in 42 Swiss Webster and 91 C57B/6J mice strains, by conducting biochemical electrophysiological and behavioural experiments.

4.1The biochemical experiment results

Regarding the biochemical experiments, the oxidative stress biomarkers and the OB proteins levels (measured in arbitrary units) were quantified and expressed as mean and Standard Deviation (SD) values for each assigned group. In addition, the body weight (expressed as mean value) of the O_3 exposed mice was measured in grams before exposing the mice, then it was measured before and after each single O_3 exposure. Moreover, the mean was calculated from the two body weight values of each single O_3 exposure.

4.1.1 Swiss Webster mouse strain

The biochemical experimental design was divided into two parts, first we conducted series of studies to test the effect of different O_3 doses on Swiss Webster mouse strain. While in the second part, we aimed to evaluate the expression levels of two oxidative stress biomarkers ,4-Hydroxynonenal (4HNE) in OB and plasma samples, Cytochrome P450 family 1 subfamily A polypeptide 1 (CYP1A1) in OB samples, and to measure the levels of OB proteins (µg/100 mg of tissue) in air and O_3 exposed mice, by using immune western blot and Bradford techniques respectively. Furthermore, we also aimed to measure the effect of O_3 exposure on the body weight of the two exposed mice strains.

In a series of preliminary studies, 22 Swiss Webster mice were exposed to different O_3 doses in order to establish the optimal conditions.

In the first series of the biochemical experiments, we analyzed the effect of 0.2 ppm O_3 dose for 2 h, 2 times for 1 day of exposure on the OB of 3 exposed females compared to the 7 air exposed mice, (5 males, 4 were 2 months old and 1 was 3 months and 12 days old, in addition to 2 females, 1 month and 29 days old) by measuring the OB 4HNE and proteins levels. In addition, the body weight of the exposed mice was measured before and after O_3 exposure.

As a result, the western immunoblot technique showed a significant ($P< 0.05$) increase in the OB 4HNE level in the O_3 exposed mice compared to the control (air exposed) mice. The mean and the standard deviation (SD) values of the two groups were: 172.31, 100 and 30.06, 24.6, respectively, **figure 4.1 (A)**. Moreover, the level of the total OB proteins was

significantly increased ($P< 0.05$) in O_3 exposed mice compared to the control mice, and the means of the two groups were 184.71, 100 and the SD values were: 39.11, 23.34, **figure 4.1 (B)**. In addition, one-way ANOVA test showed a significant decrease in the body weight after O_3 exposure, ($P< 0.05$), **figure 4.1 (C).**

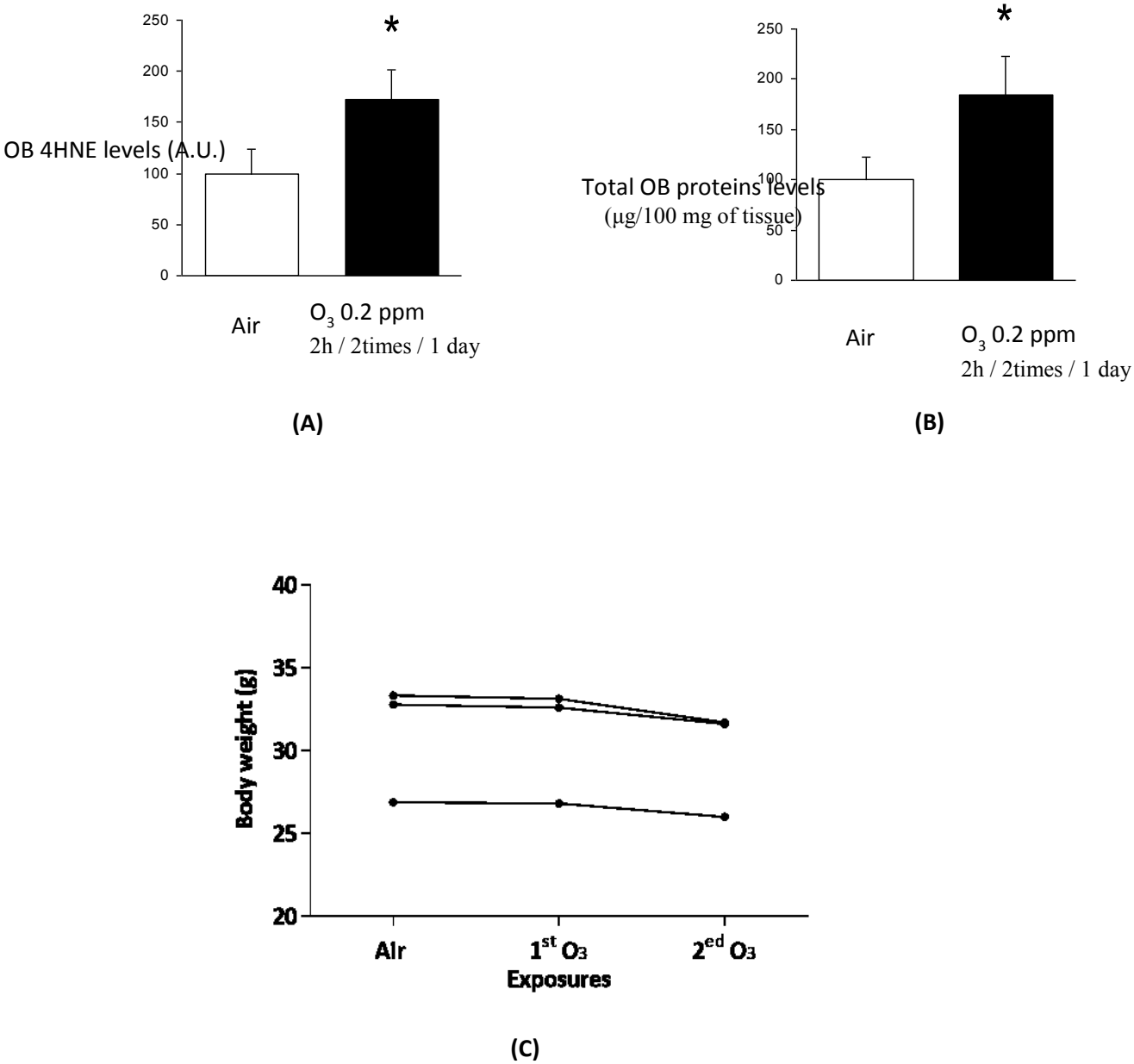

Figure 4. 1: Air and 0.2ppm/2times/1day ozone exposed Swiss Webster mice. (A): shows the 4HNE level (A.U.), and **(B):** shows the total proteins level in the OB. Whereas, **(C):** shows the effect of O_3 exposure on the body weight of the O_3 exposed mice before (air) and after O_3 exposure. (*$P< 0.05$).

Based on the first series of studies, we further studied the effect of different O_3 doses for different times and number of exposures on other 12 Swiss Webster mice. Then, the 4HNE in plasma and OB samples, CYP1A1 in OB samples and the total OB proteins levels were analyzed and compared to the same parameters of the 7 air exposed mice. In addition, the body weight of the O_3 exposed mice was measured before and after O_3 exposure as well.

Of the 12 O_3 exposed Swiss Webster mice, 2 females (3 months and 1day old), were exposed to 0.5ppm O_3 dose for 30 min/ once, the statistical analysis did not show a significant difference in the OB 4HNE level compared to the control mice (air exposed mice), and the means of both groups were: 111.46 and 100, while the SD values were 21.24 and 13.72, respectively **figure 4.2 (A).** Also, we measured the expression level of CYP1A1in OB of both groups, as shown in **figure 4.2 (B),** there was a significant increase ($P< 0.05$) in the expression level of CYP1A1 on the OB samples of the O_3 exposed mice (the mean and the SD values were: 221.55 and 43.68) compared to air exposed mice (the mean and the SD values were: 100 and 25.67). In addition, the O_3 exposed mice had a significant increase ($P< 0.05$) in the OB proteins level compared to the control mice, the mean and the SD values of the two groups were 146.49, 100 and 23.07, 15.91, respectively as shown in **figure 4.2 (C)**. Whereas, **figure 4.2 (D),** shows a significant decrease in the body weight of the O_3 exposed mice, ($P< 0.05$).

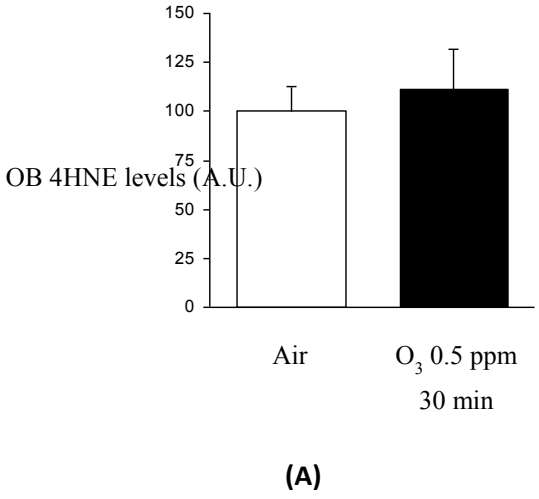

(A)

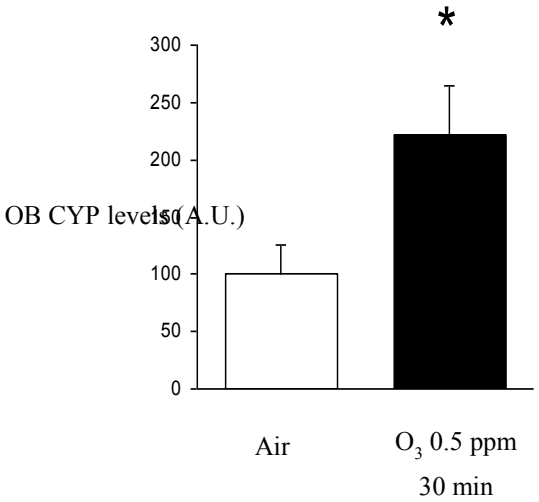

(B)

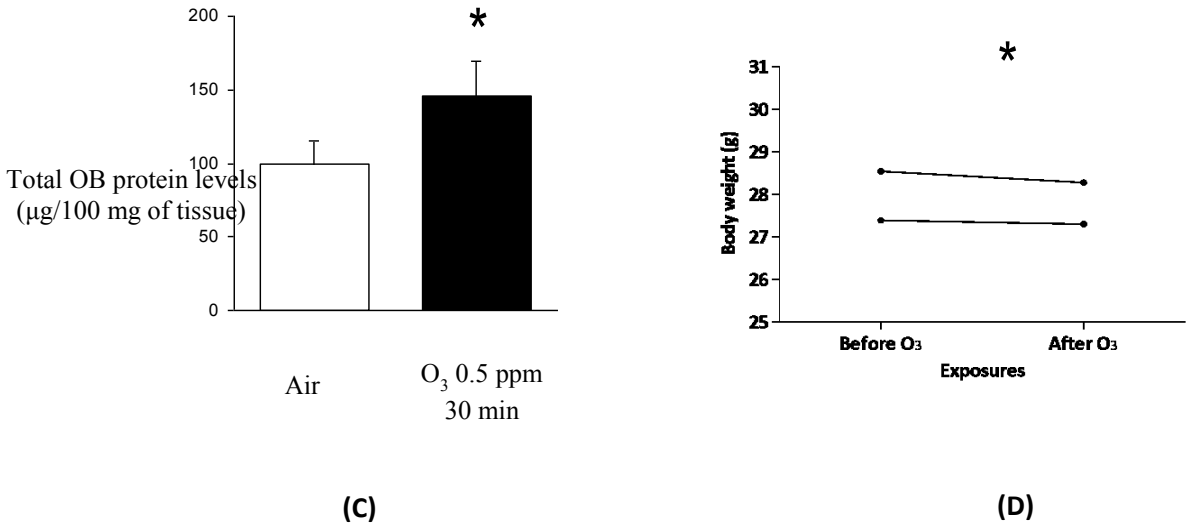

Figure 4. 2: Air and 0.5 ppm/30 min ozone exposed Swiss Webster mice. (A): shows the OB 4HNE level (A.U.), **(B):** shows the OB CYP1A1 level (A.U.), **(C):** shows the total proteins level in the OB, and **(D):** shows the effect of O_3 exposure on the body weight of the O_3 exposed mice before (air) and after O_3 exposure. (*P< 0.05).

The 3 females (3 months and 1day old), of the 12 O_3 exposed Swiss Webster mice which were exposed to 0.5ppm O_3 dose for 60 min/once, their immune blot western blot technique showed statistically significant increase in the levels of the oxidative stress biomarkers (4HNE and CYP1a) and in the total OB proteins level in the O_3 exposed mice compared to the control mice. As shown in **figure 4.3 (A)**, the mean values of OB 4HNE level of the O_3 and control group were: 148.81, 100 and the SD values were: 19.13, 11.93 respectively). While, **figure 4.3 (B),** shows the CYP1A1 level means (148.77 and 100) and the SD (24.4 and 18.78) values of the two groups respectively. On the other hand, **figure 4.3 (C),** shows the comparison of the OB proteins level between O_3 and air exposed mice, the mean values were: 223.43 and 100, while the SD values were: 39.65 and 16.34. Moreover, one-way ANOVE test showed a significant decrease in the body weight of the O_3 exposed mice, (P< 0.05) **figure 4.3 (D)**.

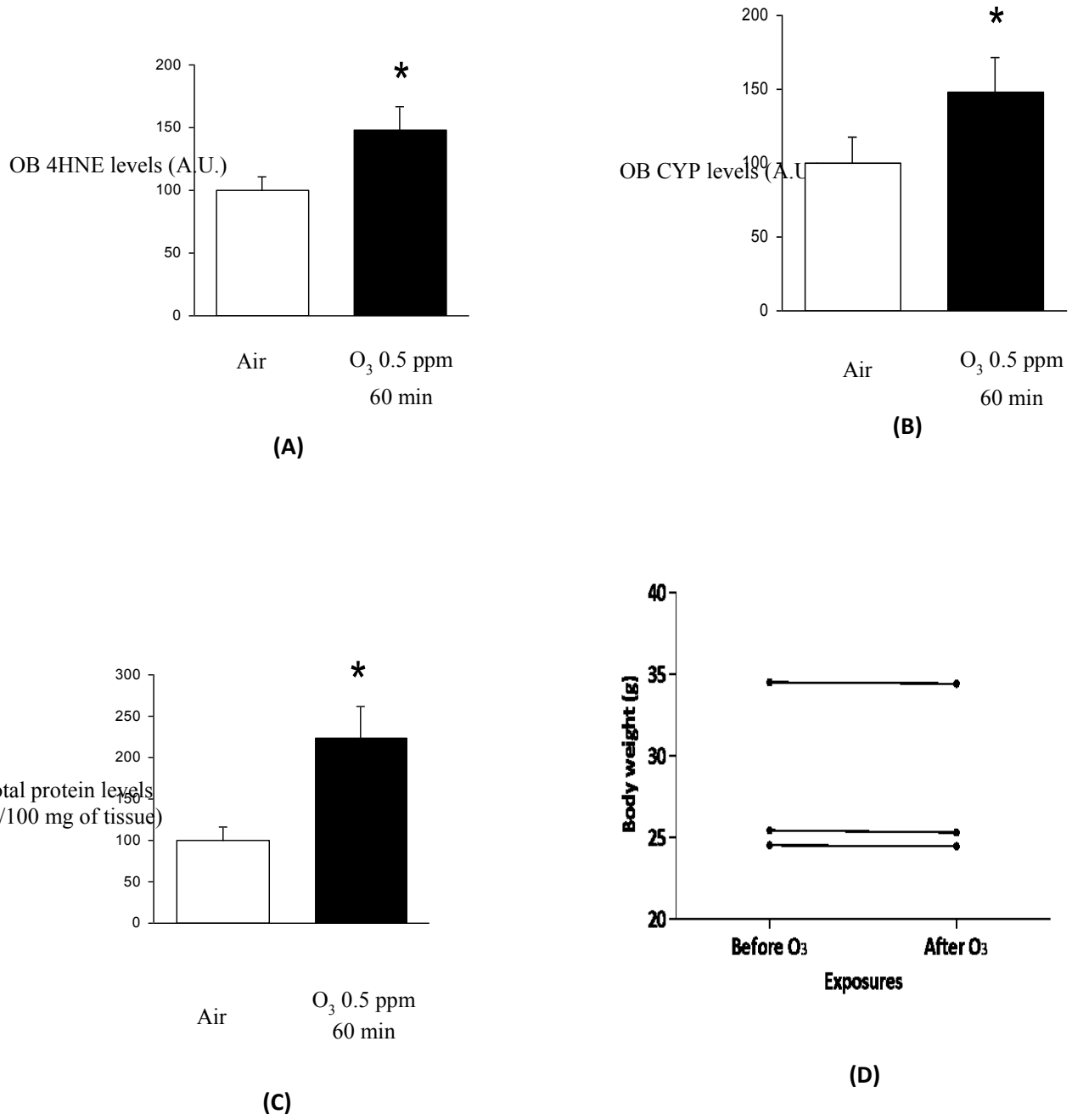

Figure 4. 3: Air and 0.5ppm/60 min/once, ozone exposed Swiss Webster mice. (A): shows the OB 4HNE level (A.U.), **(B):** shows the OB CYP1A1 level (A.U.), **(C):** shows the total protein level in the OB, and **(D):** shows the effect of O_3 exposure on the body weight of the O_3 exposed mice. (*P< 0.05).

Of the 12 O_3 exposed Swiss Webster mice, 7 were exposed (4 females, 3 months and 17 days and 3 old and 3 males, 3 months and 3 days old) to 0.2ppm O_3 dose for 2h, 2times for 2days, and were compared to the air exposed mice. As shown in **figure 4.4 (A)**, they had a significantly increased plasma 4HNE level (the mean and the SD values were 162.39, 100 and 31.78, 20.87 in both groups, respectively). While, the difference in the OB 4HNE level was statistically increased (the mean and the SD values were: 181.32, 100 and 18.19, 13.23 in the O_3 and air exposed mice, respectively), as shown in **figure 4.4 (B).** Furthermore, the O_3 exposed mice had a significantly increased OB CYP1A1 level compared to the control group (air exposed mice), as shown in **figure 4.4 (C).** The mean and the SD values were: 149.56, 100 and 21.71, 8.65for the O_3 and air exposed mice, respectively. In addition, the O_3 exposed mice showed statistically increased total OB proteins level (the mean the and the SD values were 322.41 and 62.03) compared to the air exposed mice (the mean and the SD were 100 and 21.74), **figure 4.4 (D).** Moreover, **figure 4.4 (E),** shows the effect of O_3 exposure on the body weight of the O_3 exposed mice before and after O_3 exposure, which was significantly decreased, ($P< 0.05$).

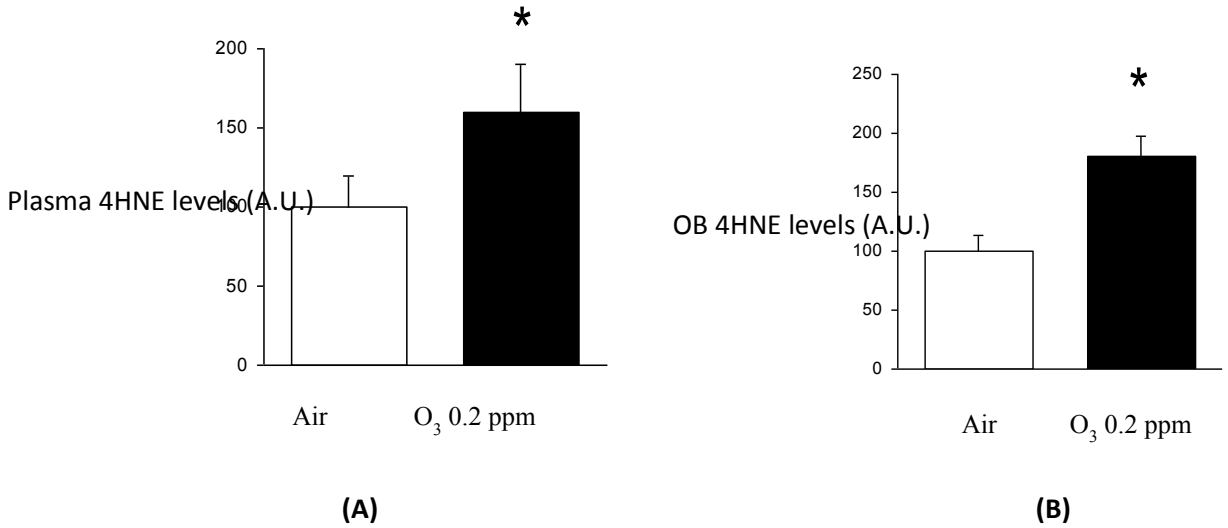

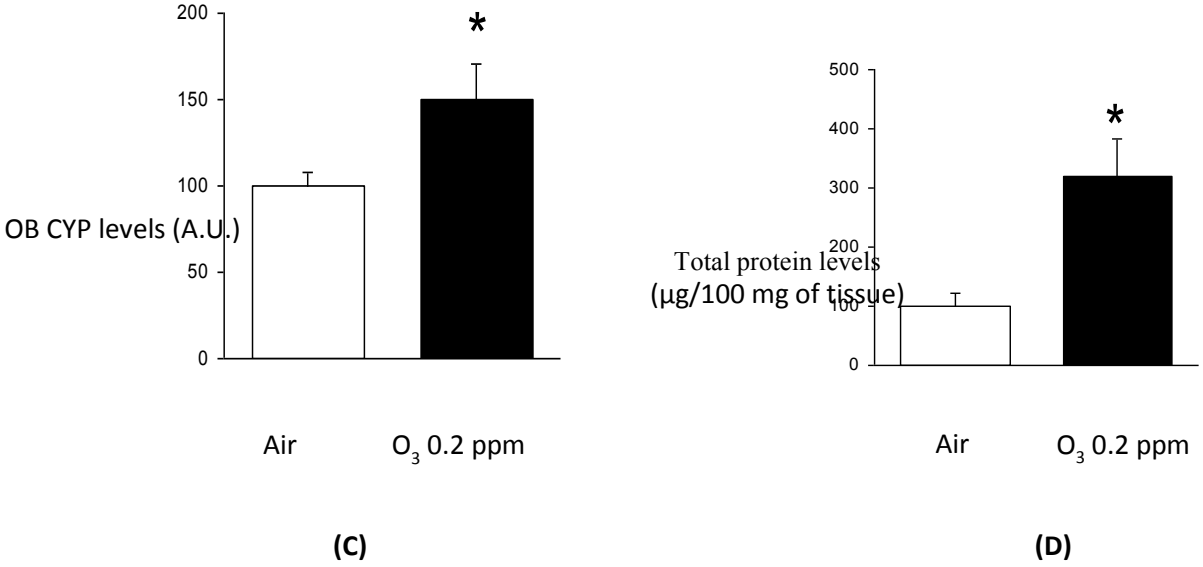

(C) **(D)**

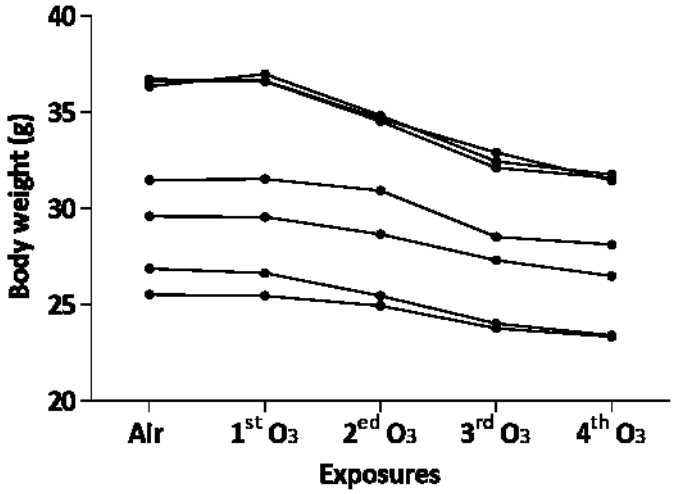

(E)

Figure 4. 4: Air exposed and 0.2ppm/2h/2times/2days ozone exposed Swiss Webster mice. **(A):** shows plasma 4HNE level (A.U.), **(B):** shows the OB 4HNE level (A.U.), (**C):** shows the CYP1A1 level (A.U.), **(D):** shows the total proteins level in the OB, and **(E):** shows the effect of O_3 exposure on the body weight of the exposed mice. (*P< 0.05).

4.1.2 C57BL/6J mouse strain

Regarding C57BL/6J mouse strain, the oxidative stress biomarkers, (4HNE in the OB and/or plasma and CYP1A1 in the OB) and the OB proteins level were measured in O_3 and air exposed mice, in the same way as described for Swiss Webster mice experiments. In addition, the body weight of the O_3 exposed mice was measured before and after O_3 exposure(s).

A total of 25 mice were divided into two groups, the first one was the air exposed group, which included 8 mice (4 males and 4 females, 2 months and 2days old) and the second one was the O_3 exposed group, which contained 17 mice (10 WT and 7 GFP). The O_3 exposed group was divided into 4 subgroups, and were exposed to different O_3 doses for different exposure times.

Of the 10 O_3 exposed C57BL/6J mice, 3 mice (2 females and 1male, 2 months and 25 days old) were exposed to 0.5ppm O_3 dose for 30 min once, and their biochemical results showed insignificant plasma 4HNE, OB 4HNE, OB CYP1A1 level and OB proteins levels. As shown in **figure 4.5 (A),** the mean and the SD values of the plasma 4HNE were: 96.17, 100 and 31.12, 25.24 in both groups, respectively. In addition, the comparison of the OB 4HNE level between the O_3 and control mice. The mean and the SD values of both groups were: 106.33, 100 and 24.32, 13.46 respectively, **figure 4.5 (B).** Furthermore, the OB CYP1A1 level of the O_3 and air exposed mice is shown in **figure 4.5 (C).** The means values were: 113.61, 100 and the SD values were: 29.34, 14.54 for the two groups respectively. Moreover, **figure 4.5 (D)** shows the levels of the total OB proteins in the O_3 and control mice. The mean and the SD values were 89.09, 100, and 11.63, 16.74, for the two groups respectively. However, O_3 exposure caused a significant decrease in the body weight of the exposed as shown in **figure 4.5 (E).**

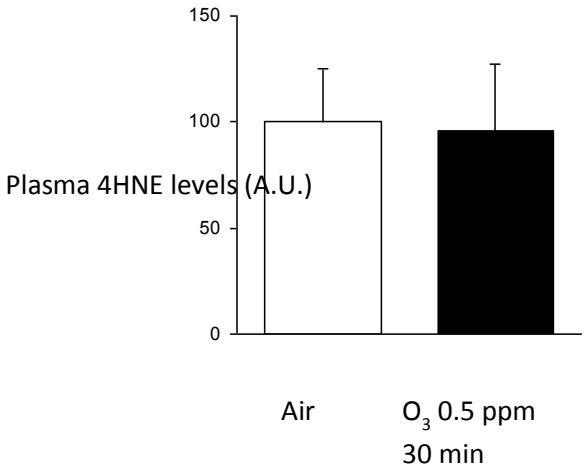
150
100
50
0
Plasma 4HNE levels (A.U.)
Air
O_3 0.5 ppm
30 min

(A)

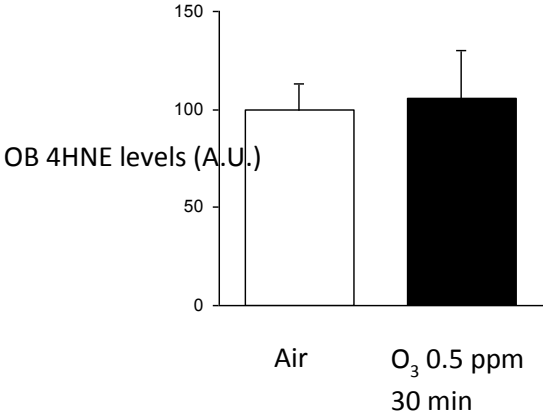
150
100
50
0
OB 4HNE levels (A.U.)
Air
O_3 0.5 ppm
30 min

(B)

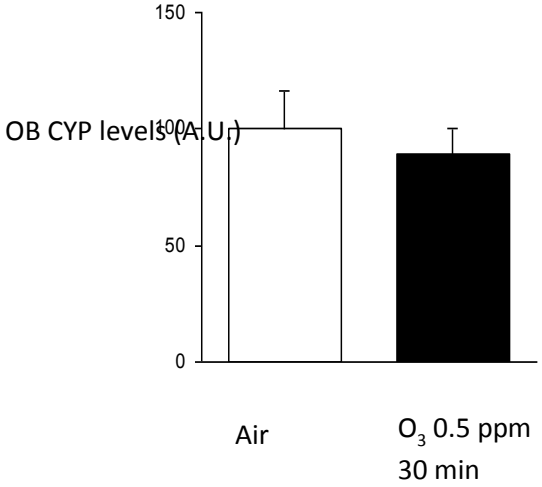
150
100
50
0
OB CYP levels (A.U.)
Air
O_3 0.5 ppm
30 min

(C)

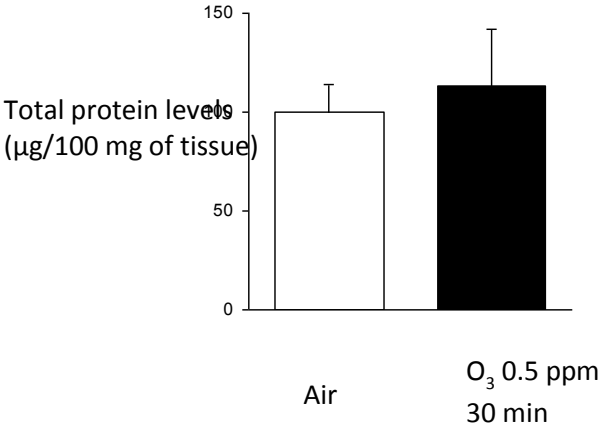
150
100
50
0
Total protein levels
(µg/100 mg of tissue)
Air
O_3 0.5 ppm
30 min

(D)

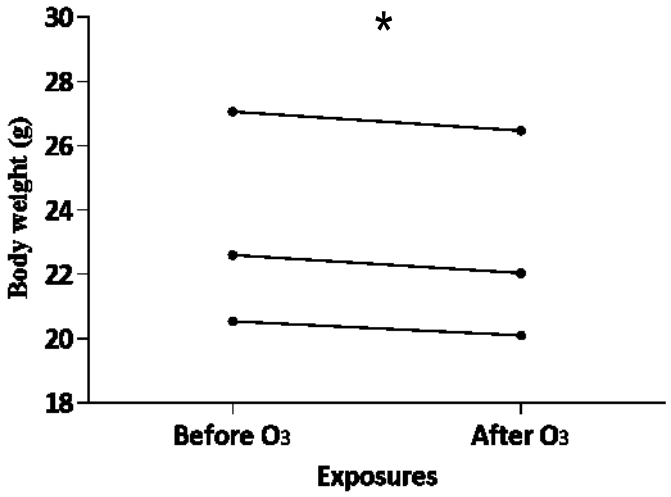

(E)

Figure 4. 5: Air exposed and 0.5ppm/30 min/once ozone exposed WT C57BL/6J mice. (A): shows the plasma 4HNE level (A.U.), **(B):** shows the OB plasma 4HNE level (A.U.), **(C):** shows the CYP1A1 level (A.U.), **(D):** shows the total proteins level in the OB, and **(E):** shows the effect of O_3 exposure on the body weight of the O_3 exposed mice. (*P< 0.05).

Figure 4.6 (A- E), shows the 3 WT mice (2 females and 1male, 2 months and 25 days old) of the 10 O_3 exposed WT mice, which were exposed to 0.5ppm O_3 dose for 60 min once. The statistical analysis results showed insignificant difference in the oxidative stress biomarkers (4HNE and CYP1A1) and in the total OB protein levels between O_3 and air exposed mice. As shown in **figure 4.6 (A),** the mean and the SD values of the plasma 4HNE level in the two groups were: 115.32, 100 and 23.71, 19.63 respectively. While for the OB 4HNE level were: 118.14, 100 and the SD values were 20.85, 13.37 respectively, **figure 4.6 (B).** In addition, the mean values of the OB CYP1A1 level were: 109.56, 100 and the SD values were 24.62, 29.84 for O_3 and control mice, **figure 4.6 (C)**. Moreover, as shown in **figure 4.6 (D),** the mean values of the total OB proteins level were: 108.49, 100 and the SD values were: 31.78, 16.46, for the two groups respectively. Also, the difference in the body weight of the O_3 exposed mice before and after O_3 exposure was statistically insignificant, **figure 4.6 (E).**

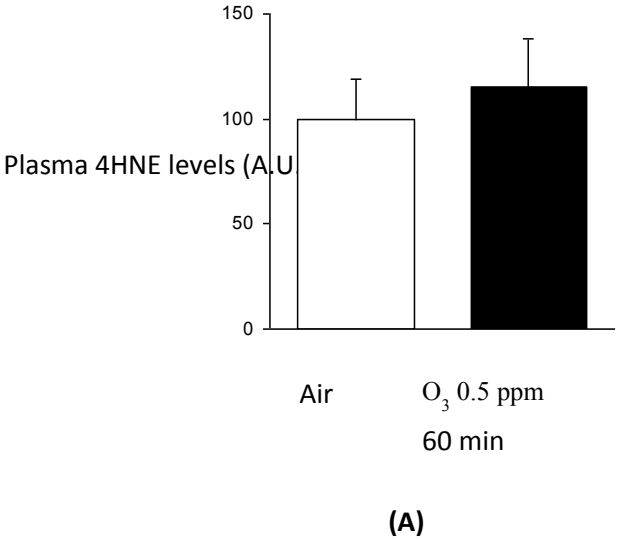
Plasma 4HNE levels (A.U.)
150
100
50
0
Air
O_3 0.5 ppm
60 min

(A)

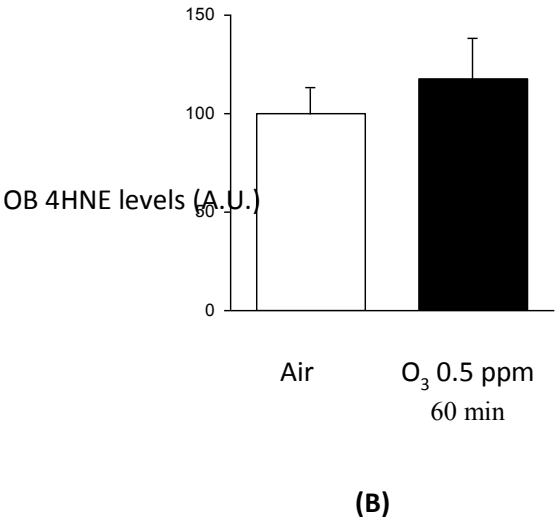
OB 4HNE levels (A.U.)
150
100
50
0
Air
O_3 0.5 ppm
60 min

(B)

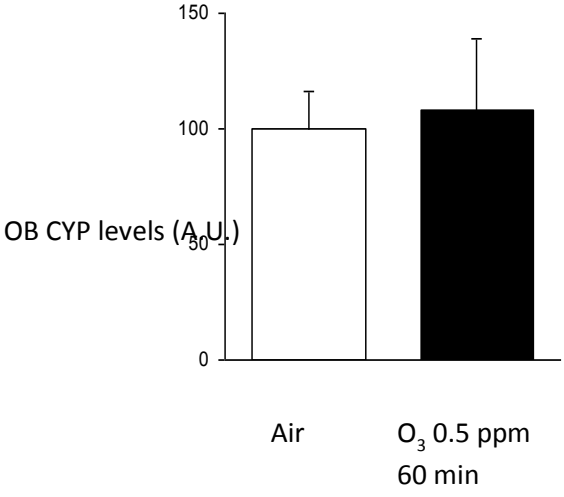
OB CYP levels (A.U.)
150
100
50
0
Air
O_3 0.5 ppm
60 min

(C)

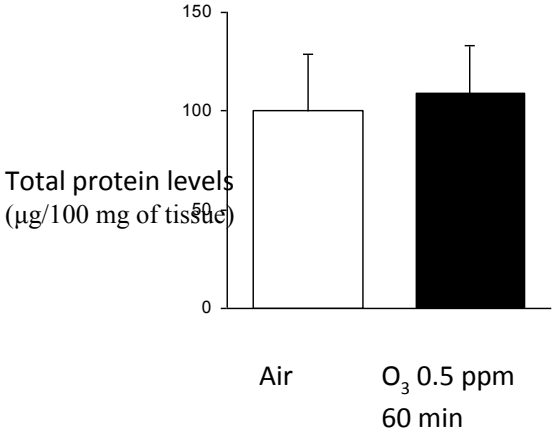
Total protein levels
(μg/100 mg of tissue)
150
100
50
0
Air
O_3 0.5 ppm
60 min

(D)

(E)

Figure 4. 6: Air and 0.5ppm/60`/once ozone exposed C57B/6J WT mice. (A): shows the plasma 4HNE level (A.U.), **(B):** shows the OB 4HNE level (A.U.), **(C):** shows the CYP1A1 level (A.U.), **(D):** shows the total protein level in the OB, and **(E):** shows the effect of O_3 exposure on the body weight of the O_3 exposed mice.

Four mice (2 females and 2 males, 2 months and 7 days old), of the 10 O_3 exposed WT mice, were exposed to 0.8ppm O_3 dose for 2h, 2times for 5 days continuously. As shown in **figure 4.7(A)**, the difference in the plasma 4HNE was statistically insignificant between the O_3 and air exposed mice**,** (the means values were: 144.36, 100 and the SD values were: 41.14, 22.02, for the two groups respectively). However, the O_3 exposed mice had a significant increase in the OB 4HNE compared to the air exposed mice. The means values were:165.33, 100 and the SD values were: 28.41, 15.34, **figure 4.7 (B).** Moreover, the two groups did not show any statistical difference in the OB CYP1A1 level. The means were: 112.33, 100 and the SD values were: 36.82, 48.41in the two groups respectively, **figure 4.7 (C).** Also, the difference in the total OB proteins level between the O_3 and control mice was statistically non-significant. The means values were: 110.87, 100 and the SD values were 23.64, 26.55, respectively, **figure 4.7 (D)**. But, **figure 4.7 (E)** shows a significant decrease in the body weight of the O_3 exposed mice after O_3 exposure, ($P< 0.05$).

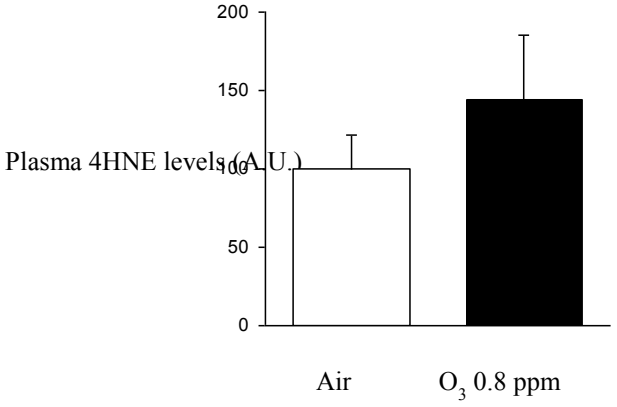
Plasma 4HNE levels (A.U.)
200
150
100
50
0
Air
O3 0.8 ppm

(A)

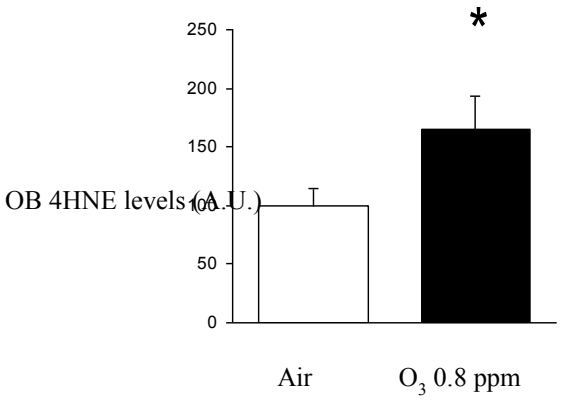
OB 4HNE levels (A.U.)
*
250
200
150
100
50
0
Air
O3 0.8 ppm

(B)

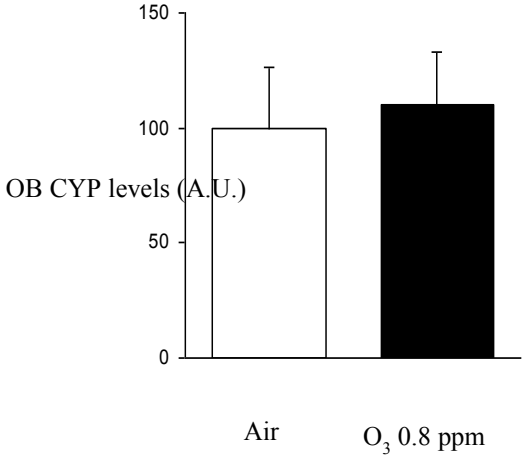
OB CYP levels (A.U.)
150
100
50
0
Air
O3 0.8 ppm

(C)

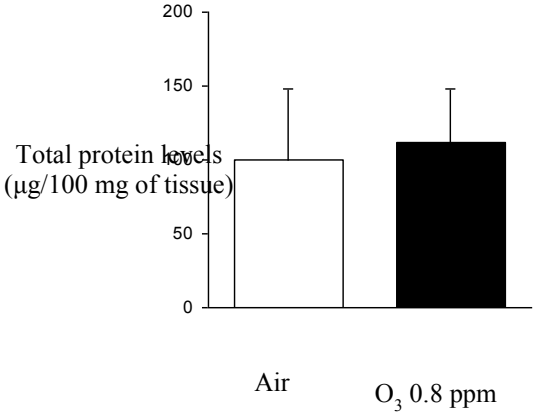
Total protein levels
(µg/100 mg of tissue)
200
150
100
50
0
Air
O3 0.8 ppm

(D)

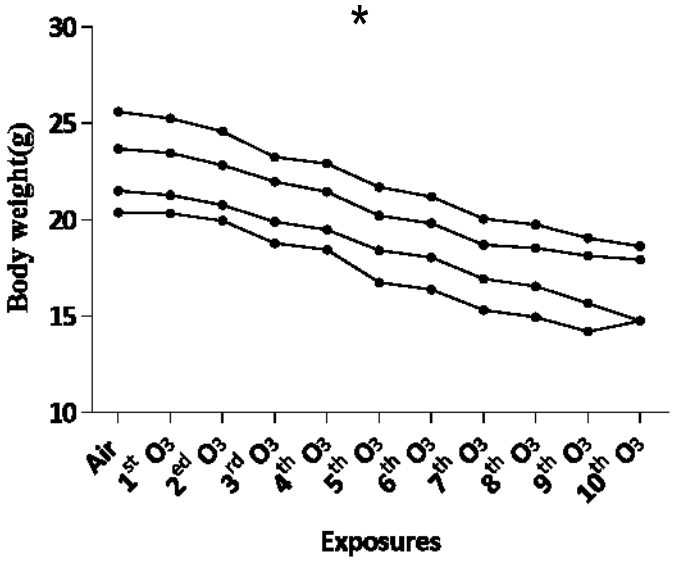

(E)

Figure 4. 7: Air and 0.8ppm/2h/2times/5days, ozone exposed C57B/6J WT mice. (A): shows the plasma 4HNE level (A.U.), (**B):** shows the OB 4HNE level (A.U.), **(C):** shows the OB CYP1A1 level (A.U.), **(D):** shows the total protein level in the OB, and (E): shows the effect of O_3 exposure on the body weight of the O_3 exposed mice, (*P< 0.05).

Of the 17 O_3 exposed mice, seven GFP mice (3 females, 2 were 2 months and 20 days old, and one was 2 months and 22 days old. In addition to 4 males, 3 were 3 months old and one was 2 months and 14 days old) were exposed to 0.8ppm O_3 dose for 2hours, 2 times for 5 days continuously. The immune western blot results of the O_3 exposed (GFP) and air exposed (WT) mice samples showed statistically insignificant 4HNE (plasma and OB) and total OB protein levels. As shown in **figure 4.8 (A),** the mean values of the plasma 4HNE were: 112.25, 100 and the SD values were: 22.39, 18.14, for the two groups respectively. While, the mean values for the OB 4HNE level were: 105.12, 100 and the SD values were: 38.56, 32.09 for the O_3 and air exposed mice, **figure 4.8 (B)**. In addition, the means values of the total OB proteins level were: 108.26, 100 and the SD values were: 32.75, 41.98 for the two groups respectively, **figure 4.8 (C)**. Moreover, the CYP1A1 wasn`t detected in all OB samples of the GFP O_3 exposed mice. However, the difference in the body weight of the O_3 exposed mice was statistically decreased after O_3 exposure, as shown in **figure 4.8 (D).**

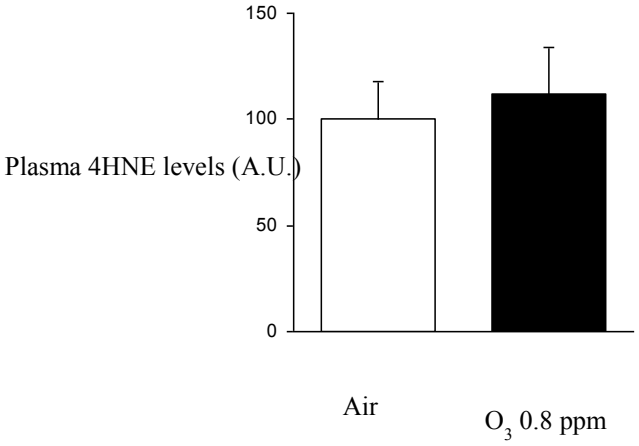

(A)

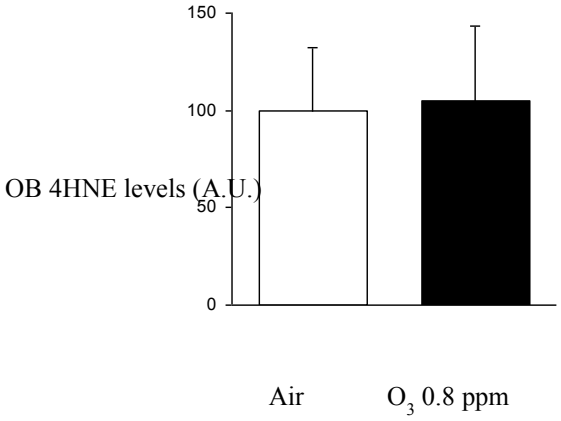

(B)

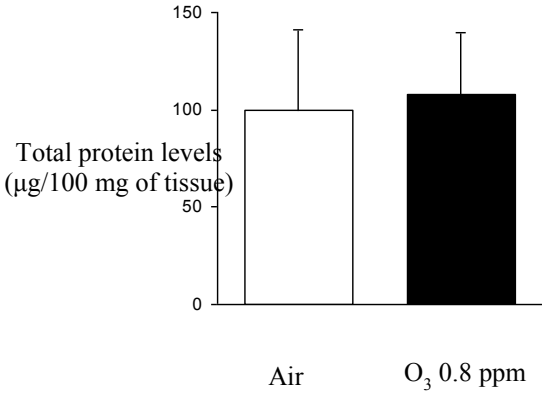

(C)

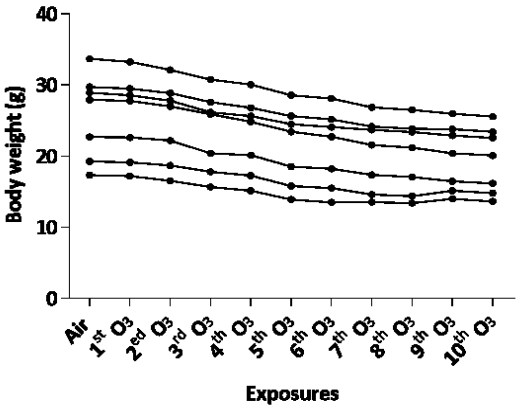

(D)

Figure 4. 8: Air and 0.8ppm/2h/2times/5days ozone exposed GFP C57BL/6J mice. (A): shows the plasma 4HNE level (A.U.), **(B):** shows the OB plasma 4HNE level (A.U.), **(C):** shows the total protein level in the OB, and **(D):** shows the effect of O_3 exposure on the body weight of the O_3 exposed GFP C57BL/6J mice, (*P< 0.05).

4.2 Electrophysiological experiments

4.2.1 Preliminary studies

In this part of the project, we aimed to test the effect(s) of O_3 exposure on the electrophysiological spontaneous activity (spontaneous firing) and on the number of TH-GFP positive cells compared to non-ozone exposed mice. Even more, to select the appropriate ozone exposure protocol that gives a clear result. Therefore, five transgenic mice TH-GFP/21-31 line that carries the eGFP gene under the control of the TH promoter (Matsushita et al., 2002; Sawamoto et al., 2001), were exposed to two different O_3 concentrations (0.5 and 0.8 ppm), for different durations of time and number of exposures. The result and the experimental conditions are summarized in **table 4.1**.

Table 4. 1: The effect of ozone on the OB DA cells in O_3 and air exposed C57B/J6 mice.

Mice sex	Male	Female	Male	Female	Female
Mice Age	1 year and 5 months **(515 days)**	2 months and 2 days **(83 days)**	1 year and 4 months **(515 days)**	1 year, 5 months and 4 days **(514 days)**	2 months and 24 days **(85 days)**
Ozone dose	**No**	**No**	0.5 ppm	0.5 ppm	0.8 ppm
Ozone exposure duration	**No**	**No**	30 min	150 min	1080 min
Exposure protocol	**None**	**None**	1 time/30'/day	2 time/30'/day	2 time/120'/day
patch clamp recording	No	No	Yes	Yes	Yes
Spontaneous activity	Yes	Yes	Yes	Yes	Yes
# of GFP cells/slice	**766.17**	**1088.83**	**757.43**	**1039.83**	**1140.67**
SD	58.48	232.10	59.73	125.87	118.19
# of slices	**6**	**6**	**7**	**6**	**6**

4.2.1.1 The spontaneous firing activity of OB DA cells

The effect of O_3 exposure on the spontaneous activity of OB DA cells was tested using the patch-clamp technique under different exposure conditions, as described in **table 4.1**.

The results indicated that in animals exposed to ozone, TH-GFP positive cells were always able to give spontaneous firing activity, as described in a previous work (Pignatelli et al., 2005), even when the ozone concentration, the duration and number of exposures were also increased.

Further analysis of the electrophysiological recordings which was measured in 15 cells showed that in the exposed mice to O_3, the spontaneous firing frequency of TH-GFP positive cells was reduced to 2.39± 0.33 Hz, a much lower frequency value compared with what measured on a large scale in the previous work in control condition (7.84± 2.44 Hz) by Pignatelli et al., (2005)**.**

In addition, the frequency distribution of the interspike intervals (inter-event time) was also measured in ozone and non-ozone (CTL) exposed mice DA cell, this parameter became much longer in O_3 exposed DA cells.

4.2.1.2 The number of TH-GFP positive cells

Also, we aimed to verify if O_3 exposure causes a death in the OB DA cells in the glomerular layer. In order to identify the eGFP expressing cells, we used a microscope equipped with epifluorescence.

As shown in **table 2**, in the preliminary study two mice were used as control (non O_3 exposed mice), and three were exposed to O_3 at different concentrations to see if there were evident differences in the number of DA cells in the two groups. There was no clear difference in the numbers of TH-GFP positive cells in the two groups, although, given the differences in age and experimental conditions, the number of tested mice was insufficient to draw any ultimate conclusion.

4.2.2 The main electrophysiological results

After having a general idea about the effect of O_3 exposure on the olfactory bulb DA cells from the preliminary study, we decided to select 0.8 ppm O_3 dose for 2 h two times per day for 4 subsequent, days followed by a single exposure on the fifth day, as suitable protocol for the electrophysiological experiment. In addition, we aimed to test the effects of ozone

exposure on the spontaneous activity (a characteristic electrophysiological feature of a typical dopaminergic cell) of O_3 exposed DA cells compared to non-O_3 exposed cells.

Concerning our electrophysiological objective, a total of 51 transgenic TH-GFP / 21-31 line mice expressing the eGFP gene under the control of TH promoter were used, (Matsushita et al., 2002; Sawamoto et al., 2001).

Following brain extraction using microsurgical procedure as described in materials and method, slices of 150 μm in thickness were obtained to be used for current clamp experiment. Then a total number of 82 PG-DA positive cells of GFP exposed mice were identified with a suitable illumination that excited the GFP.

The results indicated that in O_3 exposed mice, the TH-GFP positive cells were always able to give spontaneous action potentials, as described previously by Pignatelli et al., (2005). f**igure 4.9 A and B.**

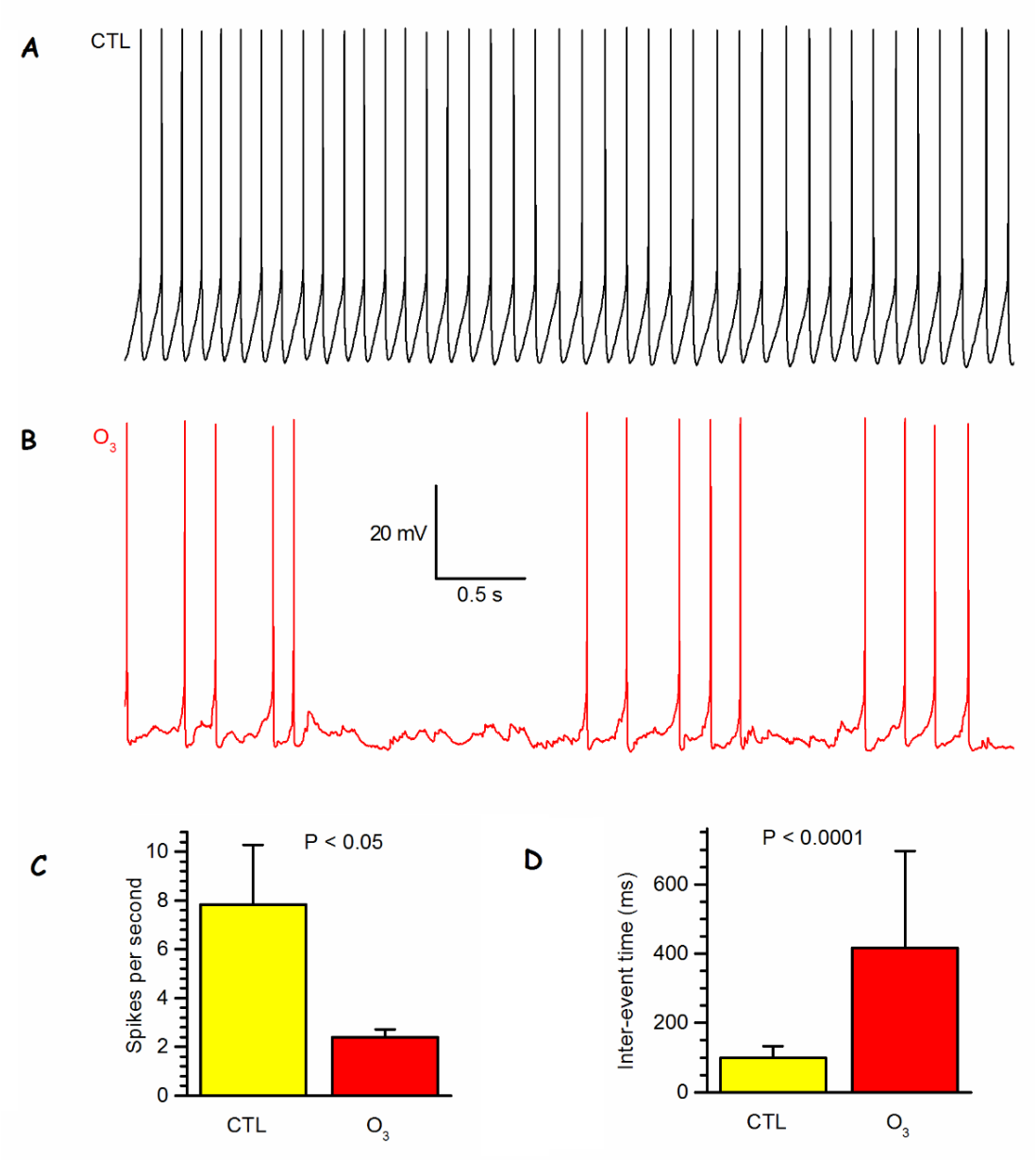

Figure 4. 9: The spontaneous activity – Frequency discharge and the inter-event time of control and O_3 exposed DA cells. (A): Spontaneous frequency discharge in control cell. **(B):** The frequency discharge in ozone exposed mice cell. **(C):** and **(D):** The Comparison of the means of the frequency discharge and the inter-event time in the controls and O_3 exposed mice.

As shown in **figure 4.9,** panels **A** and **B** show the spontaneous activity of the periglomerular GFP positive cells in control (A) and in ozone exposed mice DA cells, respectively. Furthermore, the comparison between the two groups (control an ozone exposed mice) showed difference in the frequency discharge.

In the **figure 4.9** panel **C**, the histogram represents the comparison between the average numbers of spikes per second (frequency in Hz) in control and O_3 exposed mice. The result indicated a statistically significant difference ($P < 0.05$). Moreover, the average of the

spikes in control cells was 7.84 ± 2.44 Hz, while for the ozone exposed mice was 2.39 ± 0.33 Hz (mean ± SE).

The inter-event time (the time between a spike and the next one) is shown in **figure 4.9** panel **D,** for the control and O_3 exposed mice. In control cells, the mean time (in ms) between one spike and the other was 99.5 ± 33 and 416.2 ± 280 (mean ± S.D.) for the O_3 exposed cells. The difference in the mean time between the two group was statistically significant ($P < 0.0001$).

Subsequently, further analysis for some electrophysiological parameters of dopaminergic cells was performed for the control and O_3 exposed cells. These parameters include: the rheobase, chronaxie, membrane resistance and the resting membrane potential.

To compare the rheobase values in O_3 and control cells, a protocol consisting of series of current steps of 200 ms width, with a progressively greater amplitude until no action potential was evoked, were injected in the O_3 and control DA cells. Then after analysing 36 control cells an average value of 11.32 ± .85 pA was obtained. While, in the ozone exposed mice 28 cells were analysed and the mean value of the rheobase was 16.64 ± .93 pA (mean ± S.E.), **figure 4.10 (A).** Moreover, the statistical analysis showed a significant difference between the two groups.

Concerning the chronaxie, after obtaining the rheobase value a depolarizing stimulus was used in which the injected current was twice as strong as the rheobase and the length of time was increased until a spike was obtained. Moreover, after analysing the chronaxie results from 28 control cells and 22 ozone exposed cells average values of 43.11 ± 3.36 and 29.6 ± .25 ms (mean ± SE) were obtained from the two groups, respectively, **figure 4.10 (B)**, the statistical analysis showed a significant difference between the two groups.

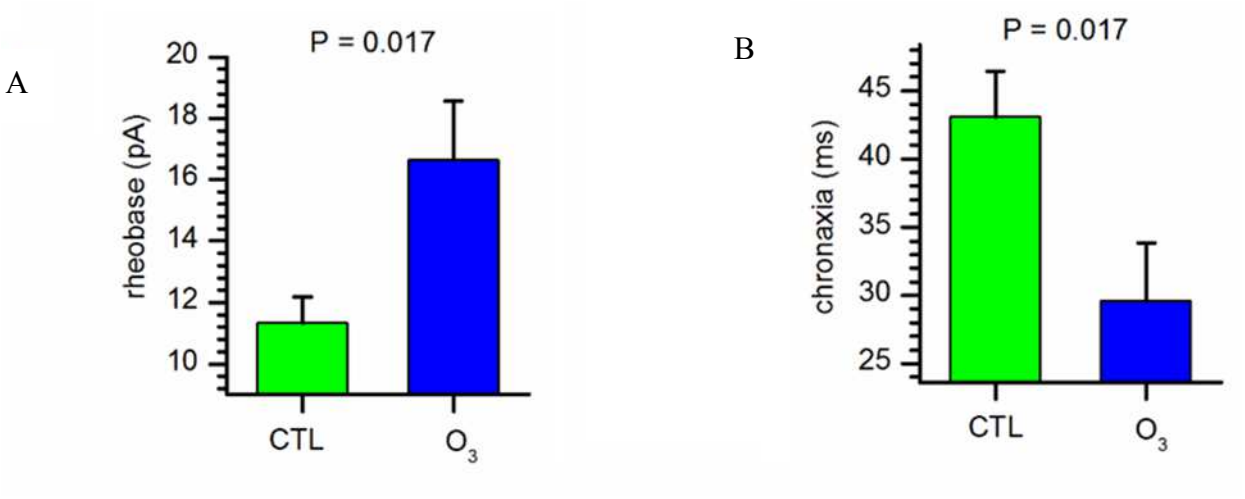

Figure 4. 10: The rheobase and chronaxie in control and O_3 exposed C57B/J6 mice. **(A):** shows the mean ± S.E of the rheobase values obtained from the controls and ozone exposed mice. **(B):** Shows the mean ± S.E of the chronaxie values obtained from the controls and ozone exposed mice.

In addition, the membrane resistance from 37 control cells and 28 O_3 exposed cells was also analysed, and the mean values were 1.21 ± 0.12 GΩ and 0.65 ± 0.08 GΩ for the two groups, respectively. Furthermore, the statistical analysis showed a significant difference between the two groups, **figure 4.11 panel (A).** Also the difference in the resting membrane values was statistically significant **figure 4.11** panel **(B).**

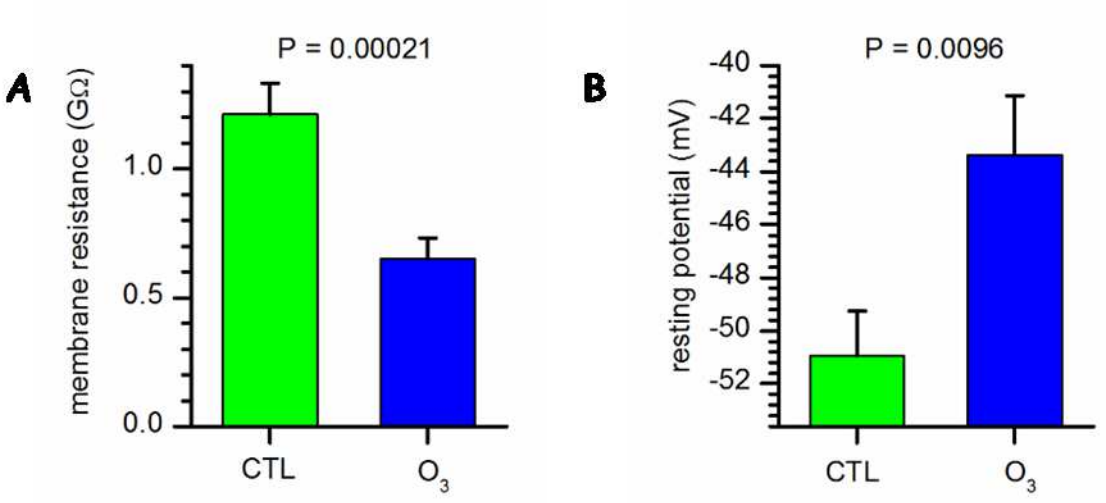

Figure 4. 11: Membrane resistance and resting potential in control and O_3 exposed mice. (A): shows the comparison of the average values of the membrane resistances in control and O_3 exposed mice. **(B)** shows the comparison of mean values of the resting potentials in control and O_3 exposed mice.

4.3 Behavioural experiment results

In this part of the work, we aimed to test the effect(s) of environmental O_3 exposure on the sense of smell of two different mouse strains (C57BL/6J and Swiss Webster), by assessing their ability to distinguish different and same odourous stimuli before and after O_3 exposure.

Total of 30 mice (C57BL/6J and Swiss Webster) were exposed to 0.8 ppm O_3 dose 2h/once for one day. In addition, all of the mice were subjected to the olfactory habituation/dishabituation test before and after O_3 exposure as described in material and method.

4.3.1 C57BL / 6J mice

Total of 10 C57BL / 6J males were used for this experiment. In addition, the presented odours were ordered as follow: water, banana, D-carvone and L-carvone (non-social odours), in addition to urine from the same sex and from the opposite sex (social odours), respectively. Furthermore, each non-social odour was presented three times, whereas social odours were presented 5 times.

Moreover, the difference in the number of repetitions between social and non-social odours was chosen to obtain a better characterization of the habituation phenomenon which was observed after the first exposure to a new smell.

Concerning C57BL/6J mice male the effects of O_3 exposure on the olfactory response was evaluated by recording the sniffing times for each non-social odour before and after O_3 exposure, as shown in **figure 4.12** These sniffing times represent the times spent by the tested mice to smell various odourous stimuli. e.g for banana the average sniffing times were: 7.14s and 1.13 s, while for D-carvone were 2.97 s and 0.55 s, before and after O_3 exposure, respectively. In addition, the statistical analysis showed a significant difference between the means of sniffing times before and after O_3 exposure.

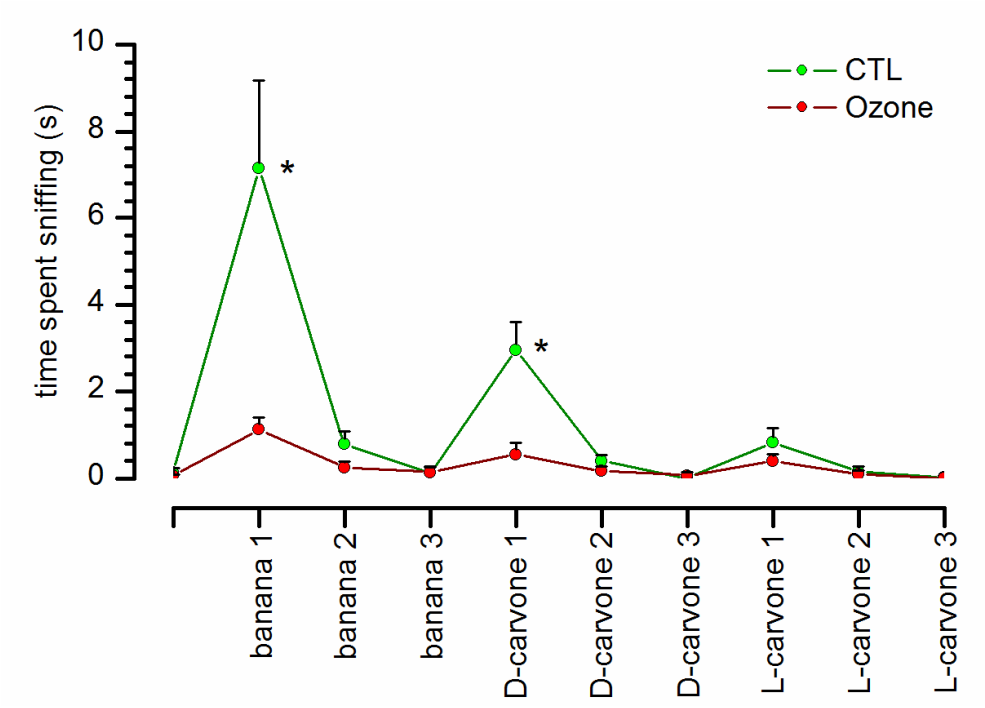

Figure 4. 12: Non-social odours- C57BL / 6J mice male. The figure shows the average times spent during sniffing of non-social odours before (green line-CTL) and after O_3 exposure (red line) for C57BL / 6J mice male.

Moreover, the statistical analysis did not show any significant difference between the means of sniffing times for social odours before and after O_3 exposure for C57BL / 6J mice male, **figure 4.13.**

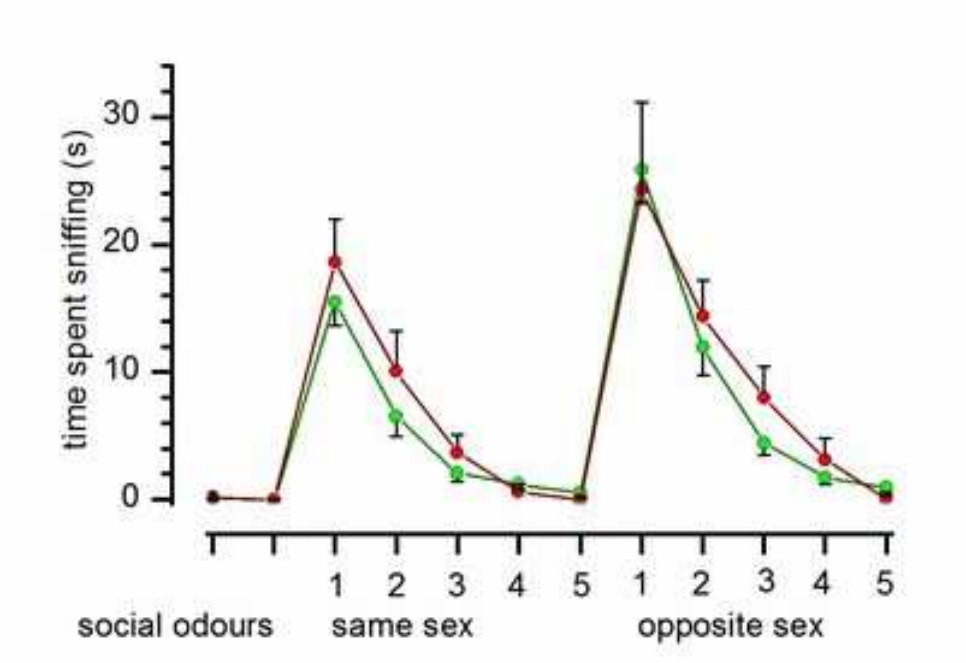

Figure 4. 13: Social odours- C57BL / 6J mice male. The figure shows the average times spent during sniffing for social odours before (green line-CTL) and after ozone exposure (red line) for C57BL / 6J mice male.

4.3.2 Swiss Webster mice

Also the olfactory habituation/dishabituation test was performed on 20 Swiss Webster mice (10 males and 10 females), to observe the effect of O_3 exposure on the olfactory response to environmental odours among different mouse strains, and to see the effect of mice gender on the olfactory response to different odourous stimuli after O_3 exposure.

The presented non-social odours were: water, banana (amyl acetate, 1: 1000), peppermint (D-carvone 1: 100) and almond (benzaldehyde 1: 100). Banana, D-carvone (peppermint) and almond represent the non-social odours that the mice have never come in contact with. While the social odours included: urine from the same and from opposite sex.

As shown in **figure 4.14**, the difference between the means of sniffing times for each presented non-social odour did not show any statistical significant before and after O_3 exposure for Swiss Webster male mice.

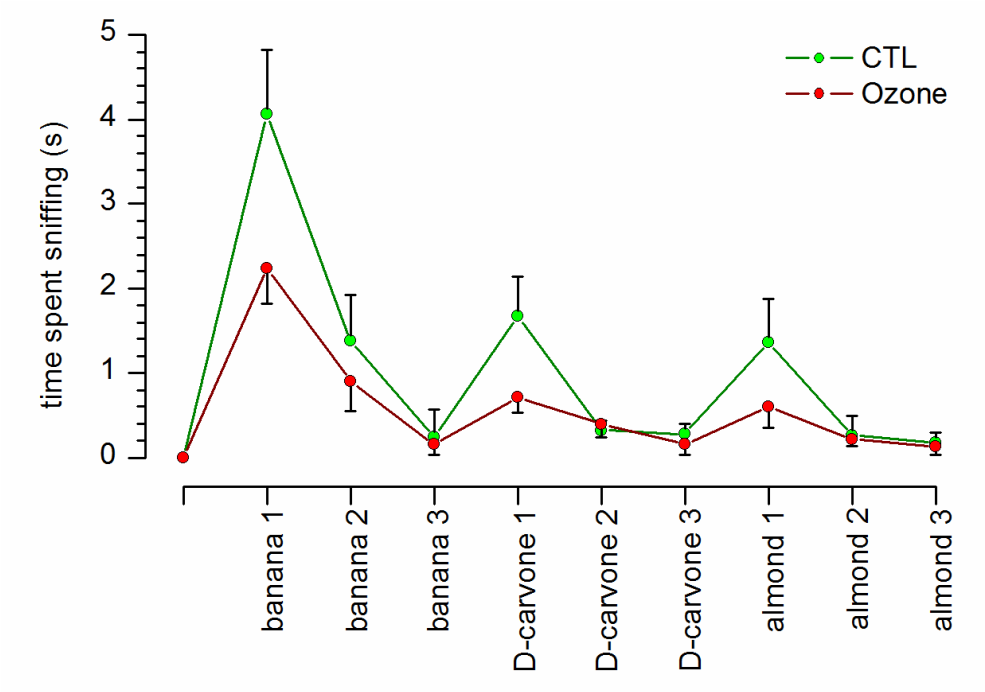

Figure 4. 14: Non-social odours- Swiss Webster male mice. The figure shows the average time spent during sniffing for non-social odours before (green line-CTL) and after ozone exposure (red line) for Swiss Webster mice male.

The representation of the social odours (urine from the same and from opposite sex) is shown in **figure 4.15.** A significant difference was observed between the means of sniffing times before and after O_3 exposure for the social odours from the opposite sex only, P-value <0.01, (the means of sniffing times were: 48.09 s and 20.73 s before and after ozone exposure, respectively).

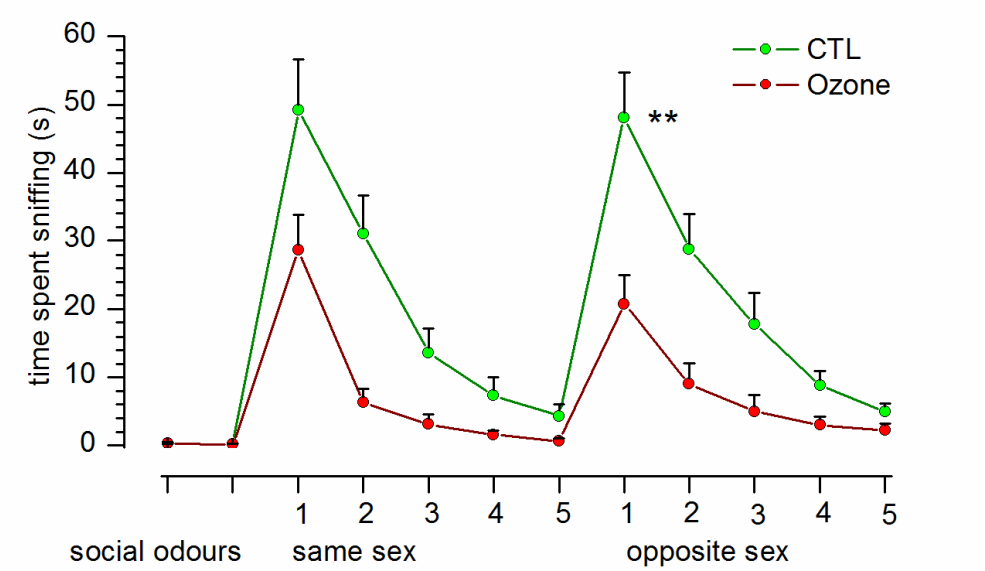

Figure 4. 15: Social odours- Swiss Webster mice male. The figure shows the average times spent during sniffing for social odours before (green line-CTL) and after ozone exposure (red line) for Swiss Webster mice male.

Furthermore, the effect of O_3 exposure on the behavioural repose of Swiss Webster female mice was completely different from males. As shown in **figure 4.16,** a statistical difference was observed between the means of sniffing times before and after O_3 exposure. Furthermore, the P value for the first exposure to banana, first exposure to D-carvone and to the first exposure to almond was $P < 0.01$.

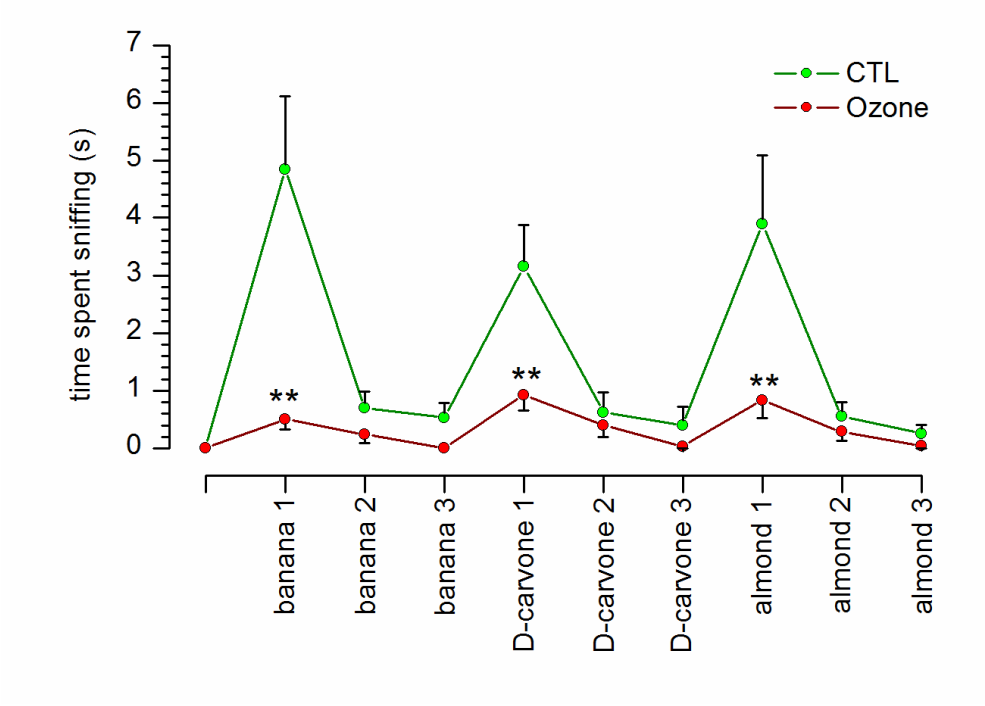

Figure 4. 16: Non-social odours- Swiss Webster mice female. The figure shows the average time spent during sniffing for non-social odours before (green line-CTL) and after O_3 exposure (red line) for Swiss Webster mice female.

Regarding the olfactory response of Swiss Webster female mice to social odours after O_3 exposure as shown in **figure 4.17**, a significant difference was observed between the means of sniffing times before and after O_3 exposure. Furthermore, this statistical significant was observed in the first three exposures to social odours from the same sex with a significant value of $P < 0.01$ in the first representation, of $P < 0.001$ in the second representation and of $P < 0.05$in the third representation.

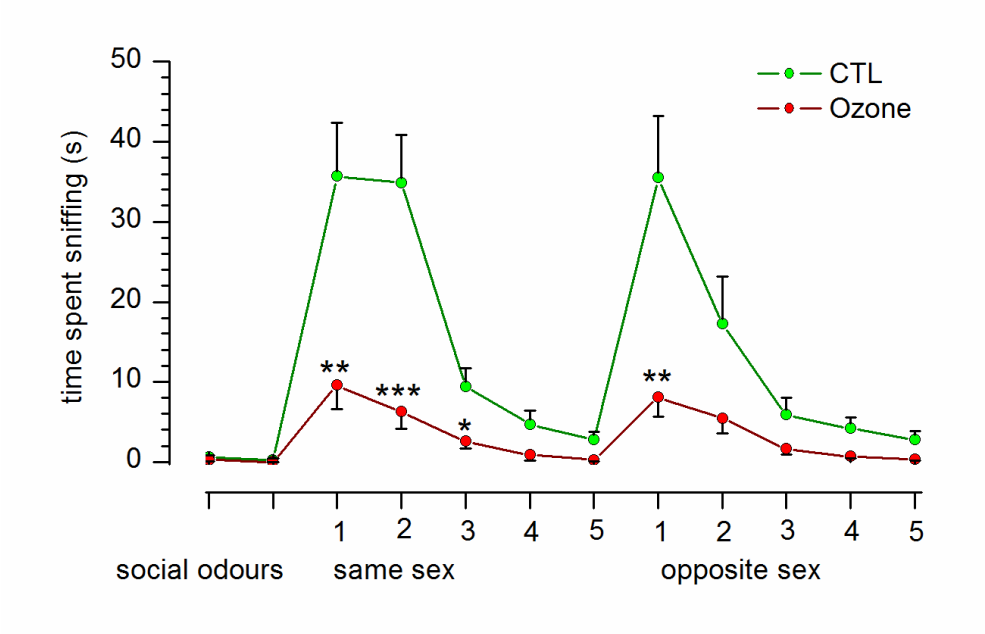

Figure 4. 17: Social odours- Swiss Webster mice female. The figure shows the average time spent during sniffing for social odours before (green line-CTL) and after O_3 exposure (red line) for Swiss Webster mice female.

Also, we aimed to understand the difference in the behavioural response between Swiss Webster male and female mice after O_3 exposure. First the olfactory response to non-social and social odours was compared between the two sexes before O_3 exposure, and the statistical analysis did not show any statistical significant neither for the non-social odours nor the social, **figure 4.18.**

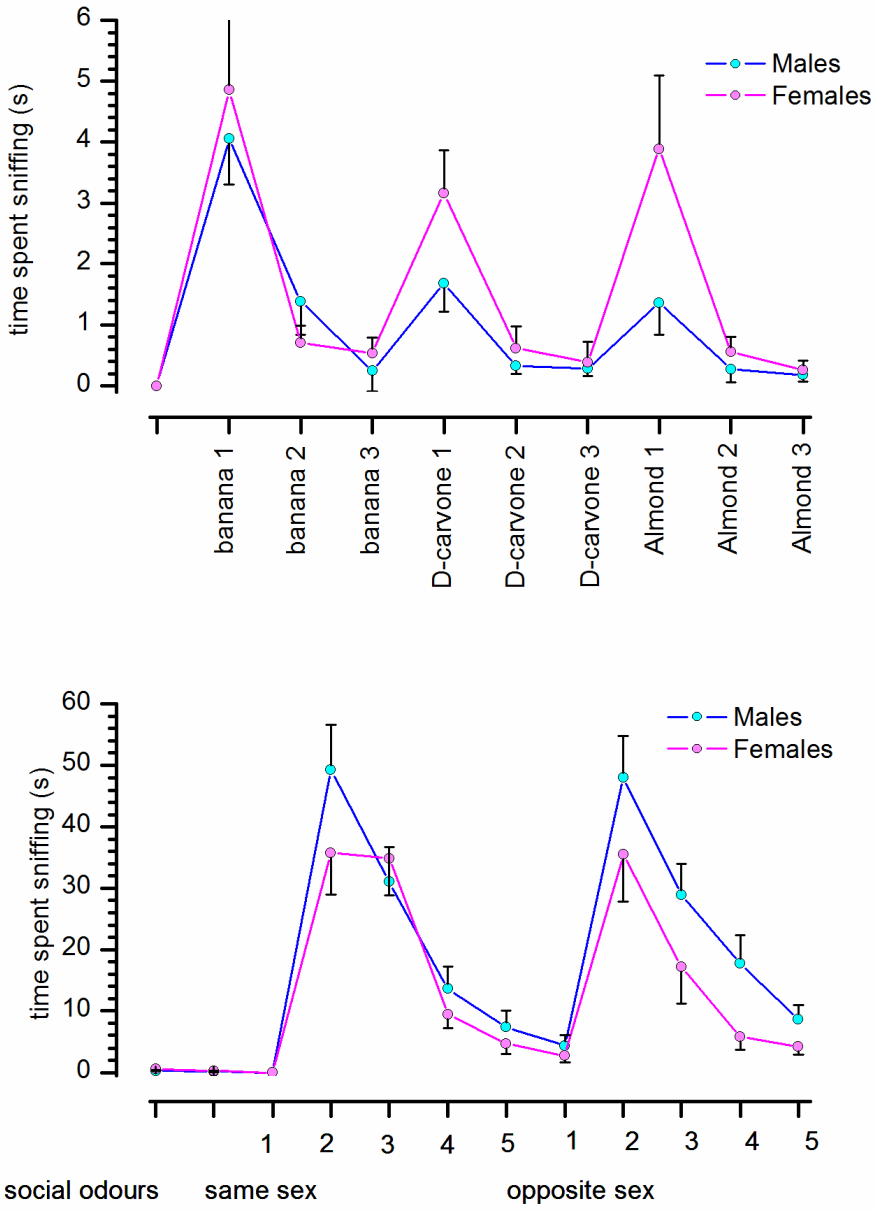

Figure 4. 18: The comparison between Swiss Webster males and females in the behavioural response to non-social and social odours. The figure shows the comparison in the sniffing times for non-social and social odours for Swiss Webster males (blue line) and females (purple line) before O_3 exposure.

As shown in **figure 4.19**, the statistical analysis showed a significant difference ($P < 0.01$) in the behavioural response to non-social odours after O_3 exposure. This difference was observed after the first exposure to banana (banana1), in both sexes. However, the difference between the two groups (males and females) for the other non-social odours did not show any statistical significant.

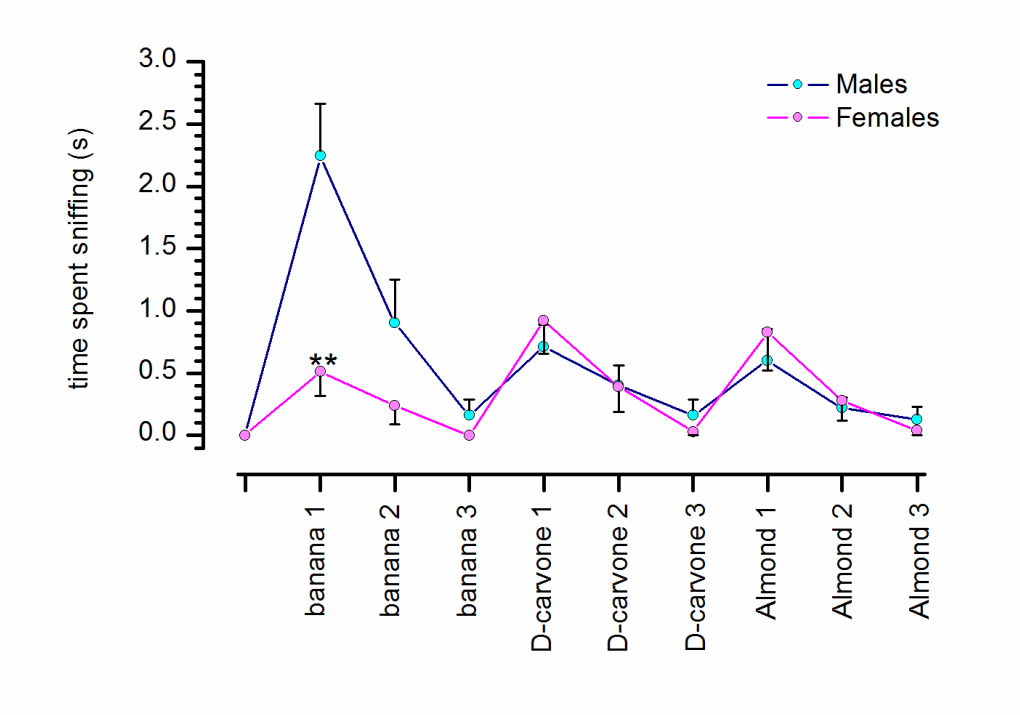

Figure 4. 19: Non-social odours -comparison between Swiss Webster male and female mice. The figure shows the comparison between the sniffing times for non-social odours for Swiss Webster males (blue line) and females (purple line) after O_3 exposure.

In addition, the comparisons of the behavioural response to social odours after O_3 exposure between Swiss Webster males and females is shown in **figure 4.20**. The statistical analysis showed a great significant difference to the first represented social odours, either from the same sex (same sex 1, $P < 0.01$) or from the opposite sex (opposite sex 1, $P < 0.05$).

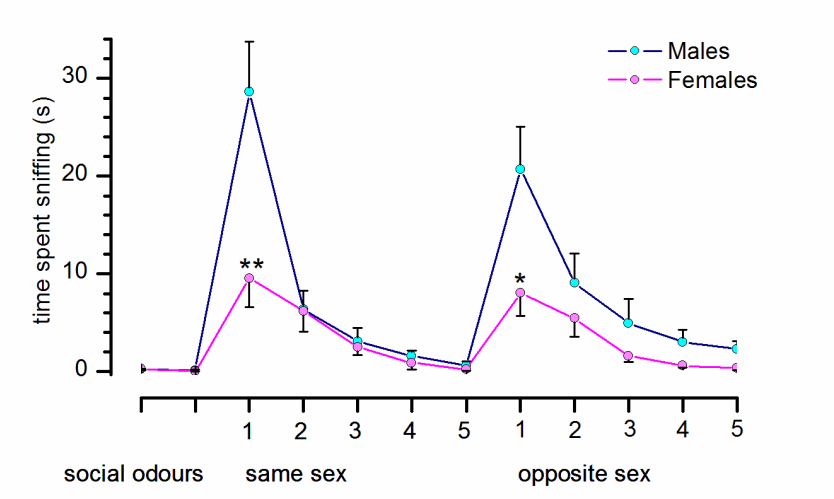

Figure 4. 20: Social odours -comparison between Swiss Webster male and female mice. The figure shows the comparison in the sniffing times for social odours for Swiss Webster males (blue line) and females (purple line) after O_3 exposure.

Moreover, for better understanding the phenomenon of habituation, normalization was carried out for the means of sniffing time for Swiss Webster male and female mice. The result showed a significant difference in the behavioural response to social odours from the same sex only. In addition, Swiss Webster female mice showed slower habituation, which indicated greater sensitivity to O_3 exposure, **figure 4.21.**

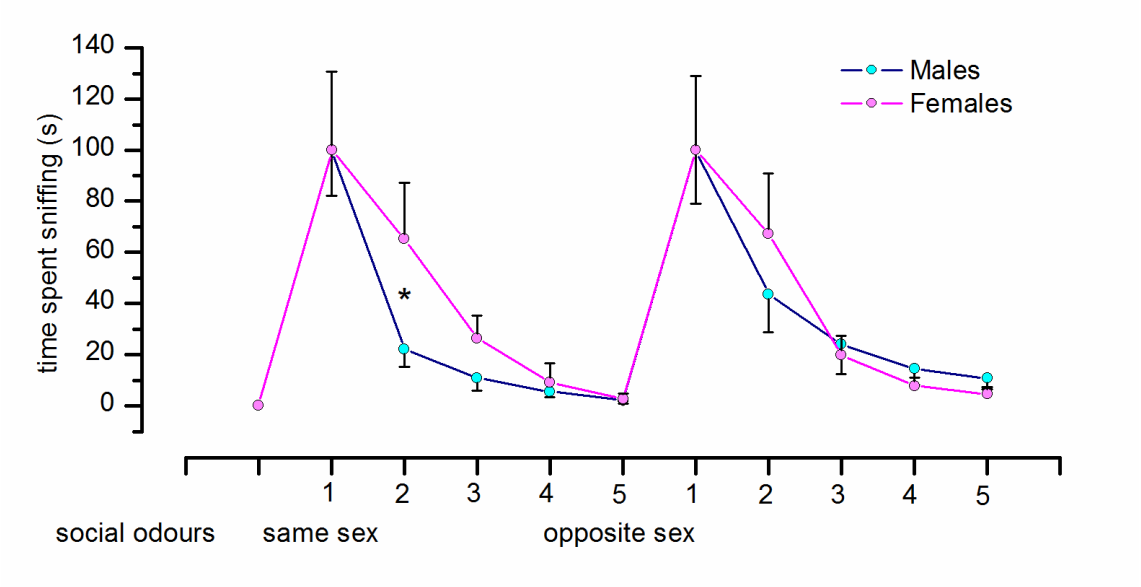

Figure 4. 21: The normalization of the behavioural response after O_3 exposure of Swiss Webster male and female mice. The figure shows the normalized values of the sniffing times for social and non-social odours between Swiss Webster males (blue line) and females (purple line) after ozone exposure.

5. DISCUSSION

In this work, we aimed to understand the effect(s) of environmental O_3 exposure on the olfactory bulb of two different mouse strains from biochemical, electrophysiological and behavioural point of view.

We used two different mouse strains basing on the results of other researchers. They found that the genetic variability plays an important role in the predisposition of the environmental diseases. In addition, studies on human and animal models revealed that O_3 toxicity is species and strain dependent, (Kleeberger et al., 2000; Prows et al., 1997; Savov et al., 2004; Vancza et al., 2009).

5.1 Biochemical study

In the biochemical experiments, we aimed to test the biological harmful effect(s) of O_3 exposure, on 15 Swiss Webster and 17 C57/J6 mice strains, compared to 7 and 8 air exposed mice from the two strains respectively, using biochemical techniques.

First in the preliminary study, we aimed to proof the harmful effect of O_3 exposure on the OB of 0.2ppm O_3 dose for 2h/2times /1day exposed mice by measuring the level of OB 4HNE and total proteins. The immune western blot results showed statistical significant increase in the OB 4HNE and total proteins levels. Also, the body weight of the O_3 exposed mice was statistically reduced after the exposure. Then, we decided to increase the days of exposure to two days because the exposed mice did not suffer.

Interestingly in our results, acute O_3 exposure (0.5ppm/30 min/once, 0.5ppm/60 min/once) and chronic exposure (0.2ppm/2h/2times/2days) showed definitive biochemical results on the effect(s) of O_3 exposure on Swiss Webster mice by showing an increase in the OB CYP1A1 and OB proteins levels in the two exposure conditions. While, the 4HNE level of the O_3 exposed mice was significantly increased after acute O_3 exposure for long duration (0.5ppm/60min/once) and chronic O_3 exposure (0.2ppm/2h/2times/2days) with a significant increase in the plasma 4HNE of the later exposure condition. However, acute O_3 exposure for short duration (0.5ppm/30 min/once) did not show any statistical significant in the 4HNE level of the O_3 exposed mice in comparison to non-O_3 exposed mice.

Our findings concerning the increase in the 4HNE and total proteins levels following O_3 exposure are similar to other published data. Connor et al., (2012) exposed TLR4 mutant C3H/HeJ mice to 0.8ppm O_3 dose for 8 hours to study the effects of O_3 exposure on the

lung. He found an increase in two oxidative stress biomarkers level: 4-hydroxynonenal modified protein, bronchoalveolar lavage lipocalin 24p3 and in lipid peroxidation level as well in the O_3 exposed mice compared to non-O_3 exposed mice. Another study in human bronchoalveolar lavage cells conducted by Hamilton et al., (1998) demonstrated the role of 4HNE in the toxicity of human lung cells after O_3 exposure. Furthermore, the results obtained by Fakhrzadeh et al., (2004b) showed a significant increase in bronchoalveolar lavage fluid protein, lung macrophages and 4-hydroxyalkenals in the lung of 0.8ppm O_3 exposed wild-type mice for 3hours. Also, another study by Kirichenko et al., (1996) demonstrate that HNE is formed *in vivo* in C3H/HeJ mice following exposure to 2.0 ppm and 0.25 ppm O_3 doses for 3 hours.

Our results regarding the increase of CYP1A1 level after O_3 exposure are similar to two studies on human epidermal keratinocytes exposed to 0.3 ppm O_3 dose, by Afaq et al., (2009) and Zaid et al., (2008) resulted in an increase in protein and mRNA expression of CYP1A1, CYP1A2, and CYP1B1 isoforms.

From our biochemical results concerning Swiss Webster mice, we could suggest an alteration in the OB cells due to the generated oxidative stress state following O_3 exposure. This assumption is supported by Colín-Barenque et al., (1999) work. He exposed rats to 1-1.5 ppm for 4 hours, to study the morphological changes of rats OB after O_3 exposure. His results indicated an alteration in the granule layer of the olfactory bulb which was indicated by a significant loss of dendritic spines on primary and secondary dendrites of OB granule cells, dilation cisterns of the rough endoplasmic reticulum, swelling of Golgi apparatus and mitochondrion and vacuolation of neuronal cytoplasm.

In addition, our results concerning the effect of acute O_3 exposure on C57BL/J6 mice did not show any statistical significant in the 4HNE (OB and plasma) after acute O_3 exposure (0.5ppm/30 min/once) and chronic exposure (0.8ppm/2h/2times/5days) for the two phenotypes. Furthermore, the statistical analysis of the total OB proteins showed insignificant results after acute (0.5ppm/30 min/once and 0.5ppm/60 min/once) and chronic (0.8ppm/2h/2times/5days) exposure conditions. Moreover, acute and chronic O_3 exposures did not show any statistical difference in the CYP1A1 level of the WT C57BL/J6 O_3 exposed mice compared to air exposed mice. However, this oxidative stress biomarker was completely absent in OB of the C57BL/J6 GFP phenotype.

Our findings concerning the effect(s) of different O_3 doses on C57BL/6J mice did not match with what has been published by many researchers` work. For example : Watkinson

et al., (1996) exposed C57BL/6J (B6) and C3H/HeJ (C3) mice to 2ppm O_3 dose for 2h to study O_3 toxicity in mice. He observed significant decrease in the core body temperature during O_3 exposure in the two strains. In addition, the response of B6 mice was less dynamic than that of C3 mice. Also, both strains showed a significant change in the level of O_3 toxicity biomarkers. Furthermore, there was a significant increase in BAL fluid protein level and cells number at 22 h after the exposure, and the percentage of neutrophil cells was significantly less in C57/J6 mice strain in comparison to C3H/HeJ strain.

Also, Kleeberger et al., (1993), used less O_3 doses to study the susceptibility of mice to ozone-induced inflammation. In his study, he exposed C57BL/J6 (B6) and C3 mice to 0.12 and 0.30 ppm O_3 doses for 72 hours, he found a significant increase in the total BAL protein level, polymorphonuclear leukocytes, lymphocytes, and in the alveolar macrophages. In contrast, his results concerning 0.30 ppm O_3 dose showed a significant greater number of inflammatory cells and broncheoalveolar protein level in B6 mice compared to C3 mice strain.

Moreover, some in vivo studies tested the effect of different O_3 doses on C57BL/6J mice. Pulfer et al., (2005) exposed C57BL/6J mice to varying O_3 concentrations (0.5-3.0 ppm) for 3 hours to study the effect of O_3 exposure on the lung toxicity. He found that β-epoxide and 6-oxo-3,5-diol have a role in O_3 toxicity in the lung of the exposed mice. In addition, the formation of these compounds was detected after the exposure to 0.5 ppm O_3 dose. Also, Johnston et al., (1999) exposed the same strain to 0.3 ppm O_3 for 0, 24, or 96 hours, 1.0 ppm O_3 dose for 0, 1, 2, or 4 hours, or 2.5 ppm O_3 dose for 0, 2, 4, or 24 hours, to observe the effect of O_3 exposure on the inflammatory and antioxidant gene expression in C57BL/6J mice. His results indicated that after 24h of O_3 exposure to 0.3 ppm there was an increases in mRNA abundance for messages encoding macrophage inflammatory protein (MIP)-1 alpha, MIP-2 and eotaxin. This increase was persisted through 96h of exposure. At the same time, messages encoding lymphotactin and metallothionein were also increased. In addition, after 4 hours of 1.0 ppm O_3 exposure the same molecules were increased with an increase in the abundance of Mt mRNA after 1 hour of O_3 exposure and persisted through 4 hours. After 2 hours of 2.5 ppm O_3 exposure, the same increase was observed and persisted through the 4 hours of exposure. Furthermore, the lung weights of the O_3 exposed mice to 2.5 ppm dose for 24 hours were approximately 2 times greater than control mice. However, 2.5 ppm O_3 dose became lethal after 36 hours of exposure, at that time there was an increase in mRNAs code for eotaxin, MIP-1 alpha, MIP-2, and Mt at higher levels than those detected after 2 and 4 hours of ozone exposure.

Moreover, in our results we observed a significant decrease in the body weight of the O_3 exposed mice of the two strains compared to the air exposed mice, except for acute O_3 exposed C57BL/J6 WT mice (0.5ppm/60min/once), and (0.5ppm/30min/once) Swiss Webster mice, as the difference in the body weight before and after O_3 was statistically insignificant, this might be due to the decreased number and variation in the sex of the tested mice. Because Vancza et al., (2009) found that the sensitivity of mice lung to the inhaled O_3 is affected by mice gender.

In addition, we correlate the decrease in the body weight following O_3 exposure to the effect of O_3 on lipid peroxidation level. This presumption is supported by several published experimental findings. Rivas-Arancibia et al., (1998, 2000, 2003, 2010) correlated the increase in lipid peroxidation level in different brain structures to the generated oxidative stress following O_3 exposure. In addition, Pereyra-Muñoz et al., (2006), observed an increased in lipid peroxidation level after exposing Wister rates to 0.25ppm O_3 dose for 4h daily for different exposure durations.

From all of our biochemical results we conclude that C57BL/6J mice are more resistance to O_3 exposure than Swiss Webster mice. In addition, the oxidative stress state following O_3 exposure caused deterioration the OB of Swiss Webster mice, which was evidenced by the increase of the oxidative stress biomarkers and elevation of OB total proteins. Moreover, O_3 caused a reduction in the body weight of the exposed mice regardless their strain.

5. 2 Electrophysiological study

Up to date, this study provides the first electrophysiological report on the effect of environmental O_3 exposure on the OB dopaminergic cells of mouse strain.

The idea of carrying out this experimental approach arose from the results of previous experimental studies which reported the death of DA cell due to ozone exposure in different brain regions. Pereyra-Muñoz et al., (2006) found that, the neurons of the *striatum* and *substantia nigra* in rats were damaged following chronic ozone exposure. Also, another study in rat *substantia nigra*, by Santiago-López et al., (2010) reported a decrease in the number of dopaminergic neurons and an increase in the p53-immunoreactive cells, with an increase in the levels of the dopamine Quinones (DAQ) in the plasma, which were correlated with lipid peroxide levels. Therefore, these DAQ could be a peripheral oxidative indicator for nigral dopaminergic neurons damage.

Moreover, Rivas-Arancibia et al., (2015) observed in rats exposed to low O_3 doses (0.25 ppm) an inflammation and progressive damage in the *substantia nigra* of O_3 exposed rats. Rivas-Arancibia et al., (2010) studied the effects of oxidative stress in the hippocampus region, they found swelling and morphological changes in the nucleus and in the cytoplasm of the hippocampal neurons, a decrease in Neu-N and doublecortin level, increased number of astrocytes and an increase in lipid peroxidation level.

Our preliminary study concerning the effect of O_3 exposure on the survival of TH-GFP positive cells was conducted in insufficient number of animals to draw a conclusive indication, but we could affirm that no evident differences were observed in controls *vs.* exposed animals.

Regarding our electrophysiological findings, first we tested the effect of O_3 exposure on the spontaneous activity TH-GFP positive cells, an electrophysiological characteristic of all dopaminergic cells, (Pignatelli et al., 2005).

In ozone exposed mice, the TH-GFP positive cells maintained their capability to generate spontaneous action potentials. However, the discharge frequency was significantly reduced and the firing became irregular with bursts followed by long pauses.

In addition, the basic parameters of the excitability profile (resting membrane potential, impedance, rheobase and chronaxie) of the control and O_3 exposed cells were further analysed. Consequently, the result of this analysis indicates an alteration in these parameters after ozone exposure. Furthermore, this alteration indicates a severe reduction in the OB DA cells excitability after O_3 exposure.

5.3 The behavioural experiments

Our electrophysiological results could suggest a functional damage to the dopaminergic neurons of the olfactory bulb. This finding is supported by several experimental studies. The results of these studies showed loss in the ability to discriminate odours as a result of alteration in the dopaminergic receptors or the absence of their transporters (knock-out), (Sullivan and Wilson, 1995; Tillerson et al., 2006).Therefore, we aimed to assess the effect of O_3 exposure on the olfactory response to environmental odours in two different mouse strains.

Our findings indicated a clear deterioration in the olfactory response after O_3 exposure, and this impairment was different among the two mouse strains. So, we suggested that the harmful effect of environmental O_3 exposure is strain dependent. This assumption is

supported by Kleeberger et al., (1990) , Gardi et al., (2012), work. They reported a difference in the inflammatory response between different mouse strains after ozone exposure.

Concerning the C57BL / 6J male mice, the effect of O_3 exposure on the sense of smell was analysed and it indicated a significant difference in the response to the non-social odours only, particularly after the first presentation to banana and D-carvone.

While for Swiss Webster mice, the olfactory response to environmental odours (social and non-social) was analysed before and after O_3 exposure. Furthermore, the result of this analysis was shown separately for males and females to understand the role of sex on the olfactory repose after O_3 exposure. The results indicated that females had greater sensitivity to the harmful effect of O_3 exposure than males. This finding agreed with what has been published by Durrani et al., (2012), Phelps et al., (2012), and Mikerov et al., (2014). In their studies, they found that females were more susceptible to air way inflammation after O_3 exposure rather than males. In addition, this could be attributed to the difference in the sex hormones that influence the response to environmental agents and to the course of the disease in animal models, (Card and Zeldin, 2009).

Moreover, concerning Swiss Webster males, O_3 exposure reduced the sniffing times to the odours to the limit of statistical significance for both non-social and social odours, and this finding could be better understood by increasing the sample size. While the females showed a great decrease in the sniffing times to environmental odours after O_3 exposure and the difference was observed in the social odours only. Furthermore, the statistical analysis showed a significant difference after the presentation of the first odour then for the subsequent representations.

For better understanding the difference between males and females in the olfactory response to environmental odours after O_3 exposure, first a comparison between Swiss Webster males and females before O_3 exposure (control) was performed to verify the absence of any significant difference between the two sexes.

Secondly, the values of sniffing times of the two sexes were compared after ozone exposure and the results showed a greater sensitivity of Swiss Webster female mice to the presented banana odour only. In addition, this sensitivity was obvious in the non-social odours. Moreover, another difference was observed after normalizing the values of sniffing times after O_3 exposure for the social odours. The result showed a significant slower decay

for females which indicated a lesser-rehabituation (a decrease in the mouse ability to recognised an odour as new smell).

Our findings concerning the behavioural results showed a clear effect of O_3 exposure on the olfactory response in all of the tested mice regardless their sex and strain. This finding is supported by the results of Guevara-Guzman et al., (2009) and Arancibia et al., (1998), they found that O_3 concentrations between 0.25 and 1 ppm were capable of altering the olfactory bulb sensitivity and memory response. Moreover, in our work, the olfactory response to social odours was different among the two strains after O_3 exposure.

6. CONCLUSION

We conclude that Swiss Webster mouse strain is more sensitive to O_3 exposure than C57BL/6J mouse strain. In addition, O_3 exposure caused oxidative stress state in Swiss Webster mice OB which was evidenced from the increase of the oxidative stress proteins in the O_3 exposed mice in comparison with the air exposed mice. While the biochemical experiment didn`t show any harmful change in C57BL/6J mouse OB. Nevertheless, the results of the electrophysiological experiment showed normal spontaneous firing activity of the C57BL/6J OB DA cells of the O_3 exposed mice. In addition, these cells showed marked alteration in their excitability profile (resting membrane potential, input impedance, Rheobase and chronaxie) following O_3 exposure. Moreover, O_3 exposure cased marked reduction in the body weight of the O_3 exposed mice regardless their strain. On the other hand, the behavioural experiments indicated an impairment in the olfactory memory response after ozone exposure which was sex dependant.

7. ACKNOWLEDGMENT

This humble work has been completed by the contribution of many people to whom I am thankful.

I would like to express my sincere gratitude to my tutor **Prof. Ottorino Belluzzi,** for his patience, supervision and assistance during my Ph.D study .

My sincere thanks also go to **Prof. Giuseppe Valacchi**, for their help, comments and advices.

I would like to show my deep respect and thanks to **Dr. Angela Pignatelli and Dr. Mascia Benedusi** for their support and the assistance during this work.

Also, I would like to thank **Dr. Franco Cervellati, Dr. Ximena Muresan and Dr. Faride Pighin** for their continuous help and valuable information.

My warm thanks go to **Prof. Naser Eldin Bilal**, previous Dean, Faculty of Medical Laboratory Sciences - University of Khartoum, for his assistance and encouragement

I am greatly indebted to **Dr**. **Yosef Mohamed Azzam** Head Department of histopathology and Cytology -University of Khartoum for his continuous support, encouragement and motivations.

Finally, I would like to thank **University of Khartoum and Ministry of High Education - Sudan** for their financial support and encouragement.

8. REFERENCES

Adelman, R., Saul, R.L., and Ames, B.N. (1988). Oxidative damage to DNA: relation to species metabolic rate and life span. Proc. Natl. Acad. Sci. U. S. A. *85*, 2706–2708.

Afaq, F., Zaid, M.A., Pelle, E., Khan, N., Syed, D.N., Matsui, M.S., Maes, D., and Mukhtar, H. (2009). Aryl hydrocarbon receptor is an ozone sensor in human skin. J. Invest. Dermatol. *129*, 2396–2403.

Ajmani, G.S., Suh, H.H., and Pinto, J.M. (2016). Effects of ambient air pollution exposure on olfaction: a review. Environ. Health Perspect. *124*, 1683–1693.

Allison, A.C., and Warwick, R.T.T. (1949). Quantitative observations on the olfactory system of the rabbit. Brain J. Neurol. *72*, 186–197.

Altman, J. (1962). Are new neurons formed in the brains of adult mammals? Science *135*, 1127–1128.

Altman, J. (1969). Autoradiographic and histological studies of postnatal neurogenesis. IV. Cell proliferation and migration in the anterior forebrain, with special reference to persisting neurogenesis in the olfactory bulb. J. Comp. Neurol. *137*, 433–457.

Altshuller, A.P. (1987). Estimation of the natural background of ozone present at surface rural locations. JAPCA *37*, 1409–1417.

Ames, B.N., Gold, L.S., and Willett, W.C. (1995). The causes and prevention of cancer. Proc. Natl. Acad. Sci. U. S. A. *92*, 5258–5265.

Arbex, M.A., Santos, U. de P., Martins, L.C., Saldiva, P.H.N., Pereira, L.A.A., and Braga, A.L.F. (2012). Air pollution and the respiratory system. J. Bras. Pneumol. *38*, 643–655.

Aroniadou-Anderjaska, V., Ennis, M., and Shipley, M.T. (1997). Glomerular synaptic responses to olfactory nerve input in rat olfactory bulb slices. Neuroscience *79*, 425–434.

Ashley, Z., Sutherland, H., Lanmuller, H., Unger, E., Li, F., Mayr, W., Kern, H., Jarvis, J.C., and Salmons, S. (2005). Determination of the chronaxie and rheobase of denervated limb muscles in conscious rabbits. Artif. Organs *29*, 212–215.

Aviado, D.M., and Salem, H. (1968). Acute effects of air pollutants on the lungs. Arch. Environ. Health Int. J. *16*, 903–907.

Baker, H., and Farbman, A.I. (1993). Olfactory afferent regulation of the dopamine phenotype in the fetal rat olfactory system. Neuroscience *52*, 115–134.

Baker, H., Kawano, T., Margolis, F.L., and Joh, T.H. (1983). Transneuronal regulation of tyrosine hydroxylase expression in olfactory bulb of mouse and rat. J. Neurosci. Off. J. Soc. Neurosci. *3*, 69–78.

Baker, H., Liu, N., Chun, H.S., Saino, S., Berlin, R., Volpe, B., and Son, J.H. (2001). Phenotypic differentiation during migration of dopaminergic progenitor cells to the olfactory bulb. J. Neurosci. Off. J. Soc. Neurosci. *21*, 8505–8513.

Barja, G., and Herrero, A. (2000). Oxidative damage to mitochondrial DNA is inversely related to maximum life span in the heart and brain of mammals. FASEB J. Off. Publ. Fed. Am. Soc. Exp. Biol. *14*, 312–318.

Bassett, D., Elbon-Copp, C., Otterbein, S., Barraclough-Mitchell, H., Delorme, M., and Yang, H. (2001). Inflammatory cell availability affects ozone-induced lung damage. J. Toxicol. Environ. Health A *64*, 547–565.

Batista-Brito, R., Close, J., Machold, R., and Fishell, G. (2008). The distinct temporal origins of olfactory bulb interneuron subtypes. J. Neurosci. *28*, 3966–3975.

Baudouin, C., Charveron, M., Tarroux, R., and Gall, Y. (2002). Environmental pollutants and skin cancer. Cell Biol. Toxicol. *18*, 341–348.

Beckman, K.B., and Ames, B.N. (1998). The free radical theory of aging matures. Physiol. Rev. *78*, 547–581.

Benignus, V.A., and Prah, J.D. (1982). Olfaction: anatomy, physiology and behavior. Environ. Health Perspect. *44*, 15–21.

Berkowicz, D.A., and Trombley, P.Q. (2000). Dopaminergic modulation at the olfactory nerve synapse. Brain Res. *855*, 90–99.

Betarbet, R., Zigova, T., Bakay, R.A., and Luskin, M.B. (1996). Dopaminergic and GABAergic interneurons of the olfactory bulb are derived from the neonatal subventricular zone. Int. J. Dev. Neurosci. Off. J. Int. Soc. Dev. Neurosci. *14*, 921–930.

Björklund, A., and Dunnett, S.B. (2007). Dopamine neuron systems in the brain: an update. Trends Neurosci. *30*, 194–202.

Bocci, V. (1996). Does ozone therapy normalize the cellular redox balance? Implications for therapy of human immunodeficiency virus infection and several other diseases. Med. Hypotheses *46*, 150–154.

Borin, M., Fogli Iseppe, A., Pignatelli, A., and Belluzzi, O. (2014). Inward rectifier potassium (Kir) current in dopaminergic periglomerular neurons of the mouse olfactory bulb. Front. Cell. Neurosci. *8*, 223.

Borisovska, M., Bensen, A., Chong, G., and Westbrook, G.L. (2013). Distinct modes of dopamine and GABA release in a dual transmitter neuron. J. Neurosci. Off. J. Soc. Neurosci. *33*, 1790–1796.

Bradford, M.M. (1976). A rapid and sensitive method for the quantitation of microgram quantities of protein utilizing the principle of protein-dye binding. Anal. Biochem. *72*, 248–254.

Calderón-Garcidueñas, L., Maronpot, R.R., Torres-Jardon, R., Henríquez-Roldán, C., Schoonhoven, R., Acuña-Ayala, H., Villarreal-Calderón, A., Nakamura, J., Fernando, R., Reed, W., et al. (2003). DNA damage in nasal and brain tissues of canines exposed to air pollutants is associated with evidence of chronic brain inflammation and neurodegeneration. Toxicol. Pathol. *31*, 524–538.

Card, J.W., and Zeldin, D.C. (2009). Hormonal influences on lung function and response to environmental agents. Proc. Am. Thorac. Soc. *6*, 588–595.

Carney, J.M., Smith, C.D., Carney, A.M., and Butterfield, D.A. (1994). Aging- and oxygen-induced modifications in brain biochemistry and behavior. Ann. N. Y. Acad. Sci. *738*, 44–53.

Cave, J.W., and Baker, H. (2009). Dopamine systems in the forebrain. Adv. Exp. Med. Biol. *651*, 15–35.

Chang, L.Y., Huang, Y., Stockstill, B.L., Graham, J.A., Grose, E.C., Menache, M.G., Miller, F.J., Costa, D.L., and Crapo, J.D. (1992). Epithelial injury and interstitial fibrosis in the proximal alveolar regions of rats chronically exposed to a simulated pattern of urban ambient ozone. Toxicol. Appl. Pharmacol. *115*, 241–252.

Chao, T.I., Kasa, P., and Wolff, J.R. (1997). Distribution of astroglia in glomeruli of the rat main olfactory bulb: exclusion from the sensory subcompartment of neuropil. J. Comp. Neurol. *388*, 191–210.

Colín-Barenque, L., Avila-Costa, M.R., Fortoul, T., Rugerio-Vargas, C., Machado-Salas, J.P., Espinosa-Villanueva, J., and Rivas-Arancibia, S. (1999). Morphologic alteration of the olfactory bulb after acute ozone exposure in rats. Neurosci. Lett. *274*, 1–4.

Connor, A.J., Laskin, J.D., and Laskin, D.L. (2012). Ozone-induced lung injury and sterile inflammation. Role of toll-like receptor 4. Exp. Mol. Pathol. *92*, 229–235.

Cross, C.E., Reznick, A.Z., Packer, L., Davis, P.A., Suzuki, Y.J., and Halliwell, B. (1992). Oxidative damage to human plasma proteins by ozone. Free Radic. Res. Commun. *15*, 347–352.

De Marchis, S., Bovetti, S., Carletti, B., Hsieh, Y.-C., Garzotto, D., Peretto, P., Fasolo, A., Puche, A.C., and Rossi, F. (2007). Generation of distinct types of periglomerular olfactory bulb interneurons during development and in adult mice: implication for intrinsic properties of the subventricular zone progenitor population. J. Neurosci. Off. J. Soc. Neurosci. *27*, 657–664.

Dorado-Martínez, C., Paredes-Carbajal, C., Mascher, D., Borgonio-Pérez, G., and Rivas-Arancibia, S. (2001). Effects of different ozone doses on memory, motor activity and lipid peroxidation levels, in rats. Int. J. Neurosci. *108*, 149–161.

Doty, R.L. (2012). Olfactory dysfunction in Parkinson disease. Nat. Rev. Neurol. *8*, 329–339.

Durrani, F., Phelps, D.S., Weisz, J., Silveyra, P., Hu, S., Mikerov, A.N., and Floros, J. (2012). Gonadal hormones and oxidative stress interaction differentially affects survival of male and female mice after lung Klebsiella pneumoniae infection. Exp. Lung Res. *38*, 165–172.

Ennis, M., Zimmer, L.A., and Shipley, M.T. (1996). Olfactory nerve stimulation activates rat mitral cells via NMDA and non-NMDA receptors in vitro. Neuroreport *7*, 989–992.

Ennis, M., Zhou, F.M., Ciombor, K.J., Aroniadou-Anderjaska, V., Hayar, A., Borrelli, E., Zimmer, L.A., Margolis, F., and Shipley, M.T. (2001). Dopamine D2 receptor-mediated presynaptic inhibition of olfactory nerve terminals. J. Neurophysiol. *86*, 2986–2997.

Fabbri, L.M., Aizawa, H., Alpert, S.E., Walters, E.H., O'Byrne, P.M., Gold, B.D., Nadel, J.A., and Holtzman, M.J. (1984). Airway hyperresponsiveness and changes in cell counts in bronchoalveolar lavage after ozone exposure in dogs. Am. Rev. Respir. Dis. *129*, 288–291.

Fakhrzadeh, L., Laskin, J.D., and Laskin, D.L. (2004a). Ozone-induced production of nitric oxide and TNF-alpha and tissue injury are dependent on NF-kappaB p50. Am. J. Physiol. Lung Cell. Mol. Physiol. *287*, L279-285.

Fakhrzadeh, L., Laskin, J.D., Gardner, C.R., and Laskin, D.L. (2004b). Superoxide dismutase–overexpressing mice are resistant to ozone-induced tissue injury and increases in nitric oxide and tumor necrosis factor-α. Am. J. Respir. Cell Mol. Biol. *30*, 280–287.

Feigenspan, A., Gustincich, S., Bean, B.P., and Raviola, E. (1998). Spontaneous activity of solitary dopaminergic cells of the retina. J. Neurosci. Off. J. Soc. Neurosci. *18*, 6776–6789.

Fukagawa, N.K., Timblin, C.R., Buder-Hoffman, S., and Mossman, B.T. (2000). Strategies for evaluation of signaling pathways and transcription factors altered in aging. Antioxid. Redox Signal. *2*, 379–389.

Gaboriau, F., Morlière, P., Marquis, I., Moysan, A., Goegze, M., and Dubertret, L. (1993). Membrane damage induced in cultured human skin fibroblasts by Uva irradiation. Photochem. Photobiol. *58*, 515–520.

Gall, C.M., Hendry, S.H., Seroogy, K.B., Jones, E.G., and Haycock, J.W. (1987). Evidence for coexistence of GABA and dopamine in neurons of the rat olfactory bulb. J. Comp. Neurol. *266*, 307–318.

Gardi, C., and Valacchi, G. (2012). Cigarette smoke and ozone effect on murine inflammatory responses. Ann. N. Y. Acad. Sci. *1259*, 104–111.

Getchell, T.V., and Shepherd, G.M. (1978). Responses of olfactory receptor cells to step pulses of odour at different concentrations in the salamander. J. Physiol. *282*, 521–540.

Golowasch, J., Thomas, G., Taylor, A.L., Patel, A., Pineda, A., Khalil, C., and Nadim, F. (2009). Membrane capacitance measurements revisited: dependence of capacitance value on measurement method in nonisopotential neurons. J. Neurophysiol. *102*, 2161–2175.

Grace, A.A., and Onn, S.P. (1989). Morphology and electrophysiological properties of immunocytochemically identified rat dopamine neurons recorded in vitro. J. Neurosci. Off. J. Soc. Neurosci. *9*, 3463–3481.

Guevara-Guzmán, R., Arriaga, V., Kendrick, K.M., Bernal, C., Vega, X., Mercado-Gómez, O.F., and Rivas-Arancibia, S. (2009). Estradiol prevents ozone-induced increases in brain lipid peroxidation and impaired social recognition memory in female rats. Neuroscience *159*, 940–950.

Haddad, E.B., Salmon, M., Koto, H., Barnes, P.J., Adcock, I., and Chung, K.F. (1996). Ozone induction of cytokine-induced neutrophil chemoattractant (CINC) and nuclear factor-kappa b in rat lung: inhibition by corticosteroids. FEBS Lett. *379*, 265–268.

Hainsworth, A.H., Röper, J., Kapoor, R., and Ashcroft, F.M. (1991). Identification and electrophysiology of isolated pars compacta neurons from guinea-pig substantia nigra. Neuroscience *43*, 81–93.

Halász, N. (1990). The vertebrate olfactory system: chemical neuroanatomy, function, and development (Akadémiai Kiadó).

Hálasz, N., and Greer, C.A. (1993). Terminal arborizations of olfactory nerve fibers in the glomeruli of the olfactory bulb. J. Comp. Neurol. *337*, 307–316.

Halász, N., Johansson, O., Hökfelt, T., Ljungdahl, A., and Goldstein, M. (1981). Immunohistochemical identification of two types of dopamine neuron in the rat olfactory bulb as seen by serial sectioning. J. Neurocytol. *10*, 251–259.

Halliwell, B., and Gutteridge, J.M. (1984). Lipid peroxidation, oxygen radicals, cell damage, and antioxidant therapy. Lancet Lond. Engl. *1*, 1396–1397.

Hamill, O.P., Marty, A., Neher, E., Sakmann, B., and Sigworth, F.J. (1981). Improved patch-clamp techniques for high-resolution current recording from cells and cell-free membrane patches. Pflugers Arch. *391*, 85–100.

Hamilton, R.F., Li, L., Eschenbacher, W.L., Szweda, L., and Holian, A. (1998). Potential involvement of 4-hydroxynonenal in the response of human lung cells to ozone. Am. J. Physiol. *274*, L8-16.

He, Q.C., Tavakkol, A., Wietecha, K., Begum-Gafur, R., Ansari, S.A., and Polefka, T. (2006). Effects of environmentally realistic levels of ozone on stratum corneum function. Int. J. Cosmet. Sci. *28*, 349–357.

Hinds, J.W. (1968a). Autoradiographic study of histogenesis in the mouse olfactory bulb. I. Time of origin of neurons and neuroglia. J. Comp. Neurol. *134*, 287–304.

Hinds, J.W. (1968b). Autoradiographic study of histogenesis in the mouse olfactory bulb. II. Cell proliferation and migration. J. Comp. Neurol. *134*, 305–322.

Holtzman, M.J., Fabbri, L.M., O'Byrne, P.M., Gold, B.D., Aizawa, H., Walters, E.H., Alpert, S.E., and Nadel, J.A. (1983). Importance of airway inflammation for hyperresponsiveness induced by ozone. Am. Rev. Respir. Dis. *127*, 686–690.

Hsia, A.Y., Vincent, J.D., and Lledo, P.M. (1999). Dopamine depresses synaptic inputs into the olfactory bulb. J. Neurophysiol. *82*, 1082–1085.

Jackowski, A., Parnavelas, J.G., and Lieberman, A.R. (1978). The reciprocal synapse in the external plexiform layer of the mammalian olfactory bulb. Brain Res. *159*, 17–28.

Joh, T.H., Geghman, C., and Reis, D. (1973). Immunochemical demonstration of increased accumulation of tyrosine hydroxylase protein in sympathetic ganglia and adrenal medulla elicited by reserpine. Proc. Natl. Acad. Sci. U. S. A. *70*, 2767–2771.

Johnson, M. (2016). Laboratory Mice and Rats. Mater. Methods.

Johnston, C.J., Stripp, B.R., Reynolds, S.D., Avissar, N.E., Reed, C.K., and Finkelstein, J.N. (1999). Inflammatory and antioxidant gene expression in C57BL/6J mice after lethal and sublethal ozone exposures. Exp. Lung Res. *25*, 81–97.

Johnston, R.A., Schwartzman, I.N., Flynt, L., and Shore, S.A. (2005). Role of interleukin-6 in murine airway responses to ozone. Am. J. Physiol. Lung Cell. Mol. Physiol. *288*, L390-397.

Kampa, M., and Castanas, E. (2008). Human health effects of air pollution. Environ. Pollut. Barking Essex 1987 *151*, 362–367.

Karten, B., Beisiegel, U., Gercken, G., and Kontush, A. (1997). Mechanisms of lipid peroxidation in human blood plasma: a kinetic approach. Chem. Phys. Lipids *88*, 83–96.

Kasowski, H.J., Kim, H., and Greer, C.A. (1999). Compartmental organization of the olfactory bulb glomerulus. J. Comp. Neurol. *407*, 261–274.

Kelly, F.J., and Fussell, J.C. (2011). Air pollution and airway disease. Clin. Exp. Allergy J. Br. Soc. Allergy Clin. Immunol. *41*, 1059–1071.

Kendrick, K.M., Guevara-Guzman, R., Zorrilla, J., Hinton, M.R., Broad, K.D., Mimmack, M., and Ohkura, S. (1997). Formation of olfactory memories mediated by nitric oxide. Nature *388*, 670–674.

Kirichenko, A., Li, L., Morandi, M.T., and Holian, A. (1996). 4-Hydroxy-2-nonenal–protein adducts and apoptosis in murine lung cells after acute ozone exposure. Toxicol. Appl. Pharmacol. *141*, 416–424.

Kleeberger, S.R., Bassett, D.J., Jakab, G.J., and Levitt, R.C. (1990). A genetic model for evaluation of susceptibility to ozone-induced inflammation. Am. J. Physiol. *258*, L313-320.

Kleeberger, S.R., Levitt, R.C., and Zhang, L.Y. (1993). Susceptibility to ozone-induced inflammation. I. Genetic control of the response to subacute exposure. Am. J. Physiol. *264*, L15-20.

Kleeberger, S.R., Reddy, S., Zhang, L.Y., and Jedlicka, A.E. (2000). Genetic susceptibility to ozone-induced lung hyperpermeability: role of toll-like receptor 4. Am. J. Respir. Cell Mol. Biol. *22*, 620–627.

Kodavanti, U.P., Costa, D.L., Dreher, K.L., Crissman, K., and Hatch, G.E. (1995). Ozone-induced tissue injury and changes in antioxidant homeostasis in normal and ascorbate-deficient guinea pigs. Biochem. Pharmacol. *50*, 243–251.

Kohen, R. (1999). Skin antioxidants: their role in aging and in oxidative stress--new approaches for their evaluation. Biomed. Pharmacother. Biomedecine Pharmacother. *53*, 181–192.

Koren, H.S., Devlin, R.B., Graham, D.E., Mann, R., McGee, M.P., Horstman, D.H., Kozumbo, W.J., Becker, S., House, D.E., and McDonnell, W.F. (1989). Ozone-induced inflammation in the lower airways of human subjects. Am. Rev. Respir. Dis. *139*, 407–415.

Kosaka, K., and Kosaka, T. (2005). Synaptic organization of the glomerulus in the main olfactory bulb: compartments of the glomerulus and heterogeneity of the periglomerular cells. Anat. Sci. Int. *80*, 80–90.

Kosaka, K., and Kosaka, T. (2007). Chemical properties of type 1 and type 2 periglomerular cells in the mouse olfactory bulb are different from those in the rat olfactory bulb. Brain Res. *1167*, 42–55.

Kosaka, T., and Kosaka, K. (2008). Tyrosine hydroxylase-positive GABAergic juxtaglomerular neurons are the main source of the interglomerular connections in the mouse main olfactory bulb. Neurosci. Res. *60*, 349–354.

Kosaka, T., and Kosaka, K. (2009). Olfactory Bulb Anatomy. In Encyclopedia of Neuroscience, (Oxford: Academic Press), pp. 59–69.

Kosaka, T., and Kosaka, K. (2011). “Interneurons” in the olfactory bulb revisited. Neurosci. Res. *69*, 93–99.

Kosaka, K., Toida, K., Margolis, F.L., and Kosaka, T. (1997). Chemically defined neuron groups and their subpopulations in the glomerular layer of the rat main olfactory bulb--II. Prominent differences in the intraglomerular dendritic arborization and their relationship to olfactory nerve terminals. Neuroscience *76*, 775–786.

Kosaka, K., Toida, K., Aika, Y., and Kosaka, T. (1998). How simple is the organization of the olfactory glomerulus?: the heterogeneity of so-called periglomerular cells. Neurosci. Res. *30*, 101–110.

Kosaka, T., Hataguchi, Y., Hama, K., Nagatsu, I., and Wu, J.Y. (1985). Coexistence of immunoreactivities for glutamate decarboxylase and tyrosine hydroxylase in some neurons in the periglomerular region of the rat main olfactory bulb: possible coexistence of gamma-aminobutyric acid (GABA) and dopamine. Brain Res. *343*, 166–171.

Kratskin, I., and Belluzzi, O. (2003). Anatomy and Neurochemistry of the Olfactory Bulb. In Handbook of Olfaction and Gustation, (CRC Press), p.

Laskin, D.L., Pendino, K.J., Punjabi, C.J., Rodriguez del Valle, M., and Laskin, J.D. (1994). Pulmonary and hepatic effects of inhaled ozone in rats. Environ. Health Perspect. *102 Suppl 10*, 61–64.

LaVoie, M.J., and Hastings, T.G. (1999). Peroxynitrite- and nitrite-induced oxidation of dopamine: implications for nitric oxide in dopaminergic cell loss. J. Neurochem. *73*, 2546–2554.

Lawrence, E., Jackson, J.M., and Jackson, A.R.W. (1998). Longman dictionary of environmental science (Harlow, Essex, England: Longman).

Lazarini, F., Gabellec, M.-M., Moigneu, C., de Chaumont, F., Olivo-Marin, J.-C., and Lledo, P.-M. (2014). Adult neurogenesis restores dopaminergic neuronal loss in the olfactory bulb. J. Neurosci. Off. J. Soc. Neurosci. *34*, 14430–14442.

Lee, H., Kim, E.K., Kang, S.W., Kim, J.H., Hwang, H.J., and Kim, T. (2013). Effects of ozone exposure on the ocular surface. Free Radic. Biol. Med. *63*, 78–89.

Lim, Y., Phung, A.D., Corbacho, A.M., Aung, H.H., Maioli, E., Reznick, A.Z., Cross, C.E., Davis, P.A., and Valacchi, G. (2006). Modulation of cutaneous wound healing by ozone: differences between young and aged mice. Toxicol. Lett. *160*, 127–134.

Lippmann, M. (2009). Ozone. In Environmental Toxicants, M. Lippmann, ed. (John Wiley and Sons, Inc.), pp. 869–936.

Lledo, P.-M., Gheusi, G., and Vincent, J.-D. (2005). Information processing in the mammalian olfactory system. Physiol. Rev. *85*, 281–317.

Lynch, C.J. (1969). The so-called Swiss mouse. Lab. Anim. Care *19*, 214–220.

Mackay-Sim, A. (1991). The vertebrate olfactory system: chemical neuroanatomy, function and development. Trends Neurosci. *14*, 476.

Macrides, F., Schoenfeld, T.A., Marchand, J.E., and Clancy, A.N. (1985). Evidence for morphologically, neurochemically and functionally heterogeneous classes of mitral and tufted cells in the olfactory bulb. Chem. Senses *10*, 175–202.

Maher, B.J., and Westbrook, G.L. (2008). Co-transmission of dopamine and GABA in periglomerular cells. J. Neurophysiol. *99*, 1559–1564.

Mahmood, T., and Yang, P.-C. (2012). Western blot: technique, theory, and trouble shooting. North Am. J. Med. Sci. *4*, 429–434.

Matsushita, N., Okada, H., Yasoshima, Y., Takahashi, K., Kiuchi, K., and Kobayashi, K. (2002). Dynamics of tyrosine hydroxylase promoter activity during midbrain dopaminergic neuron development. J. Neurochem. *82*, 295–304.

McLean, J.H., and Shipley, M.T. (1988). Postmitotic, postmigrational expression of tyrosine hydroxylase in olfactory bulb dopaminergic neurons. J. Neurosci. Off. J. Soc. Neurosci. *8*, 3658–3669.

Meisami, E., and Safari, L. (1981). A quantitative study of the effects of early unilateral olfactory deprivation on the number and distribution of mitral and tufted cells and of glomeruli in the rat olfactory bulb. Brain Res. *221*, 81–107.

Mekada, K., Abe, K., Murakami, A., Nakamura, S., Nakata, H., Moriwaki, K., Obata, Y., and Yoshiki, A. (2009). Genetic differences among C57BL/6 substrains. Exp. Anim. *58*, 141–149.

Menzel, D.B. (1984). Ozone: An overview of its toxicity in man and animals. J. Toxicol. Environ. Health *13*, 181–204.

Menzel, D.B. (1994). The toxicity of air pollution in experimental animals and humans: the role of oxidative stress. Toxicol. Lett. *72*, 269–277.

Merkle, F.T., Fuentealba, L.C., Sanders, T.A., Magno, L., Kessaris, N., and Alvarez-Buylla, A. (2014). Adult neural stem cells in distinct microdomains generate previously unknown interneuron types. Nat. Neurosci. *17*, 207–214.

Mikerov, A.N., Phelps, D.S., Gan, X., Umstead, T.M., Haque, R., Wang, G., and Floros, J. (2014). Effect of ozone exposure and infection on bronchoalveolar lavage: sex differences in response patterns. Toxicol. Lett. *230*, 333–344.

Mizrahi, A., Lu, J., Irving, R., Feng, G., and Katz, L.C. (2006). In vivo imaging of juxtaglomerular neuron turnover in the mouse olfactory bulb. Proc. Natl. Acad. Sci. U. S. A. *103*, 1912–1917.

Moran, D.T., Rowley, J.C., Jafek, B.W., and Lovell, M.A. (1982). The fine structure of the olfactory mucosa in man. J. Neurocytol. *11*, 721–746.

Mori, K., Kishi, K., and Ojima, H. (1983). Distribution of dendrites of mitral, displaced mitral, tufted, and granule cells in the rabbit olfactory bulb. J. Comp. Neurol. *219*, 339–355.

Mori, K., Nagao, H., and Yoshihara, Y. (1999). The olfactory bulb: coding and processing of odor molecule information. Science *286*, 711–715.

Morin, J.G., and Hastings, J.W. (1971). Energy transfer in a bioluminescent system. J. Cell. Physiol. *77*, 313–318.

Mudway, I.S., and Kelly, F.J. (2000). Ozone and the lung: a sensitive issue. Mol. Aspects Med. *21*, 1–48.

Mustafa, M.G. (1990). Biochemical basis of ozone toxicity. Free Radic. Biol. Med. *9*, 245–265.

Nagatsu, T., Levitt, M., and Udenfriend, S. (1964). Tyrosine hydroxylase. The initial step in norepinephrine biosynthesis. J. Biol. Chem. *239*, 2910–2917.

Nagayama, S., Takahashi, Y.K., Yoshihara, Y., and Mori, K. (2004). Mitral and tufted cells differ in the decoding manner of odor maps in the rat olfactory bulb. J. Neurophysiol. *91*, 2532–2540.

Neher, E., and Sakmann, B. (1976). Single-channel currents recorded from membrane of denervated frog muscle fibres. Nature *260*, 799–802.

Neuhoff, H., Neu, A., Liss, B., and Roeper, J. (2002). I(h) channels contribute to the different functional properties of identified dopaminergic subpopulations in the midbrain. J. Neurosci. Off. J. Soc. Neurosci. *22*, 1290–1302.

Nichols, B.G., Woods, J.S., Luchtel, D.L., Corral, J., and Koenig, J.Q. (2001). Effects of ozone exposure on nuclear factor-kappaB activation and tumor necrosis factor-alpha expression in human nasal epithelial cells. Toxicol. Sci. Off. J. Soc. Toxicol. *60*, 356–362.

O'Byrne, P.M., Walters, E.H., Gold, B.D., Aizawa, H.A., Fabbri, L.M., Alpert, S.E., Nadel, J.A., and Holtzman, M.J. (1984). Neutrophil depletion inhibits airway hyperresponsiveness induced by ozone exposure. Am. Rev. Respir. Dis. *130*, 214–219.

Olanow, C.W. (1993). A radical hypothesis for neurodegeneration. Trends Neurosci. *16*, 439–444.

Orona, E., Rainer, E.C., and Scott, J.W. (1984). Dendritic and axonal organization of mitral and tufted cells in the rat olfactory bulb. J. Comp. Neurol. *226*, 346–356.

Packer, L., and Valacchi, G. (2002). Antioxidants and the response of skin to oxidative stress: vitamin E as a key indicator. Skin Pharmacol. Appl. Skin Physiol. *15*, 282–290.

Panzanelli, P., Fritschy, J.M., Yanagawa, Y., Obata, K., and Sassoè-Pognetto, M. (2007). GABAergic phenotype of periglomerular cells in the rodent olfactory bulb. J. Comp. Neurol. *502*, 990–1002.

Parrish-Aungst, S., Shipley, M.T., Erdelyi, F., Szabo, G., and Puche, A.C. (2007). Quantitative analysis of neuronal diversity in the mouse olfactory bulb. J. Comp. Neurol. *501*, 825–836.

Pereyra-Muñoz, N., Rugerio-Vargas, C., Angoa-Pérez, M., Borgonio-Pérez, G., and Rivas-Arancibia, S. (2006). Oxidative damage in substantia nigra and striatum of rats chronically exposed to ozone. J. Chem. Neuroanat. *31*, 114–123.

Phelps, D.S., Umstead, T.M., and Floros, J. (2012). Sex differences in the response of the alveolar macrophage proteome to treatment with exogenous surfactant protein-A. Proteome Sci. *10*, 44.

Pignatelli, A., Kobayashi, K., Okano, H., and Belluzzi, O. (2005). Functional properties of dopaminergic neurones in the mouse olfactory bulb. J. Physiol. *564*, 501–514.

Pignatelli, A., Ackman, J.B., Vigetti, D., Beltrami, A.P., Zucchini, S., and Belluzzi, O. (2009). A potential reservoir of immature dopaminergic replacement neurons in the adult mammalian olfactory bulb. Pflugers Arch. *457*, 899–915.

Pignatelli, A., Borin, M., Fogli Iseppe, A., Gambardella, C., and Belluzzi, O. (2013). The h-current in periglomerular dopaminergic neurons of the mouse olfactory bulb. PloS One *8*, e56571.

Pinching, A.J., and Powell, T.P.S. (1971). The Neuropil of the Glomeruli of the Olfactory Bulb. J. Cell Sci. *9*, 347–377.

Prasher, D.C., Eckenrode, V.K., Ward, W.W., Prendergast, F.G., and Cormier, M.J. (1992). Primary structure of the Aequorea victoria green-fluorescent protein. Gene *111*, 229–233.

Price, J.L., and Powell, T.P. (1970a). The mitral and short axon cells of the olfactory bulb. J. Cell Sci. *7*, 631–651.

Price, J.L., and Powell, T.P. (1970b). The synaptology of the granule cells of the olfactory bulb. J. Cell Sci. *7*, 125–155.

Price, J.L., and Powell, T.P.S. (1970c). The Morphology of the Granule Cells of the Olfactory Bulb. J. Cell Sci. *7*, 91–123.

Prows, D.R., Shertzer, H.G., Daly, M.J., Sidman, C.L., and Leikauf, G.D. (1997). Genetic analysis of ozone-induced acute lung injury in sensitive and resistant strains of mice. Nat. Genet. *17*, 471–474.

Pulfer, M.K., Taube, C., Gelfand, E., and Murphy, R.C. (2005). Ozone exposure in vivo and formation of biologically active oxysterols in the lung. J. Pharmacol. Exp. Ther. *312*, 256–264.

Puopolo, M., and Belluzzi, O. (1998). Functional heterogeneity of periglomerular cells in the rat olfactory bulb. Eur. J. Neurosci. *10*, 1073–1083.

Rahman, I., Clerch, L.B., and Massaro, D. (1991). Rat lung antioxidant enzyme induction by ozone. Am. J. Physiol. *260*, L412-418.

Rall, W., Shepherd, G.M., Reese, T.S., and Brightman, M.W. (1966). Dendrodendritic synaptic pathway for inhibition in the olfactory bulb. Exp. Neurol. *14*, 44–56.

Rittié, L., and Fisher, G.J. (2002). UV-light-induced signal cascades and skin aging. Ageing Res. Rev. *1*, 705–720.

Rivas-Arancibia, S., Vazquez-Sandoval, R., Gonzalez-Kladiano, D., Schneider-Rivas, S., and Lechuga-Guerrero, A. (1998). Effects of ozone exposure in rats on memory and levels of brain and pulmonary superoxide dismutase. Environ. Res. *76*, 33–39.

Rivas-Arancibia, S., Dorado-Martínez, C., Borgonio-Pérez, G., Hiriart-Urdanivia, M., Verdugo-Diaz, L., Durán-Vázquez, A., Colin-Baranque, L., and Avila-Costa, M.R. (2000).

Effects of taurine on ozone-induced memory deficits and lipid peroxidation levels in brains of young, mature, and old rats. Environ. Res. *82*, 7–17.

Rivas-Arancibia, S., Dorado-Martínez, C., Colin-Barenque, L., Kendrick, K.M., de la Riva, C., and Guevara-Guzmán, R. (2003). Effect of acute ozone exposure on locomotor behavior and striatal function. Pharmacol. Biochem. Behav. *74*, 891–900.

Rivas-Arancibia, S., Guevara-Guzmán, R., López-Vidal, Y., Rodríguez-Martínez, E., Zanardo-Gomes, M., Angoa-Pérez, M., and Raisman-Vozari, R. (2010). Oxidative stress caused by ozone exposure induces loss of brain repair in the hippocampus of adult rats. Toxicol. Sci. Off. J. Soc. Toxicol. *113*, 187–197.

Rivas-Arancibia, S., Zimbrón, L.F.H., Rodríguez-Martínez, E., Maldonado, P.D., Borgonio Pérez, G., and Sepúlveda-Parada, M. (2015). Oxidative stress-dependent changes in immune responses and cell death in the substantia nigra after ozone exposure in rat. Front. Aging Neurosci. *7*, 65.

Salvi, S. (2001). Pollution and allergic airways disease. Curr. Opin. Allergy Clin. Immunol. *1*, 35–41.

Sánchez-Andrade, G., James, B.M., and Kendrick, K.M. (2005). Neural encoding of olfactory recognition memory. J. Reprod. Dev. *51*, 547–558.

Santiago-López, D., Bautista-Martínez, J.A., Reyes-Hernandez, C.I., Aguilar-Martínez, M., and Rivas-Arancibia, S. (2010). Oxidative stress, progressive damage in the substantia nigra and plasma dopamine oxidation, in rats chronically exposed to ozone. Toxicol. Lett. *197*, 193–200.

Savov, J.D., Whitehead, G.S., Wang, J., Liao, G., Usuka, J., Peltz, G., Foster, W.M., and Schwartz, D.A. (2004). Ozone-induced acute pulmonary injury in inbred mouse strains. Am. J. Respir. Cell Mol. Biol. *31*, 69–77.

Sawamoto, K., Nakao, N., Kobayashi, K., Matsushita, N., Takahashi, H., Kakishita, K., Yamamoto, A., Yoshizaki, T., Terashima, T., Murakami, F., et al. (2001). Visualization, direct isolation, and transplantation of midbrain dopaminergic neurons. Proc. Natl. Acad. Sci. U. S. A. *98*, 6423–6428.

Schmut, O., Gruber, E., el-Shabrawi, Y., and Faulborn, J. (1994). Destruction of human tear proteins by ozone. Free Radic. Biol. Med. *17*, 165–169.

Schneider, S.P., and Macrides, F. (1978). Laminar distributions of interneurons in the main olfactory bulb of the adult hamster. Brain Res. Bull. *3*, 73–82.

Schoenfeld, T.A., Marchand, J.E., and Macrides, F. (1985). Topographic organization of tufted cell axonal projections in the hamster main olfactory bulb: An intrabulbar associational system. J. Comp. Neurol. *235*, 503–518.

Schroeder, P., Schieke, S.M., and Morita, A. (2006). Premature skin aging by infrared radiation, tobacco smoke and ozone. In Skin Aging, P.D.B.A. Gilchrest, and P.D.J. Krutmann, eds. (Springer Berlin Heidelberg), pp. 45–53.

Shipley, M.T., and Ennis, M. (1996). Functional organization of olfactory system. J. Neurobiol. *30*, 123–176.

Shusterman, D. (2011). The effects of air pollutants and irritants on the upper airway. Proc. Am. Thorac. Soc. *8*, 101–105.

Simonian, N.A., and Coyle, J.T. (1996). Oxidative stress in neurodegenerative diseases. Annu. Rev. Pharmacol. Toxicol. *36*, 83–106.

Smith, M.A., Nunomura, A., Zhu, X., Takeda, A., and Perry, G. (2000). Metabolic, metallic, and mitotic sources of oxidative stress in Alzheimer disease. Antioxid. Redox Signal. *2*, 413–420.

Stadtman, E.R. (1992). Protein oxidation and aging. Science *257*, 1220–1224.

Stockstill, B.L., Chang, L.Y., Ménache, M.G., Mellick, P.W., Mercer, R.R., and Crapo, J.D. (1995). Bronchiolarized metaplasia and interstitial fibrosis in rat lungs chronically exposed to high ambient levels of ozone. Toxicol. Appl. Pharmacol. *134*, 251–263.

Sullivan, R.M., and Wilson, D.A. (1995). Dissociation of behavioral and neural correlates of early associative learning. Dev. Psychobiol. *28*, 213–219.

Thiele, J.J., Traber, M.G., Tsang, K., Cross, C.E., and Packer, L. (1997). In vivo exposure to ozone depletes vitamins C and E and induces lipid peroxidation in epidermal layers of murine skin. Free Radic. Biol. Med. *23*, 385–391.

Tillerson, J.L., Caudle, W.M., Parent, J.M., Gong, C., Schallert, T., and Miller, G.W. (2006). Olfactory discrimination deficits in mice lacking the dopamine transporter or the D2 dopamine receptor. Behav. Brain Res. *172*, 97–105.

Timblin, C., BeruBe, K., Churg, A., Driscoll, K., Gordon, T., Hemenway, D., Walsh, E., Cummins, A.B., Vacek, P., and Mossman, B. (1998). Ambient particulate matter causes activation of the c-jun kinase/stress-activated protein kinase cascade and DNA synthesis in lung epithelial cells. Cancer Res. *58*, 4543–4547.

Toida, K., Kosaka, K., Aika, Y., and Kosaka, T. (2000). Chemically defined neuron groups and their subpopulations in the glomerular layer of the rat main olfactory bulb--IV. Intraglomerular synapses of tyrosine hydroxylase-immunoreactive neurons. Neuroscience *101*, 11–17.

Tsien, R.Y. (1998). The green fluorescent protein. Annu. Rev. Biochem. *67*, 509–544.

Urbani, A., and Belluzzi, O. (2000). Riluzole inhibits the persistent sodium current in mammalian CNS neurons. Eur. J. Neurosci. *12*, 3567–3574.

Valacchi, G., van der Vliet, A., Schock, B.C., Okamoto, T., Obermuller-Jevic, U., Cross, C.E., and Packer, L. (2002). Ozone exposure activates oxidative stress responses in murine skin. Toxicology *179*, 163–170.

Valacchi, G., Sticozzi, C., Pecorelli, A., Cervellati, F., Cervellati, C., and Maioli, E. (2012). Cutaneous responses to environmental stressors. Ann. N. Y. Acad. Sci. *1271*, 75–81.

Vancza, E.M., Galdanes, K., Gunnison, A., Hatch, G., and Gordon, T. (2009). Age, strain, and gender as factors for increased sensitivity of the mouse lung to inhaled ozone. Toxicol. Sci. Off. J. Soc. Toxicol. *107*, 535–543.

Ventura, R.E., and Goldman, J.E. (2007). Dorsal radial glia generate olfactory bulb interneurons in the postnatal murine brain. J. Neurosci. Off. J. Soc. Neurosci. *27*, 4297–4302.

Watkinson, W.P., Highfill, J.W., Slade, R., and Hatch, G.E. (1996). Ozone toxicity in the mouse: comparison and modeling of responses in susceptible and resistant strains. J. Appl. Physiol. Bethesda Md 1985 *80*, 2134–2142.

Weber, S.U., Thiele, J.J., Cross, C.E., and Packer, L. (1999). Vitamin C, uric acid, and glutathione gradients in murine stratum corneum and their susceptibility to ozone exposure. J. Invest. Dermatol. *113*, 1128–1132.

Wersinger, S.R., Caldwell, H.K., Martinez, L., Gold, P., Hu, S.-B., and Young, W.S. (2007). Vasopressin 1a receptor knockout mice have a subtle olfactory deficit but normal aggression. Genes Brain Behav. *6*, 540–551.

Wesson, D.W., Donahou, T.N., Johnson, M.O., and Wachowiak, M. (2008). Sniffing behavior of mice during performance in odor-guided tasks. Chem. Senses *33*, 581–596.

Whitman, M.C., and Greer, C.A. (2007). Adult-generated neurons exhibit diverse developmental fates. Dev. Neurobiol. *67*, 1079–1093.

Winner, B., Cooper-Kuhn, C.M., Aigner, R., Winkler, J., and Kuhn, H.G. (2002). Long-term survival and cell death of newly generated neurons in the adult rat olfactory bulb. Eur. J. Neurosci. *16*, 1681–1689.

Woodley, S.K., and Baum, M.J. (2003). Effects of sex hormones and gender on attraction thresholds for volatile anal scent gland odors in ferrets. Horm. Behav. *44*, 110–118.

Wrenn, C.C., Kinney, J.W., Marriott, L.K., Holmes, A., Harris, A.P., Saavedra, M.C., Starosta, G., Innerfield, C.E., Jacoby, A.S., Shine, J., et al. (2004). Learning and memory performance in mice lacking the GAL-R1 subtype of galanin receptor. Eur. J. Neurosci. *19*, 1384–1396.

Xu, F., Yan, S., Wu, M., Li, F., Xu, X., Song, W., Zhao, J., Xu, J., and Kan, H. (2011). Ambient ozone pollution as a risk factor for skin disorders. Br. J. Dermatol. *165*, 224–225.

Yang, M., and Crawley, J.N. (2009). Simple behavioral assessment of mouse olfaction. Curr. Protoc. Neurosci. Editor. Board Jacqueline N Crawley Al *Chapter*, Unit-8.24.

Yang, W., and Omaye, S.T. (2009). Air pollutants, oxidative stress and human health. Mutat. Res. *674*, 45–54.

Yang, F., Moss, L.G., and Phillips, G.N. (1996). The molecular structure of green fluorescent protein. Nat. Biotechnol. *14*, 1246–1251.

Yung, W.H., Häusser, M.A., and Jack, J.J. (1991). Electrophysiology of dopaminergic and non-dopaminergic neurones of the guinea-pig substantia nigra pars compacta in vitro. J. Physiol. *436*, 643–667.

Zaid, M.A., Afaq, F., Khan, N., Pelle, E., Matsui, M., Maes, D., and Mukhtar, H. (2008). Exposure of normal human epidermal keratinocytes to ozone results in increased expression of cytochrome P450 through activation of aryl hydrocarbon receptor. Cancer Res. *68*, 595–595.